

# PROPERTIES OF MATERIALS IN HIGH PRESSURE HYDROGEN AT CRYOGENIC, ROOM, AND ELEVATED TEMPERATURES



## ANNUAL REPORT

Contract NAS8-26191

Prepared for:

George C. Marshall Space Flight Center  
National Aeronautics and Space Administration  
Marshall Space Flight Center, Alabama 35812

Prepared by:

*J. A. Harris, Jr.*

J. A. Harris, Jr.  
Responsible Engineer

*M. C. Van Wanderham*

M. C. Van Wanderham  
Program Manager

**Pratt & Whitney Aircraft**  
FLORIDA RESEARCH AND DEVELOPMENT CENTER  
BOX 2691, WEST PALM BEACH, FLORIDA 33402

DIVISION OF UNITED AIRCRAFT CORPORATION  
**U  
A**®

## CONTENTS

SECTION		PAGE
	ILLUSTRATIONS . . . . .	iv
	TABLES . . . . .	ix
I	INTRODUCTION . . . . .	I-1
II	CONCLUSIONS . . . . .	II-1
III	MATERIALS AND SPECIMENS . . . . .	III-1
	A. Test Material . . . . .	III-1
	B. Test Gases . . . . .	III-3
	C. Test Specimens . . . . .	III-4
IV	LOW CYCLE FATIGUE . . . . .	IV-1
	A. Conclusions and Discussion . . . . .	IV-1
	B. Test Procedures . . . . .	IV-15
	C. Test Results . . . . .	IV-19
V	HIGH CYCLE FATIGUE	
	A. Introduction . . . . .	V-1
	B. Conclusions and Discussion . . . . .	V-1
	C. Test Procedure . . . . .	V-4
	D. Results . . . . .	V-6
VI	FRACTURE TOUGHNESS . . . . .	VI-1
	A. Introduction . . . . .	VI-1
	B. Conclusions and Discussion . . . . .	VI-1
	C. Test Procedure . . . . .	VI-3
	D. Test Results . . . . .	VI-6
VII	CREEP RUPTURE . . . . .	VII-1
	A. Introduction . . . . .	VII-1
	B. Conclusions . . . . .	VII-1
	C. Test Procedure . . . . .	VII-12
VIII	TENSILE PROPERTIES . . . . .	VIII-1
	A. Introduction . . . . .	VIII-1
	B. Conclusions . . . . .	VIII-1
	C. Test Procedure . . . . .	VIII-2
	D. Test Results . . . . .	VIII-5

ILLUSTRATIONS

FIGURE		PAGE
III-1	Specimen Blank Preparation Prior to Welding . . . . .	III-3
III-2	Typical Test Specimens Used To Determine Effect of High Pressure Gaseous Hydrogen on Mechanical Properties of Materials . . . . .	III-4
III-3	Constant Strain Low Cycle Fatigue Specimen . . . . .	III-6
III-4	Smooth Axial High Cycle Fatigue Specimen . . . . .	III-7
III-5	Fracture Toughness Specimen (ASTM) . . . . .	III-8
III-6	Flat End Creep Rupture Specimen . . . . .	III-9
III-7	Ambient-Cryogenic Tensile Specimen (Notch) . . . . .	III-10
III-8	Ambient-Elevated Temperature Tensile Specimen (Smooth) . . . . .	III-11
IV-1	Typical Load-Strain Hysteresis Curve Obtained During a Specimen Low Cycle Fatigue Test . . . . .	IV-1
IV-2	Low Cycle Fatigue Life of AMS 5666 (INCO 625) at 80°F . . . . .	IV-3
IV-3	Effect of Gaseous Hydrogen and Strain Range on Low Cycle Fatigue Life of AMS 5666 (INCO 625) . . . . .	IV-3
IV-4	Effect of Heat Treatment on Microstructure of AMS 5662 (INCO 718) Heat BVTO . . . . .	IV-5
IV-5	Low Cycle Fatigue Life of AMS 5662 at 80°F (INCO 718, 1750°F Solution Plus Age) . . . . .	IV-6
IV-6	Low Cycle Fatigue Life of AMS 5662 at 1250°F (INCO 718, 1750°F Solution Plus Age) . . . . .	IV-6
IV-7	Effect of Gaseous Hydrogen and Strain Range on Low Cycle Fatigue Life of AMS 5662 (INCO 718, 1750°F Solution Plus Age) . . . . .	IV-7
IV-8	Low Cycle Fatigue Life of AMS 5662 at 80°F (INCO 718, 1900°F Solution Plus Age) . . . . .	IV-7
IV-9	Low Cycle Fatigue Life of AMS 5662 at -260°F (INCO 718, 1900°F Solution Plus Age) . . . . .	IV-8
IV-10	Low Cycle Fatigue Life of AMS 5662 at 1250°F (INCO 718, 1900°F Solution Plus Age) . . . . .	IV-8
IV-11	Effect of Gaseous Hydrogen and Strain Range on Low Cycle Fatigue Life of AMS 5662 (INCO 718, 1900°F Solution Plus Age) . . . . .	IV-9
IV-12	Effect of Gaseous Hydrogen and Temperature on Low Cycle Fatigue Life of AMS 5662 (INCO 718, 1900°F Solution Plus Age) . . . . .	IV-9

## ILLUSTRATIONS (Continued)

FIGURE		PAGE
IV-13	Low Cycle Fatigue Life of AMS 5754 (Hastelloy X) at 80°F . . . . .	IV-10
IV-14	Effect of Gaseous Hydrogen and Strain Range on Low Cycle Fatigue Life of AMS 5754 (Hastelloy X) . . . . .	IV-10
IV-15	Low Cycle Fatigue Life of AMS 4928 (Ti 6-4) at 80°F . . . . .	IV-11
IV-16	Low Cycle Fatigue Life of AMS 4928 (Ti 6-4) at 200°F . . . . .	IV-11
IV-17	Effect of Gaseous Hydrogen and Strain Range on Low Cycle Fatigue Life of AMS 4928 (Ti 6-4) . . . . .	IV-12
IV-18	Low Cycle Fatigue Life of AMS 4926 (A-110) at 80°F . . . . .	IV-12
IV-19	Low Cycle Fatigue Life of AMS 4926 (A-110) at 200°F . . . . .	IV-13
IV-20	Effect of Gaseous Hydrogen and Strain Range on Low Cycle Fatigue Life of AMS 4926 (A-110). . . . .	IV-13
IV-21	Low Cycle Fatigue Life of AMS 5735 (A-286) at 80°F . . . . .	IV-14
IV-22	Low Cycle Fatigue Life of AMS 5735 (A-286) at 1250°F . . . . .	IV-14
IV-23	Effect of Gaseous Hydrogen and Strain Range on Low Cycle Fatigue Life of AMS 5735 (A-286). . . . .	IV-15
IV-24	Low Cycle Fatigue Life of AMS 5646 (AISI 347) at 80°F . . . . .	IV-16
IV-25	High Pressure Gaseous Environment, Low Cycle Fatigue Test Vessel . . . . .	IV-17
IV-26	Typical Load-Strain Hysteresis Curves for a High Pressure Gaseous Environment Low Cycle Fatigue Test (AMS 5646, 1.3% Total Strain Range, 80°F, 5000-psig Hydrogen) . . . . .	IV-18
V-1	Life of AMS 5662 at 80°F (INCO 718 , 1750°F Solution Plus Age) . . . . .	V-1
V-2	High Cycle Fatigue Life of AMS 5662 at 80°F (INCO 718, 1900°F Solution Plus Age) . . . . .	V-2
V-3	High Cycle Fatigue Life of AMS 5646 (AISI 347) at 80°F . . . . .	V-2
V-4	High Cycle Fatigue Life of AMS 4926 (A-110) at 80°F . . . . .	V-3
V-5	High Cycle Fatigue Life of AMS 5662 (INCO 718) 1750°F Solution at 1250°F. . . . .	V-3



## ILLUSTRATIONS (Continued)

FIGURE		PAGE
V-6	High Cycle Fatigue Life of AMS 5662 (INCO 718) 1900°F Solution at 1250°F . . . . .	V-4
V-7	High Pressure Gaseous Environment High Cycle Fatigue Testing Equipment . . . . .	V-5
VI-1	Engineering Ratio, $K_{IC}/\sigma_{ys}$ or $K_{IE}/\sigma_{ys}$ , for Alloys Tested in High Pressure Gaseous Environments . . . . .	VI-3
VI-2	Tensile Machine, Test Environment Controls, and Data Acquisition Equipment Located in the Blockhouse . . . . .	VI-4
VI-3	High Pressure Gaseous Environment Fracture Toughness Test Vessel Installed on Tensile Machine in the Test Cell . . . . .	VI-5
VI-4	High Pressure Gaseous Environment Fracture Toughness Test Vessel With Outer Chamber Removed and Fracture Toughness Specimen With COD Gage Attached . . . . .	VI-5
VI-5	Actual Load-Displacement Record for a Fracture Toughness Test Conducted in a High Pressure Gaseous Environment [AMS 4928 (6-4 Titanium), 5000-psig Hydrogen, 80°F] . . . . .	VI-7
VI-6	Fracture Appearances . . . . .	VI-9
VII-1	Stress Rupture of AMS 5662 at 1250°F (INCO 718); 1750°F Solution Plus Age) . . . . .	VII-2
VII-2	Stress Rupture of AMS 5662 at 1250°F (INCO 718, 1900°F Solution Plus Age) . . . . .	VII-2
VII-3	Stress Rupture of AMS 5662 (INCO 625) at 1250°F . . . . .	VII-3
VII-4	Stress Rupture of AMS 5735 (A-286) at 1250°F . . . . .	VII-3
VII-5	Stress Rupture of AMS 5646 (AISI 347) at 1250°F . . . . .	VII-4
VII-6	Stress Rupture of AMS 4928 (Ti 6-4) at 200°F . . . . .	VII-4
VII-7	Stress Rupture of AMS 4926 (A-110) at 200°F . . . . .	VII-5
VII-8	Creep-Stress-Time of AMS 5662 at 1250°F (INCO 718, 1750°F Solution Plus Age) . . . . .	VII-6
VII-9	Creep-Stress-Time AMS 5735 (A-286) at 1250°F . . . . .	VII-6
VII-10	Creep-Stress Rupture of AMS 5662 at 1250°F (INCO 718, 1750°F Solution Plus Age) . . . . .	VII-7
VII-11	Creep-Stress Rupture of AMS 5666 (INCO 625) at 1250°F . . . . .	VII-7

## ILLUSTRATIONS (Continued)

FIGURE		PAGE
VII-12	Creep-Stress Rupture of AMS 5735 (A-286) at 1250°F . . . . .	VII-8
VII-13	Creep-Stress Rupture of AMS 5646 (AISI 347) at 1250°F . . . . .	VII-8
VII-14	Creep-Stress Rupture of AMS 4928 (Ti 6-4) at 200°F . . . . .	VII-9
VII-15	Creep-Stress Rupture of AMS 4926 (Ti A-110) at 200°F . . . . .	VII-9
VII-16	Creep-Rupture Specimen of AMS 4926 (A-110) Showing Hydrating After Exposure to 5000-psig Hydrogen, 115,000-psi Stress and 200°F for 45 hr Until Rupture . . . . .	VII-10
VII-17	Creep-Rupture Pressure Vessel Complete Assembly . . .	VII-12
VII-18	Creep-Rupture Pressure Vessel With Chamber Wall Removed, Specimen, Extensometer, Universal Pin Joints and Half of Oven in Place . . . . .	VII-13
VII-19	Typical Creep-Time Strip Chart Record for Creep-Rupture Test Conducted in High Pressure Gaseous Environment . . . . .	VII-14
VIII-1	Tensile Machine and Test Environment Controls and Data Acquisition Equipment . . . . .	VIII-2
VIII-2	Various Views of Test Vessel . . . . .	VIII-3
VIII-3	Test Vessel With Outer Chamber Removed Showing Specimen, Extensometer, and Half of Furnace in Place . . . . .	VIII-4
VIII-4	Tensile Properties of AMS 5662 (INCO 718), 1750°F Solution in High Pressure Gaseous Environments . . . . .	VIII-14
VIII-5	Tensile Properties of AMS 5662 (INCO 718), 1900°F Solution in High Pressure Gaseous Environments . . . . .	VIII-15
VIII-6	Tensile Properties of AMS 5666 (INCO 625) in High Pressure Gaseous Environments . . . . .	VIII-16
VIII-7	Tensile Properties of AMS 5662 (INCO 718), 1900°F Solution Welds, and AMS 5666 (INCO 625) Welds, in High Pressure Gaseous Environments at Room Temperature (80°F) . . . . .	VIII-17
VIII-8	Tensile Properties of AMS 5735 (A-286) in High Pressure Gaseous Environments . . . . .	VIII-18

ILLUSTRATIONS (Continued)

FIGURE		PAGE
VIII-9	Tensile Properties of AMS 5646 (AISI 347) in High Pressure Gaseous Environments . . . . .	VIII-19
VIII-10	Tensile Properties of AMS 5754 (Hastelloy X) in High Pressure Gaseous Environments . . . . .	VIII-20
VIII-11	Tensile Properties of AMS 4928 (Ti 4-6) in High Pressure Gaseous Environments . . . . .	VIII-21
VIII-12	Tensile Properties of AMS 4926 (A-110) in High Pressure Gaseous Environments . . . . .	VIII-22

## TABLES

TABLE		PAGE
II-1	Degree of Degradation of Various Alloys . . . . .	II-2
III-1	Materials for Hydrogen Degradation Testing . . . . .	III-1
III-2	Specimens Used to Determine Influence of Elevated Temperature on Metals in Gaseous Hydrogen . . . . .	III-5
IV-1	Degradation of Alloys Due to High Pressure Hydrogen . . .	IV-2
IV-2	Room Temperature Low Cycle Fatigue Properties of Materials in High Pressure Gaseous Environment . . . .	IV-20
IV-3	Cryogenic Temperature Low Cycle Fatigue Properties of Materials in High Pressure Gaseous Environment . . . . .	IV-23
IV-4	Elevated Temperature Low Cycle Fatigue Properties of Materials in High Pressure Gaseous Environment . . . . .	IV-24
V-1	Room Temperature High Cycle Fatigue Properties of Materials in High Pressure Gaseous Environment . . . . .	V-7
V-2	Elevated Temperature High Cycle Fatigue Properties of Materials in High Pressure Gaseous Environment . . . . .	V-9
VI-1	Fracture Toughness of Materials in High Pressure Gaseous Environment . . . . .	VI-8
VII-1	Creep-Rupture Properties of Materials in High Pressure Gaseous Environment . . . . .	VII-11
VIII-1	Room Temperature Tensile Properties of Materials in High Pressure Gaseous Environment . . . . .	VIII-6
VIII-2	Cryogenic Temperature Properties of Materials in High Pressure Gaseous Environment . . . . .	VIII-10
VIII-3	Elevated Temperature Tensile Properties of Materials in High Pressure Gaseous Environment . . . . .	VIII-11

SECTION I  
INTRODUCTION

This report is submitted in accordance with the requirements of Contract NAS8-26191 and represents the first annual report covering the period 29 June 1970 to 29 June 1971. Experimental efforts in this program have consisted of mechanical property tests of nickel-base, titanium-base, and iron-base alloys in 5000-psig gaseous helium and hydrogen at various temperatures, and the comparison of test results to determine degradation of properties due to the hydrogen environment. The testing program for the first year's work under this contract is outlined below:

Material	Temperature, °F	Low Cycle Fatigue, H <sub>2</sub> /He <sup>1</sup>	High Cycle Fatigue, H <sub>2</sub> /He <sup>1</sup>	Fracture Toughness, H <sub>2</sub> /He <sup>1</sup>	Creep Rupture, H <sub>2</sub> /He <sup>1</sup>	Notched Tensile, H <sub>2</sub> /He <sup>1</sup>	Smooth Tensile, H <sub>2</sub> /He <sup>1</sup>
Inconel 718 <sup>(2)</sup>	80	4/4	4/4	2/2		3/2	2/2
	1250	4/4	4/4		2/2	3/2	2/2
Inconel 718 <sup>(3)</sup>	-260	4/4					
	80	4/4	4/4	2/2		3/2	2/2
	1250	4/4	4/4		2/2	3/2	2/2
Inconel 718 Welds <sup>(3)</sup>	80			2/2		3/2	2/2
Inconel 625	80	4/4		2/2		3/2	2/2
	1250				2/2	3/2	2/2
Inconel 625 Welds	80			2/2		3/2	2/2
A-286	80	4/4		2/2		3/2	2/2
	1250	4/4			2/2	3/2	2/2
AISI 347	-260					3/2	2/2
	80	4/4	4/4	2/2		3/2	2/2
	1250				2/2	3/2	2/2
Hastelloy X	80	4/4				3/2	2/2
	1250					3/2	2/2
Ti-6Al-4V	80	4/4		2/2		3/2	2/2
	200	4/4			2/2	3/2	2/2
Ti-5Al-2.5 Sn	80	4/4	4/4	2/2		3/2	2/2
	200	4/4			2/2	3/2	2/2

(1) Numbers (X/X) are number of tests in hydrogen/helium.

(2) Anneal 1750 °F, 1 hour, air cool, plus aging at 1325 °F for 8 hours, furnace cool to 1150 °F, hold at 1150 °F for a total aging time of 18 hours, and air cool.

(3) Solution 1900 °F, 1 hour, air cool 50 °F/minute or faster, plus aging at 1325 °F for 8 hours, furnace cool to 1150 °F, hold at 1150 °F for total aging time of 18 hours, and air cool.

# Pratt & Whitney Aircraft

PWA FR-4566

All testing was conducted on solid specimens exposed to external gaseous pressure. Specific mechanical properties determined and the testing methods used are summarized below:

- Low Cycle Fatigue - Low cycle fatigue life was established by constant-total-strain-testing using smooth specimens and total-strain closed-loop testing machines.
- High Cycle Fatigue - High cycle fatigue life was established by load (stress) controlled tension-tension testing using smooth specimens and servo-actuated, closed-loop machines.
- Fracture Toughness - Fracture toughness tests were conducted using single-edged, notched, fatigue-precracked, compact tensile specimens.
- Creep-Rupture - Creep rate and time to failure were determined using smooth specimens and a standard creep-rupture machine equipped with a recording extensometer.
- Tensile - Smooth and notched tensile tests were conducted on solid specimens using ASTM tensile testing techniques.

This report is arranged in sections, which cover the program conclusions, materials tested, and results and conclusions of the individual property tests.

This program has been conducted using the Program Manager - Project Group System by the Pratt & Whitney Aircraft, Florida Research and Development Center, Materials Development Laboratory under the cognizance of Mr. W. B. McPherson, Materials Division, Astronautics Laboratory, Marshall Space Flight Center.

Acknowledgement is given to the following personnel of the Project Group:

Mr. J. E. Bearden	- High Cycle Fatigue Testing
Mr. R. B. Bogard	- Low Cycle Fatigue Testing
Mr. W. H. Carver	- Test Support, Rocket Test Facility
Mr. J. E. Gies	- Test Support, Rocket Test Facility
Mrs. A. Kirkpatrick	- Proposal and Report Efforts
Mr. P. E. Newett	- Tensile and Fracture Toughness Testing
Mr. J. F. Schratt	- Creep-Rupture Testing
Mrs. C. B. Stevens	- Metallurgical Investigations
Mr. C. T. Torrey	- Metallographic Investigations
Mr. B. H. Walker	- Tensile and Fracture Toughness Testing

SECTION II  
CONCLUSIONS

The following system is established to weigh the degree of degradation and serve as an aid in comparing the various alloys.

Extremely Degraded (ED) - Hydrogen reduced the property or life (in helium) greater than 50%

$$ED = \left( \frac{H_e - H_2}{H_e} \right) \times 100 \text{ is } > 50\%$$

Severely Degraded (SD) - Hydrogen reduced the property or life (in helium) greater than 25% but less than 50%

$$SD = \left( \frac{H_e - H_2}{H_e} \right) \times 100 \text{ is } > 25\% \text{ but } < 50\%$$

Degraded (D) - Hydrogen reduced the property or life (in helium) greater than 10% but less than 25%

$$D = \left( \frac{H_e - H_2}{H_e} \right) \times 100 \text{ is } > 10\% \text{ but } < 25\%$$

Negligible Degradation (ND) - Hydrogen reduced the property or life (in helium) less than 10%

Using the above rating system, table II-1 displays the degree of degradation of each alloy investigated with various tests.

Table II-1. Degree of Degradation of Various Alloys

Material	Temperature °F	Fatigue		Fracture Toughness	Creep Rupture Based On		Tensile
		Low Cycle Cyclic Life	High Cycle Cyclic Life		Life (hr) at 100 hr H <sub>2</sub>	Stress at 100 hr	
		1%-2% Strain					
<u>Nickel Base</u>							
INCO 625	80°	ED		ND			ED
AMS 5666	1250°				ED	D	D
INCO 625 Weld	80°			ND			ND
INCO 718, 1900 °F Solution Plus Age	-260°	ND*					
AMS 5662	80°	ED	ED	ND			SD
	1250°	SD	ED		ED	SD	ND
INCO 718, 1750 °F Solution Plus Age	80°	ED	ED	ND			ED
AMS 5662	1250°	SD	ED		ED	SD	ND
INCO 718 (1900°) Weld	80°			ND			ED
Hastelloy X	80°	ED					D
AMS 5754	1250°						ND
<u>Titanium Base</u>							
Ti-A110	80°	ND	ND	ND			D
AMS 4926	200°	ED			ED	ND	SD
Ti-6-4	80°	ND		ND			ED
AMS 4928	200°	SD			ED	D	SD
<u>Iron Base</u>							
A-286	80°	ND		ND			ND
AMS 5735	1250°	ND			ED	SD	D
AISI 347	-260°						ND
AMS 5646	80°	ND	ND	ND			ND
	1250°				ND	ND	ND

\*Not degraded at -260°F



### Nickel Base Alloys

Tested were: INCO 718 (AMS 5662) 1750 °F Solution plus Age  
INCO 718 (AMS 5662) 1900 °F Solution plus Age  
INCO 625 (AMS 5666)  
Hastelloy X (AMS 5754)

The low-cycle and high-cycle fatigue life, both strain controlled and tension-tension load controlled, at 80 °F was extremely degraded (ED) for all nickel base alloys tested in 5000-psig hydrogen. The degree of degradation of INCO 718 was less severe at 1250 °F (rated SD) and was not degraded at -260 °F.

The fracture toughness,  $K_{IC}$  or  $K_{IE}$ , was rated ND (Negligible Degradation) for all nickel base alloys.

The rupture life at 1250 °F in 5000-psig hydrogen, comparing  $H_2$  life (hr) to  $H_e$  life (hr) at stress required for 100 hr  $H_2$  life, is extremely degraded (ED) for INCO 625 and both heat treatments of INCO 718. However, making a comparison on a stress basis for 100 hr life, the degradation is rated severe for INCO 718 and degraded for INCO 625.

The tensile properties; 0.2% yield, ultimate, elongation and reduction in area for smooth specimens, and ultimate and reduction in area for notched specimens ( $K_t = 8.0$ ), were all evaluated, and the degradation rating is based on any of these properties being degraded. INCO 718 (1750 °F Solution Heat Treated), INCO 625, and GTA welded INCO 718 (1900 °F Solution Heat Treated), were extremely degraded at 80 °F in 5000-psig hydrogen. INCO 718 (1900 °F Solution Heat Treated) was severely degraded at 80 °F. GTA welded INCO 625 was not degraded at 80 °F. Hastelloy X was rated as degraded at 80 °F. Less degradation was noted on all alloys, INCO 718, INCO 625, and Hastelloy X, when tested at 1250 °F.

### Iron Base Alloys

Tested were: A-286 (AMS 5735)  
AISI 347 (AMS 5646)

These alloys as a class exhibited the least degradation of properties in hydrogen of all the materials tested. In fact, AISI 347 had negligible property degradation for all the tests and conditions investigated during this program. A-286 material, tested in the fully heat treated condition (AMS 5735) exhibited negligible property degradation at 80 °F. At an elevated temperature of 1250 °F, however, the creep rupture 100 hr life was extremely degraded and the stress level for 100 hr life was severely degraded. The elevated temperature tensile strength was also degraded. Low cycle fatigue life had negligible degradations.

### Titanium Base Alloys

Tested were: Ti 6-4 (AMS 4928)  
Ti A-110 (AMS 4926)

A-110 and 6-4 titanium alloys were rated ND (Negligible Degradation) for fatigue and fracture toughness at 80°F. Low cycle fatigue and stress rupture lives, and tensile RA (reduction in area) of both A-110 and 6-4 Ti were either severely or extremely degraded at 200°F in 5000-psig hydrogen.

This program was established to determine degradation of specific material properties and to enable general observations in regard to the susceptibility of a particular material to hydrogen degradation. Certain tests did not indicate any conclusive degradation due to the hydrogen environment on materials known to be degraded. An example of this is the fracture toughness of INCO 718 with the 1750°F Solution plus Age heat treatment. This test indicated negligible degradation of this material by the hydrogen environment. The low and high cycle fatigue, creep rupture, and tensile tests, however, indicated extreme hydrogen degradation.

A-286 material exhibited negligible degradation at 80°F in all tests. At elevated temperature, the creep-rupture test indicated severe to extreme degradation. This emphasizes the fact that no one test can be used as a basis for declaring a material to be free of hydrogen degradation. For this reason, a material should be subjected to several different tests in a high pressure hydrogen environment before a definite conclusion regarding the degree of hydrogen degradation can be made.

The experience of this program has been that creep-rupture and low cycle fatigue are the most severe tests of a material for hydrogen degradation, followed by high cycle fatigue, tensile and fracture toughness tests, in that order.

SECTION III  
MATERIALS AND SPECIMENS

A. TEST MATERIAL

The purpose of this contract is to determine the susceptibility of various alloys proposed for use in hydrogen-fueled rocket engines to hydrogen degradation. For this phase of the program, wrought nickel-, iron-, and titanium-base materials were tested. Table III-1 lists materials and conditions in which they were purchased.

Table III-1. Materials for Hydrogen Degradation Testing

Name	Base	Purchasing Specification	P&WA Heat	As-Received Condition
INCO 718	Nickel	AMS 5662	BVTO	0.750-in. diameter barstock, solution annealed at 1750°F only.
INCO 718	Nickel	AMS 5662	BZMK	4.0-in. diameter barstock, solution annealed at 1750°F only.
INCO 625	Nickel	AMS 5666	BZCV	0.750-in. diameter barstock, annealed at 1800°F.
INCO 625	Nickel	AMS 5666	BYAP	4.250-in. diameter barstock, annealed at 1800°F.
A-286	Iron	AMS 5735	BZCU	0.750-in. diameter barstock fully heat-treated, solution at 1800°F, age at 1350°F.
A-286	Iron	AMS 5735	BXOY	4.500-in. diameter barstock fully heat treated, solution at 1800°F, age at 1350°F.
AISI 347	Iron	AMS 5646	BZCT	0.750-in. diameter barstock, solution at 1875°F, cold finished.
AISI 347	Iron	AMS 5646	BUJR	4.250-in. diameter barstock, solution at 1875°F only.
Hastelloy X	Nickel	AMS 5754	BZCR	0.750-in. diameter barstock, solution at 2150°F only.

Table III-1. Materials for Hydrogen Degradation Testing  
(Continued)

Name	Base	Purchasing Specification	P&WA Heat	As-Received Condition
Titanium 6A1-4V	Titanium	AMS 4928	BZCR	0.750-in. diameter barstock, annealed at 1375°F only.
Titanium 6A1-4V	Titanium	AMS 4928	BZAX	4.500-in. diameter barstock, annealed at 1375°F only.
Titanium A-110 (5A1.2.5Sn)	Titanium	AMS 4926	BZCW	0.750-in. diameter barstock, annealed at 1200°F only.
Titanium A-110 (5A1-2.5Sn)	Titanium	AMS 4926	BZMP	4.500-in. diameter barstock, annealed at 1200°F only.
INCO 718	Nickel	AMS 5832		Weld wire, annealed.
INCO 625	Nickel	AMS 5837		Weld wire, annealed.

## Notes:

1. Specimens used to test tensile strength, low and high cycle fatigue, and creep rupture were made of 0.750-in. diameter barstock, of single heats.
2. Specimens used to test fracture toughness were made of larger diameter material (4.0 to 4.5 in.), and of heats other than those of the 0.750-in. diameter barstock.
3. Weld wire was from single heats.

Specimen blanks were cut and heat-treated as required. Only the INCO 718 and the A-286 materials were tested in a fully heat-treated condition. The A-286 material was received fully heat-treated (per AMS 5735), and no subsequent heat treatment was done. The INCO 718 material was received in the 1750°F annealed condition (per AMS 5662). It was heat-treated according to the two requirements of contract Work Statement as follows:

1. Anneal at 1750°F, 1 hour, air cool (as received); age at 1325°F, 8 hours, furnace cool to 1150°F; hold at 1150°F for total age time of 18 hours, air cool.
2. Anneal at 1750°F, 1 hour, air cool (as received); solution at 1900°F, 1 hour, air cool 50°F/min; age at 1325°F, 8 hours, furnace cool to 1150°F; hold at 1150°F for total age time of 18 hours, air cool.

All other materials were tested in the solution-annealed (as received) condition.

Blanks from which the welded specimens of INCO 718 and INCO 625 were machined were prepared as shown in figure III-1, and gas-tungsten-arc (GTA) welded. The INCO 718 blanks were welded using AMS 5832 as filler material; INCO 625 blanks were welded using AMS 5837 filler material. The INCO 718 welded blanks were then subjected to the heat treatment described in item 2 above. INCO 625 welded specimen blanks were subjected to an 1800°F, one hour, air cool, stress-relief cycle.

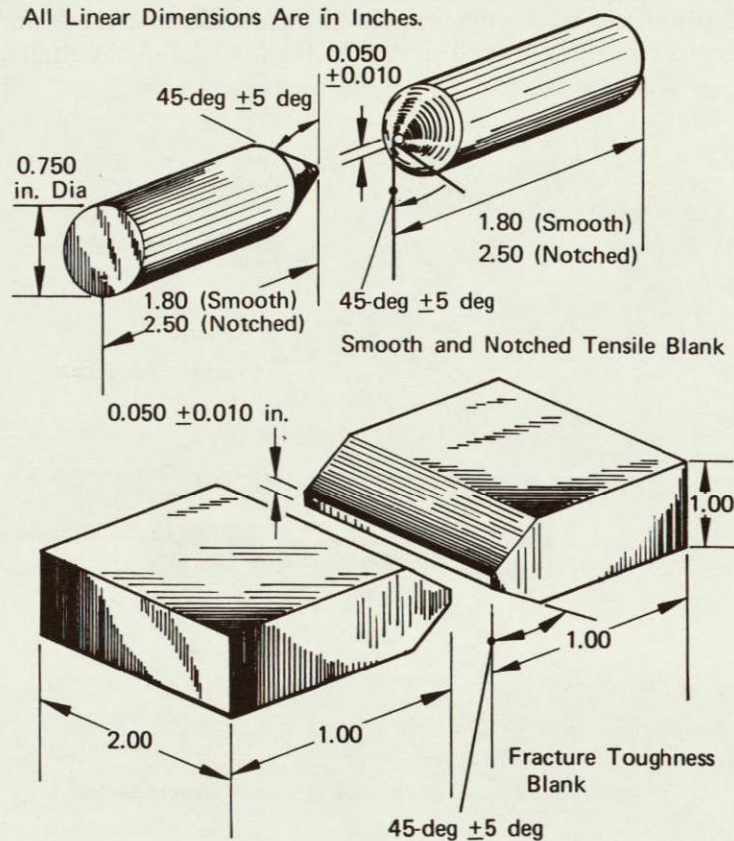


Figure III-1. Specimen Blank Preparation Prior To Welding FD 51835

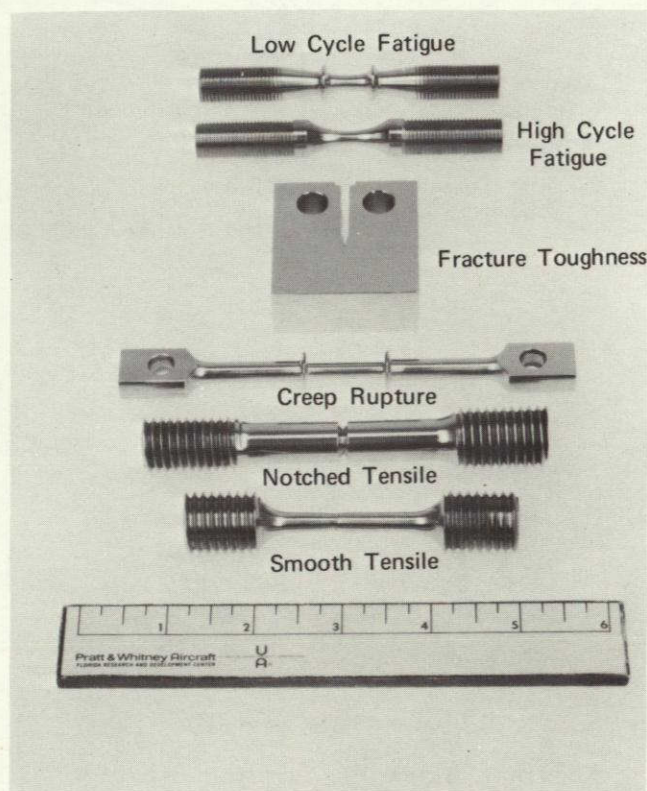
## B. TEST GASES

Helium and hydrogen were used during the testing of specimens and nitrogen was used as a preliminary purge gas. Hydrogen was provided under Military Specification P-27201, which requires the gas to have an oxygen content of less than 1 part per million. Gas handling systems supplying the test vessels were equipped to enable sampling before and after specimen tests. Samples were analyzed using a modified gas chromatograph with accuracy in the parts per billion range. Typical oxygen content of hydrogen samples was found to be in the 1.3 to 1.5 parts per million range, with one batch having an oxygen content of less than 4 parts per billion. No appreciable difference was noted between pretest and post-test samples, indicating no gas contamination by the test rig and/or test itself.



## C. TEST SPECIMENS

Surfaces of all specimens were machined<sup>1</sup> and finished to an average roughness of  $16\ \mu$  in. RMS or less except for one outer surface of the fracture toughness specimens, which was machined to a roughness of  $32\ \mu$  in. RMS in accordance with ASTM E-399T. Gage sections of specimens were polished prior to testing. The notch used for tensile specimens to obtain a stress concentration factor of 8.0 was designed according to Peterson<sup>2</sup> and was machined by grinding. Dimensions of the notch were checked optically (shadowgraph) several times during machining to ensure that the required 0.002-in. notch radius and the notch depth were obtained. Smooth tensile specimens had a gage section diameter of 0.251 in. minimum. A typical set of specimens is shown in figure III-2 and specimen prints are listed in table III-2 and shown in figures III-3 through III-7.



FE 108806A

Figure III-2. Typical Test Specimens Used To Determine Effect of High Pressure Gaseous Hydrogen on Mechanical Properties of Materials

FE 108806A

<sup>1</sup>Test specimens were machined by both the Pratt & Whitney Aircraft Laboratory Machine Shop and outside vendors operating under Pratt & Whitney Materials Control Laboratory surveillance and control.

<sup>2</sup>R. E. Peterson, Stress Concentration Design Factors, John Wiley & Sons, Inc., New York, 1953.



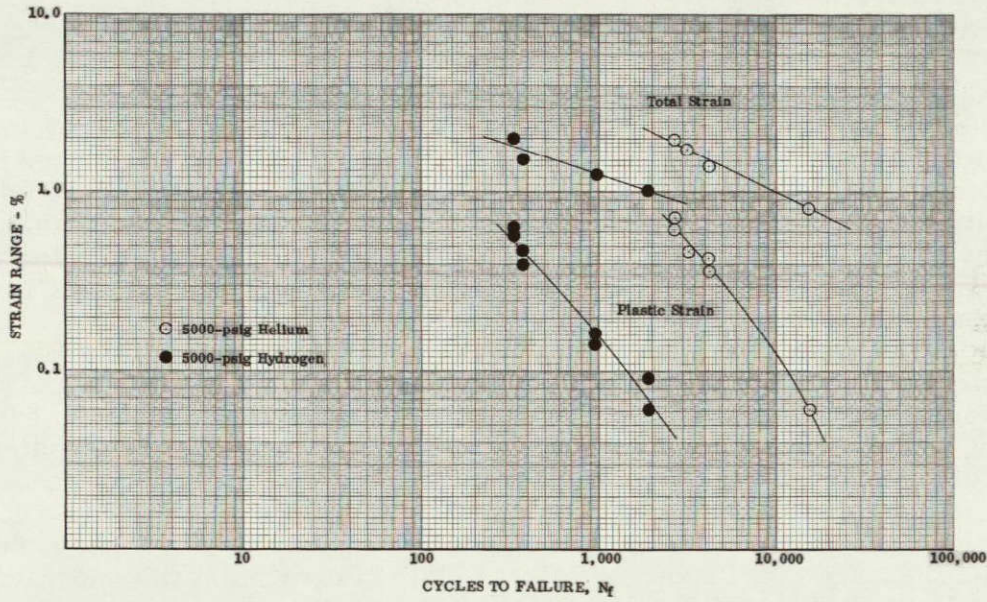


Figure IV-2. Low Cycle Fatigue Life of AMS 5666 (INCO 625) at 80°F DF 86830

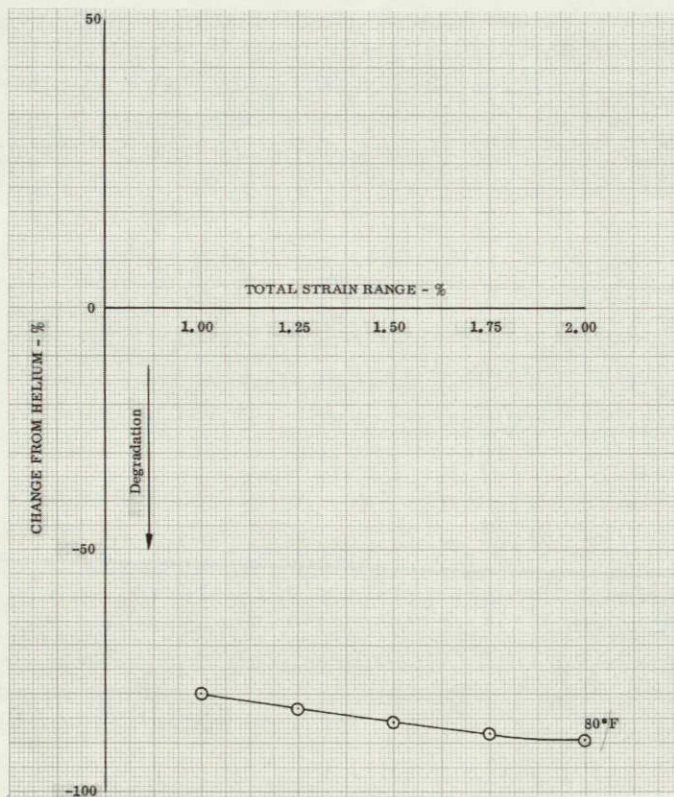


Figure IV-3. Effect of Gaseous Hydrogen and Strain Range on Low Cycle Fatigue Life of AMS 5666 (INCO 625) DF 86831



### 3. INCO 718 (AMS 5662)

INCO 718 material was the most thoroughly investigated. Two heat treatments were applied to specimens from the same stock, differing only in solution temperature. The effect of 1750 and 1900°F solution temperatures upon microstructure is shown in figure IV-4. Both microstructures were fully recrystallized with the 1900°F solution temperature producing larger grain size. The 1900°F-solutioned material was slightly more degraded in hydrogen than the 1750°F-solutioned material, indicating microstructure affects LCF performance with small grain, recrystallized structures more desirable. Investigations by Harris and VanWanderham<sup>(1)</sup> have also described this relationship. Cyclic strain level and temperature also influence the degree of degradation (figure IV-5 through IV-11). The 1750°F-solutioned material has increasing degradation at increasing cyclic strain level. The 1900°F-solutioned material did not exhibit this trend. The most influential effect on LCF life resulted from temperature. Both materials were less susceptible (almost 65% less) to life degradation at 1250°F than at 80°F. The 1900°F-solutioned material was tested at -260°F, 80°F, and 1250°F. A plot of degradation vs temperature (figure IV-12) indicates that degradation is most severe in the range of temperatures around 80°F, and with decreasing degradation with decreasing temperature. In fact, at a temperature of -260°F LCF life in hydrogen was significantly better than LCF life in helium at that temperature. The reason for this great improvement in LCF life at cryogenic temperature is not presently understood. It is believed that the 1750°F-solutioned material and perhaps other nickel-base alloys will also show similar influences of temperature. It is clear, however, that INCO 718 LCF life is most severely degraded in the room (80°F) temperature range. Additional testing at temperature ranges between -100 and 600°F would define the point of inflection in the temperature-degradation curve.

### 4. Hastelloy X

Hastelloy X (AMS 5754) was tested at 80°F only and exhibited the lowest average degradation of all the nickel-base alloys tested. Degradation of this alloy was strain level sensitive, with degradation inversely proportional to increasing cyclic strain level (figures IV-13 and IV-14).

### 5. Titanium-Base Alloys

The LCF life of the two titanium-base alloys tested, Ti 6-4 (AMS 4928) and A-110 (AMS 4926) was not as severely degraded as that of the nickel-base alloys. Both alloys showed an influence of cyclic strain level upon degree of degradation. The Ti 6-4 exhibited decreasing degradation with increasing cyclic strain level at both 80°F and 200°F (figures IV-15 through IV-17); whereas, the A-110 exhibited increasing degradation with increasing cyclic strain level at 200°F. This alloy (A-110) displayed no degradation at 80°F, however there was more scatter in the test data for this condition than for any other material tested (figures IV-18 through IV-20).

---

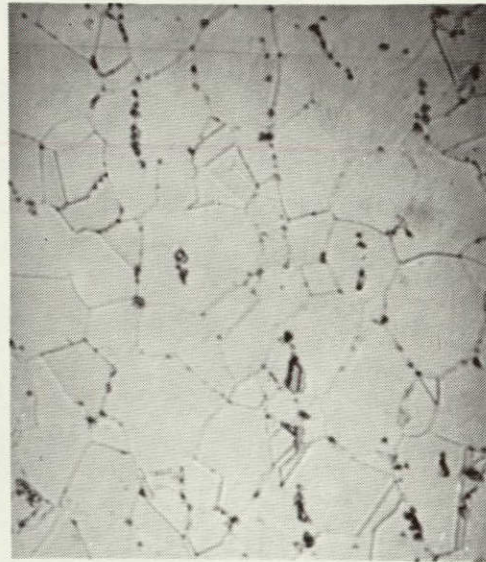
(1) VanWanderham, M., and J. A. Harris, Jr., "Low Cycle Fatigue of Metals in High Pressure Gaseous Hydrogen at Cryogenic, Ambient, and Elevated Temperatures," presented to the 1971 WESTEC Conference, Los Angeles, California.



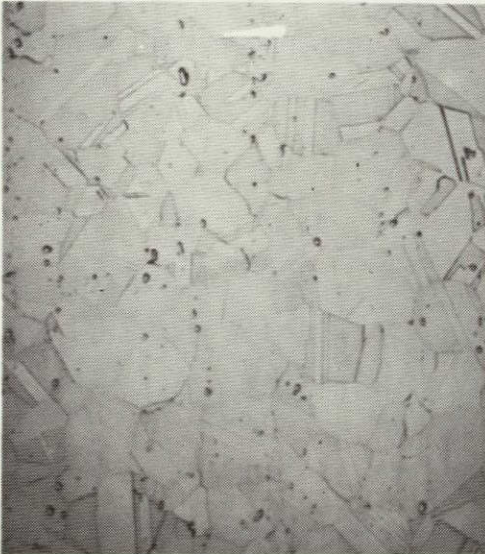


Mag: 100X

1750°F Solution Plus Age Heat Treatment

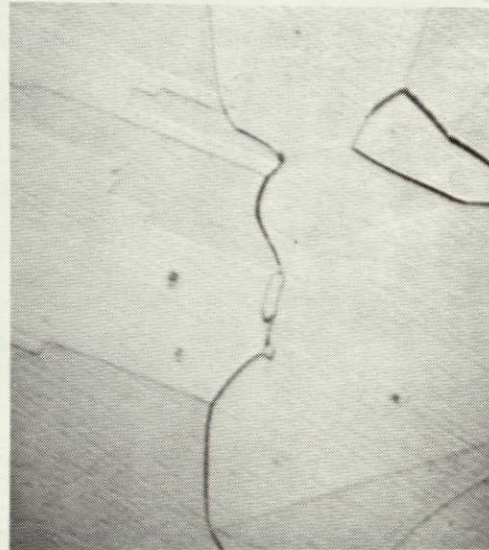


Mag: 1000X



Mag: 100X

1900°F Solution Plus Age Heat Treatment



Mag: 1000X

NOT REPRODUCIBLE

Figure IV-4. Effect of Heat Treatment on Microstructure of AMS 5662 (INCO 718) Heat BVTO

FD 53146



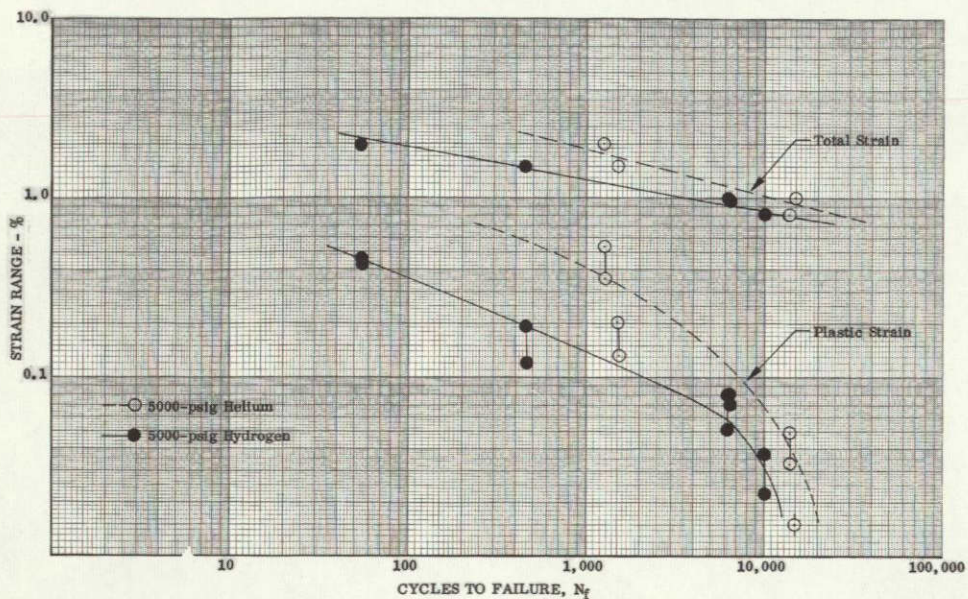


Figure IV-5. Low Cycle Fatigue Life of AMS 5662 at 80 °F (INCO 718 , 1750 °F Solution Plus Age)

DF 86832

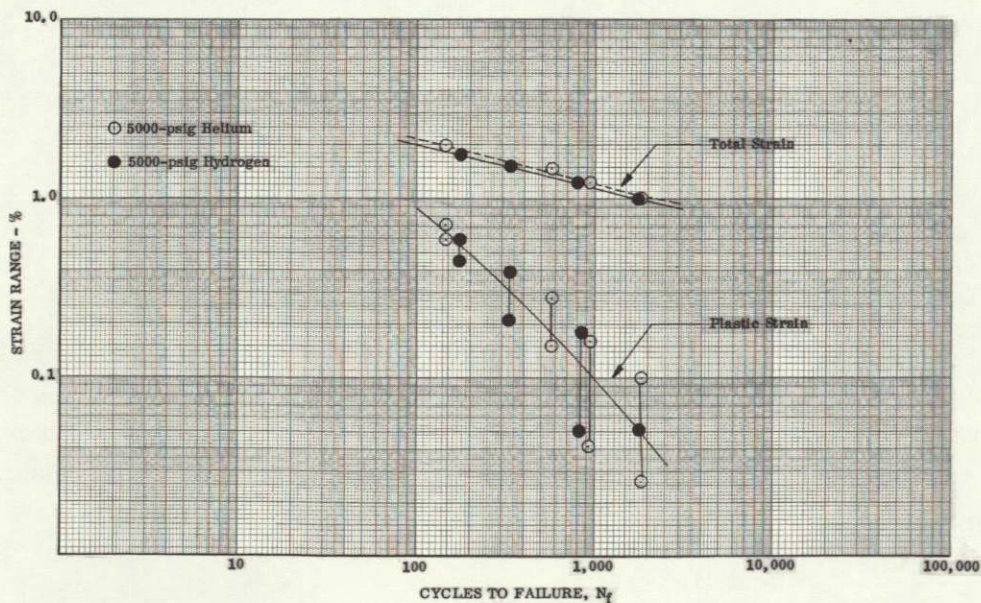


Figure IV-6. Low Cycle Fatigue Life of AMS 5662 at 1250 °F (INCO 718 , 1750 °F Solution Plus Age)

DF 86833

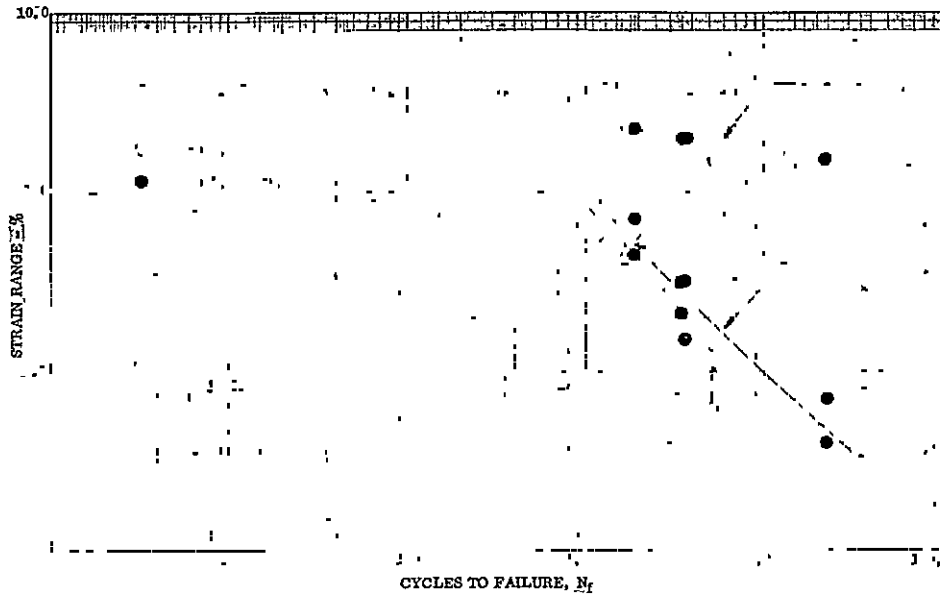


Figure IV-9. Low Cycle Fatigue Life of AMS 5662 at -260°F (INCO 718, 1900°F Solution Plus Age) DF 86836

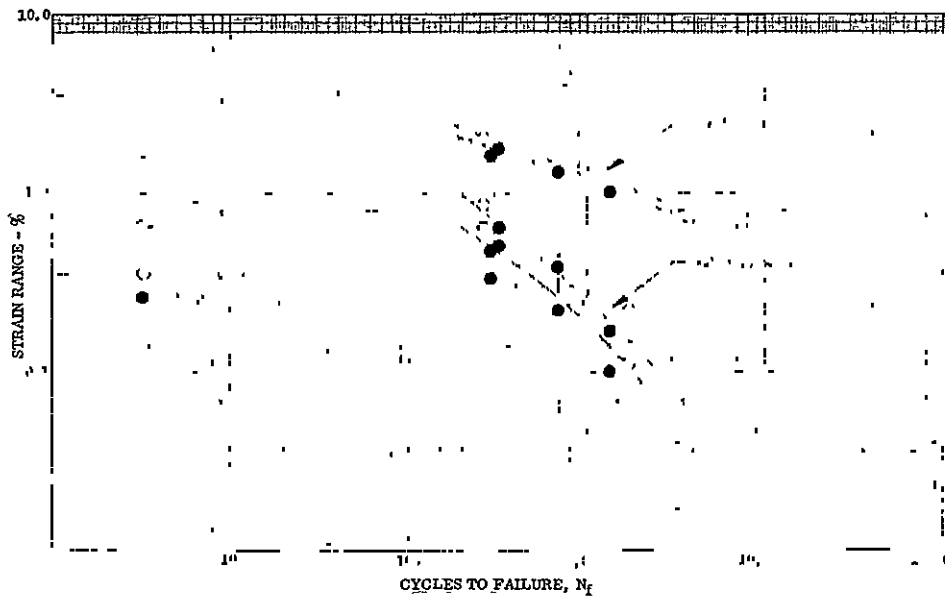


Figure IV-10. Low Cycle Fatigue Life of AMS 5662 at 1250°F (INCO 718, 1900°F Solution Plus Age) DF 86837

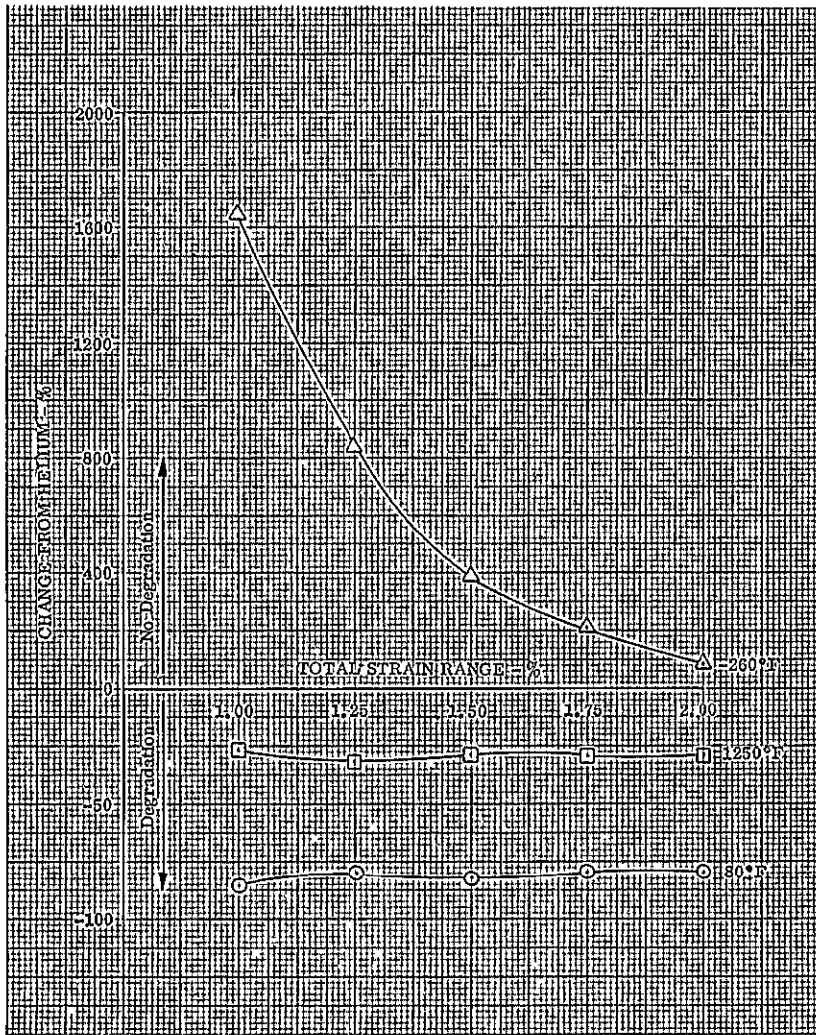


Figure IV-11. Effect of Gaseous Hydrogen DF 86838 and Strain Range on Low Cycle Fatigue Life of AMS 5662 (INCO 718, 1900°F Solution Plus Age)

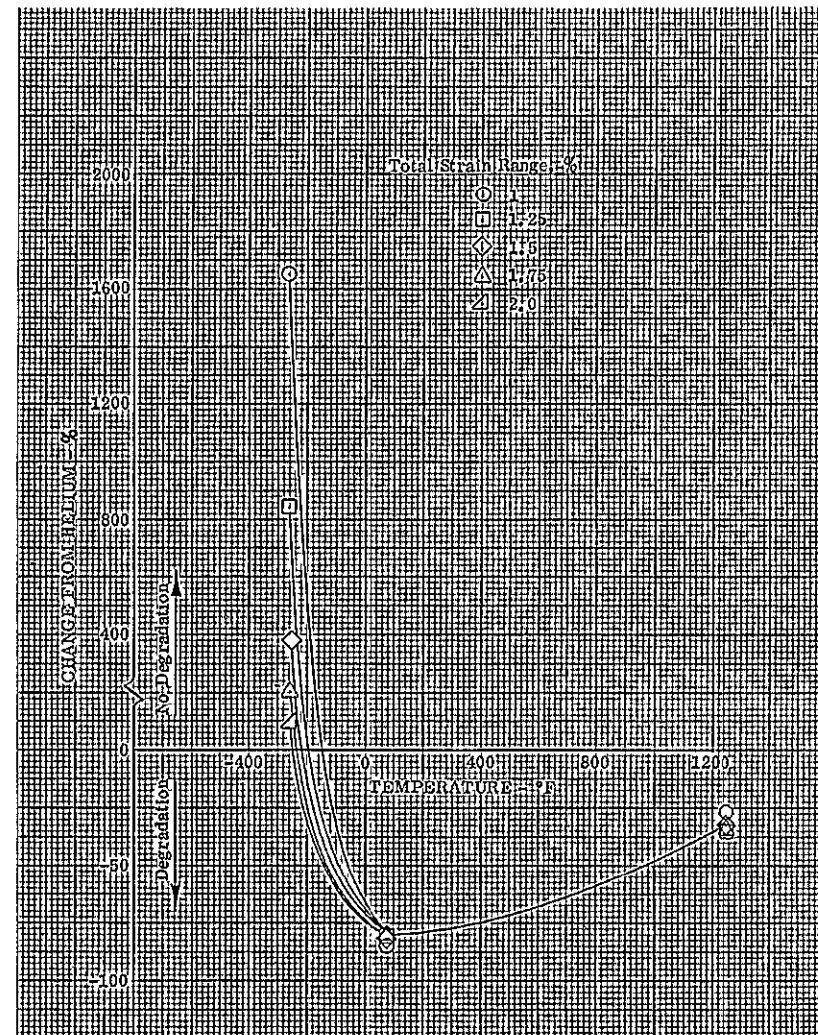


Figure IV-12. Effect of Gaseous Hydrogen DF 86839 and Temperature on Low Cycle Fatigue Life of AMS 5662 (INCO 718, 1900°F Solution Plus Age)

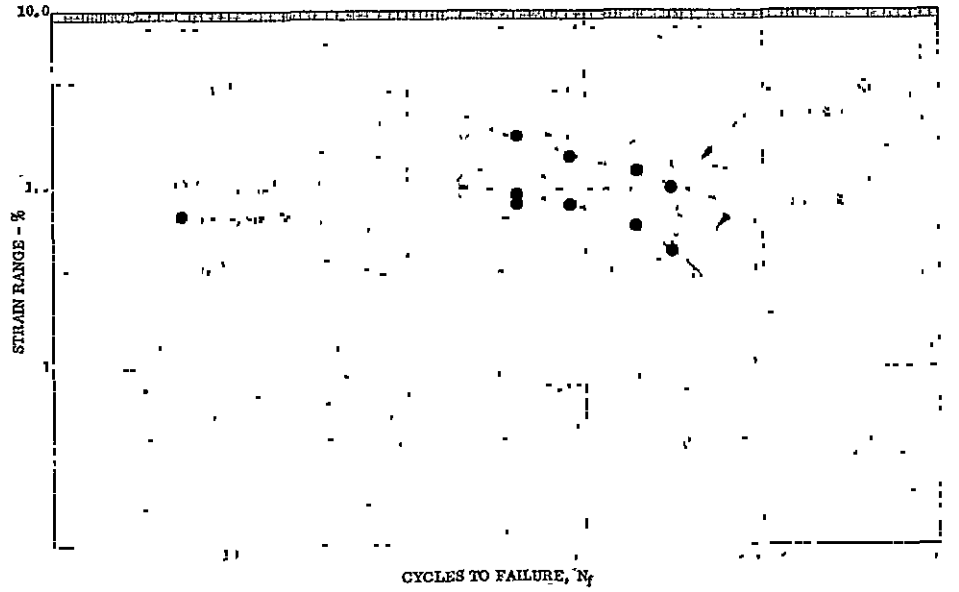


Figure IV-13. Low Cycle Fatigue Life of AMS 5754 DF 86840  
(Hastelloy X) at 80°F

---

Figure IV-14. Effect of Gaseous Hydrogen and Strain DF 86841  
Range on Low Cycle Fatigue Life of  
AMS 5754 (Hastelloy X)

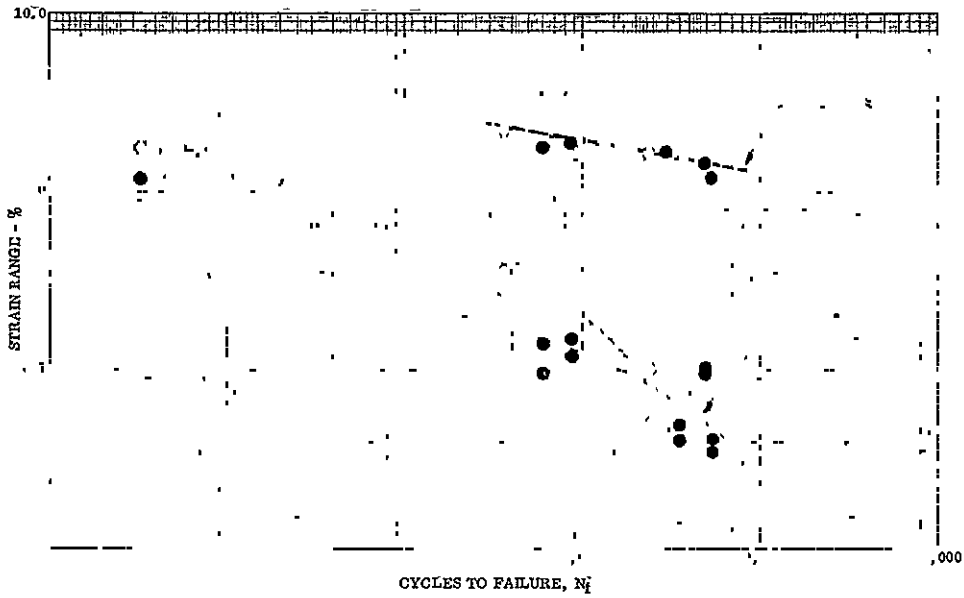


Figure IV-15. Low Cycle Fatigue Life of AMS 4928 DF 86842  
(Ti 6-4) at 80°F

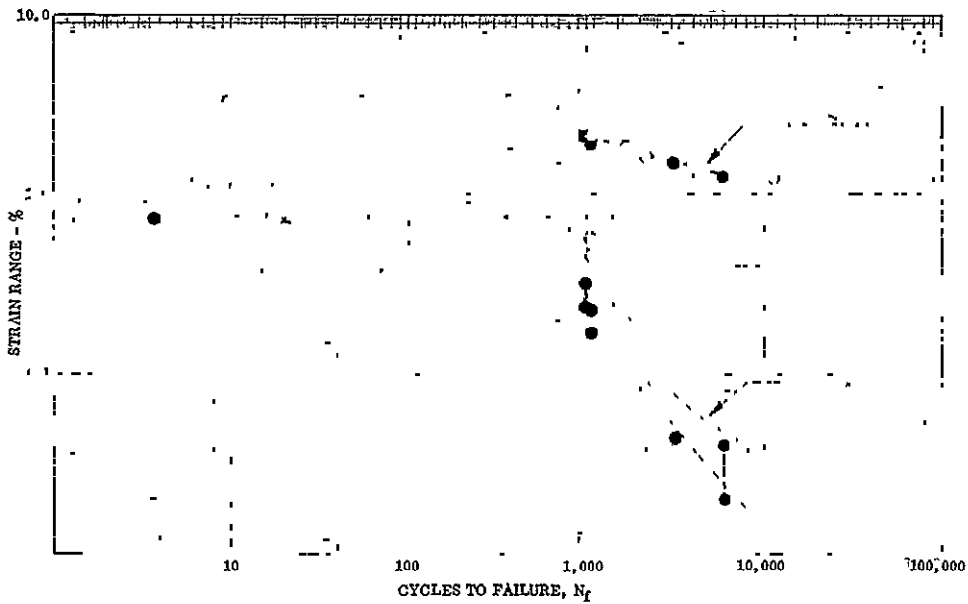


Figure IV-16. Low Cycle Fatigue Life of AMS 4928 DF 86843  
(Ti 6-4) at 200°F



Figure IV-17. Effect of Gaseous Hydrogen and Strain Range on Low Cycle Fatigue Life of AMS 4928 (Ti 6-4) DF 86844

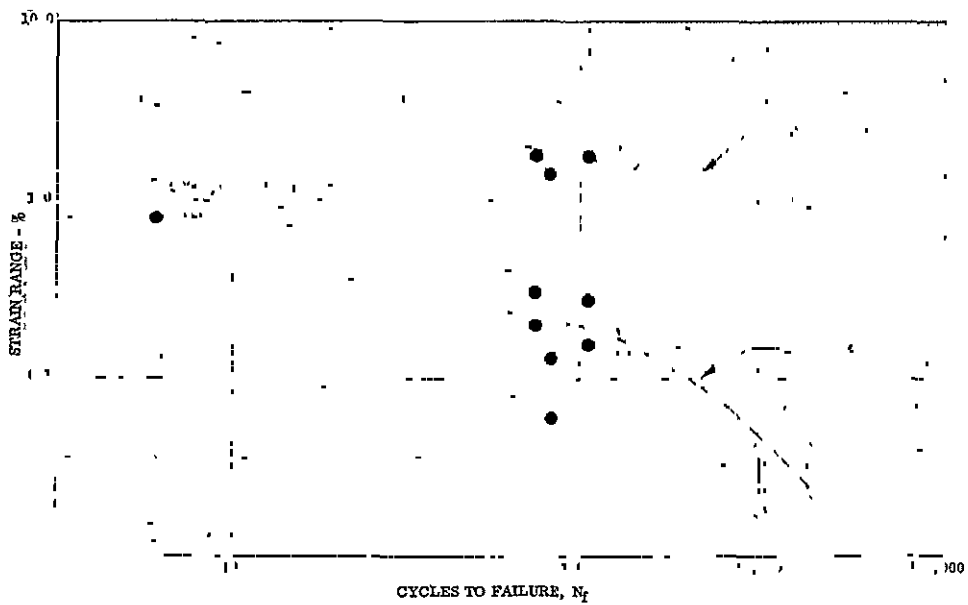


Figure IV-18. Low Cycle Fatigue Life of AMS 4926 (A-110) at 80°F DF 86845

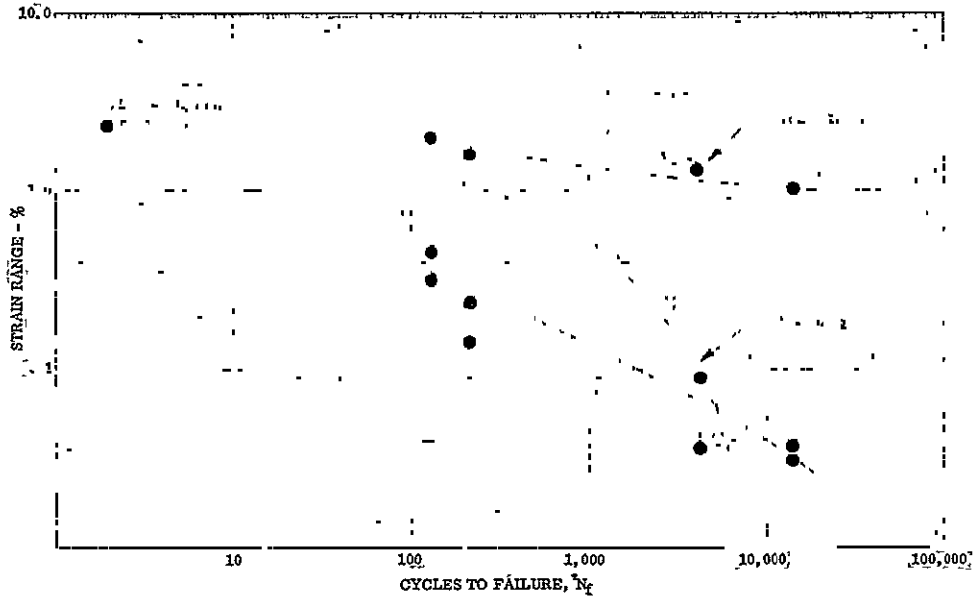


Figure IV-19. Low Cycle Fatigue Life of AMS 4926 (A-110) at 200°F DF 86846

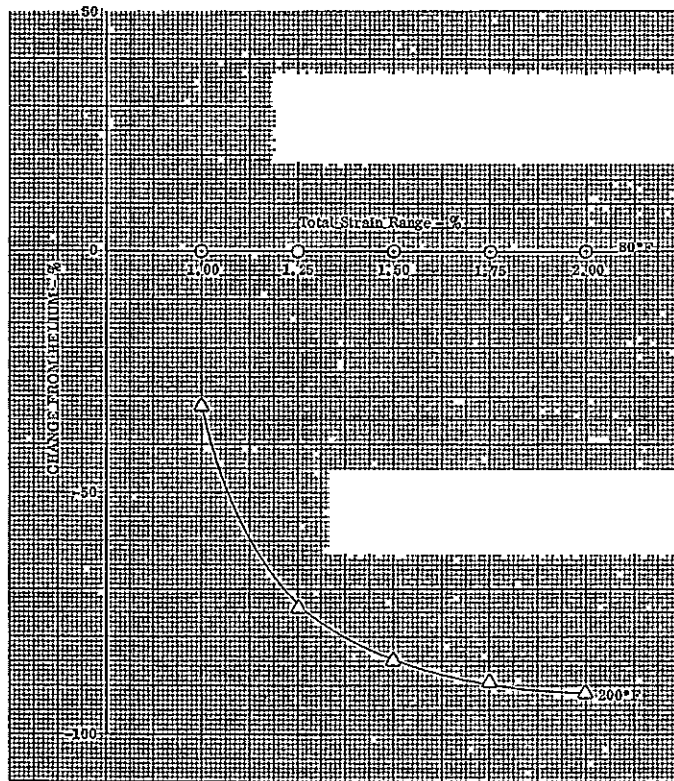


Figure IV-20. Effect of Gaseous Hydrogen and Strain Range on Low Cycle Fatigue Life of AMS 4926 (A-110) DF 86847



6. A-286

The A-286 (AMS 5735) iron-base material was not degraded at room temperature (80°F) and only slightly degraded (average of 9%) at 1250°F (figures IV-21 through IV-23). No definite trend is apparent in the degradation vs cyclic strain level plot at elevated temperature; however no degradation occurred at the maximum cyclic strain level tested (2.0%).

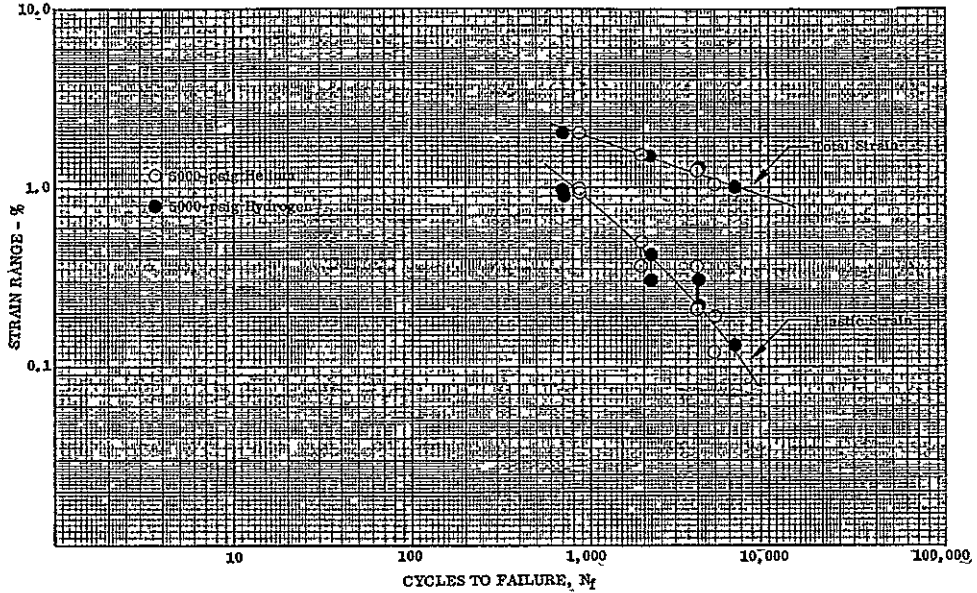


Figure IV-21. Low Cycle Fatigue Life of AMS 5735 DF 86848 (A-286) at 80°F

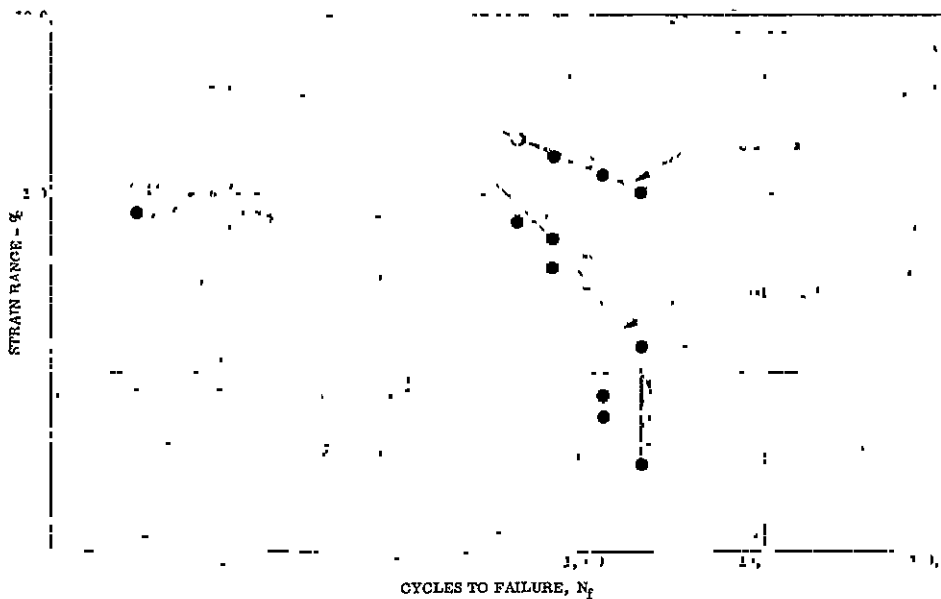


Figure IV-22. Low Cycle Fatigue Life of AMS 5735 DF 86849 (A-286) at 1250°F

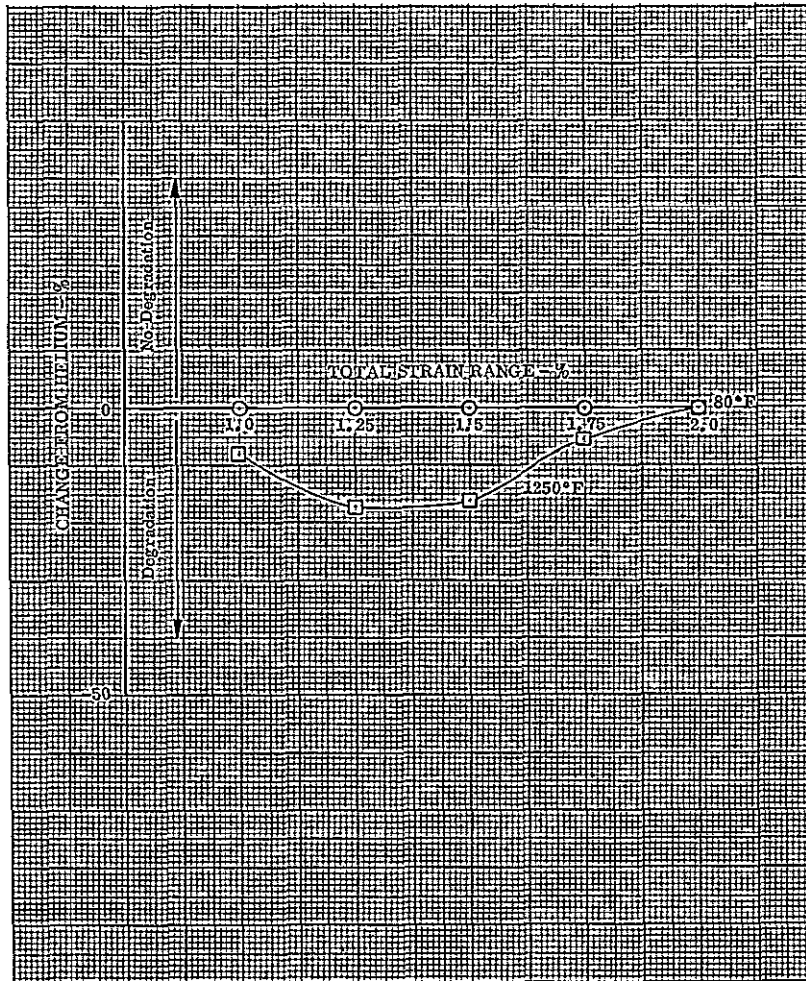


Figure IV-23. Effect of Gaseous Hydrogen and Strain Range on Low Cycle Fatigue Life of AMS 5735 (A-286) DF 86850

#### 7. AISI 347

AISI type 347 stainless steel (AMS 5646) was tested at 80°F only and was not degraded at that temperature (figure IV-24).

#### B. TEST PROCEDURES

Smooth, round, solid specimens were used for the strain-controlled LCF tests discussed in this report. The test specimen used is described in Section III and detailed by print FML 95500B (figure III-3). The specimen configuration, which incorporates integral machined extensometer collars, was arrived at experimentally through the use of photoelastic and elastic-plastic strain analyses. A calibration procedure is established for each material to relate the maximum strain to collar deflection during both the elastic and plastic portion of the strain cycle. The specimen design and calibration procedure

have also been verified analytically through the use of finite element analyses technique and also mathematical model analyses.

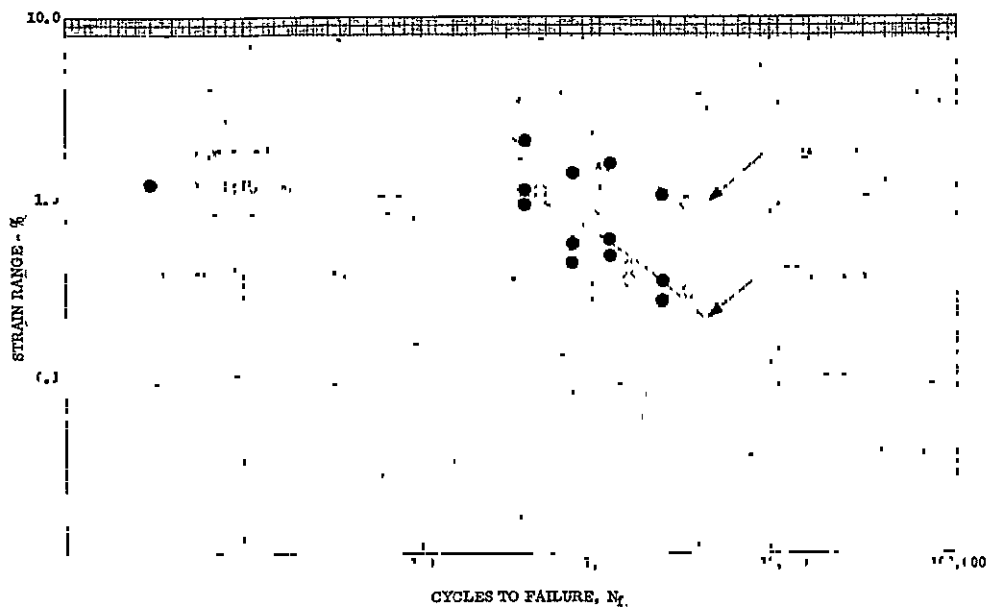
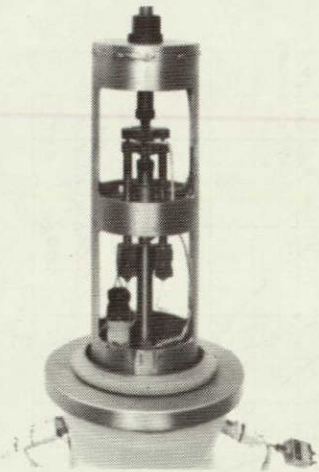


Figure IV-24. Low Cycle Fatigue Life of AMS 5646 DF 86851  
(AISI 347) at 80°F

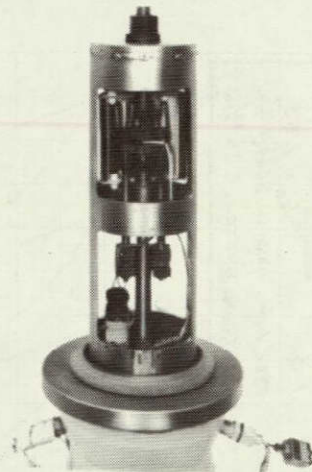
After machining, specimen material was verified by either eddy current (Dermatron) or spectrographic techniques. Gage sections were then polished and dimensions measured. Prior to installation in the test rig, specimens were thoroughly cleaned with a nonchlorinated solvent.

Tests were conducted on a P&WA designed and built, closed loop type, hydraulically actuated test machine, located in an isolated test cell, utilizing the constant strain control mode. Specimen axial strain is measured and controlled by means of a proximity probe extensometer. A heavy walled pressure vessel made of AISI type 347 stainless steel was mounted on the upper platen of the test machine. This vessel (shown in figure IV-25) incorporates a Gray Loc type flange and seal because of the relative ease of assembly and the reliability of the seal in high pressure. The base of the vessel includes a pressure compensating device to eliminate the axial tensile load acting over the differential specimen and adapter areas. Both internal (to the pressure vessel) and external load cells are used, thus the effect of friction at the seals where the load rods enter the vessel is known and accounted for. During testing, load strain hysteresis curves, similar to figure IV-26, are plotted using the extensometer and internal load cell outputs. Electrical connections to the load cell, extensometer system, furnace (for elevated temperature tests only) and thermocouples are made through the vessel wall via high-pressure bulkhead connectors. Cryogenic temperatures are obtained by surrounding the test chamber with a liquid nitrogen bath. The test gas passes through a heat exchanger coil submerged in the liquid nitrogen bath and into the test chamber. Thermocouples attached to the specimen are used to monitor temperature during test.



FE 100028

Specimen and Extensometer in Place



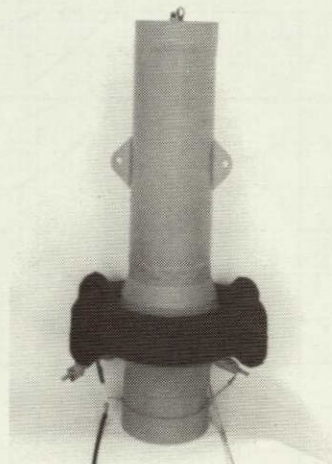
FE 100027

Specimen, Extensometer and Half  
Furnace in Place



FE 100026

Specimen, Extensometer and Furnace in  
Place



FE 100025

Closed Pressure Vessel, Cooling Jacket  
Not Shown

Figure IV-25. High Pressure Gaseous Environment, FD 53147  
Low Cycle Fatigue Test Vessel



MATL	AMS 5646	SHT.	1 OF 1
	(347)		
SER. NO.	508	DATE	3-11-71
HEAT OR CODE	BZCT	TEMP. F	80
$\Delta T$	1.3	CYCLIC OR SIGNAL	4 CYCLES/MIN
AREA	.0352 IN <sup>2</sup>	$\epsilon/\sigma =$	1.35
	5000 PSIG - HYDROGEN	STRAIN CAL	3500 $\mu\text{IN}/\text{IN}$
		LOAD CAL	920 $\text{Lb}/\text{IN}$

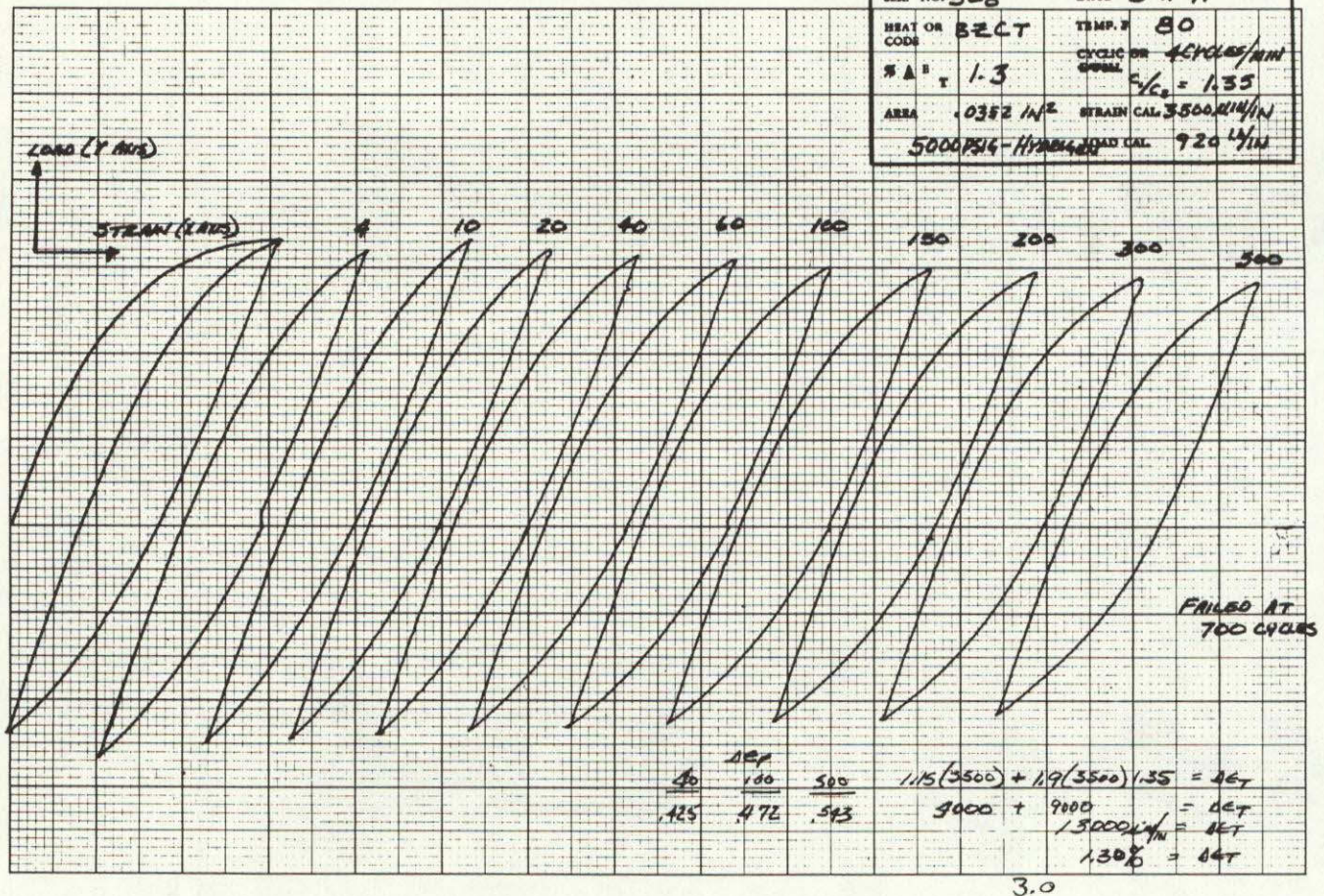


Figure IV-26. Typical Load-Strain Hysteresis Curves for a High Pressure Gaseous Environment Low Cycle Fatigue Test (AMS 5646, 1.3% Total Strain Range, 80° F, 5000-psig Hydrogen)

FD 53148

Table IV-2. Room Temperature Low Cycle Fatigue Properties of Materials in High Pressure Gaseous Environment

Material	Test Conditions				Test Results		
	Test Temperature °F	Environment	Pressure, psig	Total Strain Range, %	Cyclic Rate, Cycles/Minute	Cycles to Failure	Plastic Strain Range, % *
AMS 5662 (INCO 718) 1750°F Sol.	80	Helium	5000	1.0	4	15,000	0.02
	80	Helium	5000	0.8	5	13,650	0.03 - 0.05
	80	Helium	5000	1.5	3	1,500	0.13 - 0.20
	80	Helium	5000	2.0	3	1,220	0.35 - 0.54
	80	Hydrogen	5000	1.0	4	6,310	0.07 - 0.08
	80	Hydrogen	5000	1.0	4	6,080	0.05 - 0.08
	80	Hydrogen	5000	1.5	3	450	0.12 - 0.19
	80	Hydrogen	5000	2.0	3	55	0.41 - 0.46
	80	Hydrogen	5000	0.8	5	9,950	0.02 - 0.04
AMS 5662 (INCO 718) 1900°F Sol.	80	Helium	5000	1.0	4	21,500	0.02 - 0.05
	80	Helium	5000	1.25	4	5,450	0.13 - 0.16
	80	Helium	5000	1.5	3	2,360	0.11 - 0.18
	80	Helium	5000	2.1	3	900	0.60 - 0.70
	80	Hydrogen	5000	1.0	4	2,220	0.03
	80	Hydrogen	5000	1.3	4	760	0.04 - 0.09
	80	Hydrogen	5000	1.5	3	460	0.18 - 0.22
	80	Hydrogen	5000	2.0	3	300	0.33 - 0.49
AMS 5666 (INCO 625)	80	Helium	5000	0.8	5	15,200	0.06
	80	Helium	5000	1.4	4	4,160	0.36 - 0.42
	80	Helium	5000	1.75	3	3,200	0.46
	80	Helium	5000	2.0	3	2,730	0.62 - 0.72
	80	Hydrogen	5000	1.0	4	1,890	0.06 - 0.09
	80	Hydrogen	5000	1.25	4	970	0.14 - 0.16
	80	Hydrogen	5000	1.5	3	360	0.39 - 0.46
	80	Hydrogen	5000	2.0	3	340	0.58 - 0.62

IV-20

Table IV-2. Room Temperature Low Cycle Fatigue Properties of Materials in High Pressure Gaseous Environment (Continued)

Material	Test Conditions			Test Results			
	Test Temperature, °F	Environment	Pressure, psig	Total Strain Range, %	Cyclic Rate, Cycles/Minute	Cycles to Failure	Plastic Strain Range, % *
AMS 5735 (A-286)	80	Helium	5000	1.0	4	4,930	0.12 - 0.19
	80	Helium	5000	1.25	4	4,012	0.20 - 0.37
	80	Helium	5000	1.5	3	1,950	0.36 - 0.50
	80	Helium	5000	2.0	3	870	0.93 - 0.98
	80	Hydrogen	5000	1.0	4	6,550	0.12
	80	Hydrogen	5000	1.3	4	4,030	0.22 - 0.31
	80	Hydrogen	5000	1.5	3	2,200	0.30 - 0.42
	80	Hydrogen	5000	2.0	3	700	0.90 - 0.95
AMS 5646 (AISI 347)	80	Helium	5000	0.9	4	3,100	0.25 - 0.29
	80	Helium	5000	1.25	4	1,450	0.33 - 0.39
	80	Helium	5000	1.5	3	905	0.60 - 0.77
	80	Helium	5000	1.7	3	460	0.96 - 1.05
	80	Hydrogen	5000	1.0	4	2,200	0.26 - 0.33
	80	Hydrogen	5000	1.5	3	1,120	0.47 - 0.58
	80	Hydrogen	5000	1.3	4	700	0.42 - 0.54
	80	Hydrogen	5000	2.0	3	380	0.90 - 1.10
AMS 5754 (Hastelloy X)	80	Helium	5000	1.5	3	3,500	0.73 - 0.79
	80	Helium	5000	1.4	4	3,300	0.58 - 0.66
	80	Helium	5000	1.85	3	1,720	1.02 - 1.08
	80	Helium	5000	2.0	3	200	0.91 - 1.08
	80	Hydrogen	5000	1.0	4	3,050	0.44 - 0.46
	80	Hydrogen	5000	1.25	4	1,964	0.61 - 0.62
	80	Hydrogen	5000	1.5	3	810	0.79 - 0.82
	80	Hydrogen	5000	2.0	3	405	0.82 - 0.92

IV-21

Table IV-2. Room Temperature Low Cycle Fatigue Properties of Materials in High Pressure Gaseous Environment (Continued)

Material	Test Conditions			Test Results			
	Test Temperature, °F	Environment	Pressure, psig	Total Strain Range, %	Cyclic Rate, Cycles/Minute	Cycles to Failure	Plastic Strain Range, % *
AMS 4928 (Ti 6-4)	80	Helium	5000	1.6	3	2,370	0.05 - 0.10
	80	Helium	5000	1.9	3	950	0.21 - 0.26
	80	Helium	5000	2.25	3	360	0.28 - 0.37
	80	Hydrogen	5000	1.4	4	4,850	0.09 - 0.10
	80	Hydrogen	5000	1.7	3	600	0.09 - 0.10
	80	Hydrogen	5000	1.7	3	2,940	0.04 - 0.05
	80	Hydrogen	5000	1.85	3	860	0.12 - 0.15
	80	Hydrogen	5000	1.2	4	5,130	0.035-0.04
AMS 4926 (A-110)	80	Helium	5000	1.8	3	1,600	0.14 - 0.19
	80	Helium	5000	1.6	3	1,620	0.18
	80	Helium	5000	1.5	3	2,000	0.13 - 0.18
	80	Helium	5000	1.0	4	9,050	0.015-0.04
	80	Hydrogen	5000	1.4	4	610	0.06 - 0.13
	80	Hydrogen	5000	1.85	3	500	0.20 - 0.31
	80	Hydrogen	5000	1.8	3	1,020	0.16 - 0.27
	80	Hydrogen	5000	1.0	4	17,500	0.02 - 0.04

\* Range includes strain hardening - softening effects.



Table IV-3. Cryogenic Temperature Low Cycle Fatigue Properties of Materials in High Pressure Gaseous Environment

Material	<u>Test Conditions</u>			<u>Test Results</u>			
	Test Temperature, °F	Environment	Pressure, psig	Total Strain Range, %	Cyclic Rate, Cycles/Minute	Cycles to Failure	Plastic Strain Range, % *
AMS 5662 (INCO 718) 1900°F Sol.	-260	Helium	5000	1.5	3	5,140	0.06 - 0.14
	-260	Helium	5000	2.0	3	1,630	0.41 - 0.61
	-260	Helium	5000	2.0	3	2,080	0.45 - 0.52
	-260	Helium	5000	2.5	3	1,300	0.51 - 0.89
	-260	Hydrogen	5000	1.5	3	22,300	0.04 - 0.07
	-260	Hydrogen	5000	2.0	3	3,460	0.21 - 0.31
	-260	Hydrogen	5000	2.0	3	3,580	0.15 - 0.32
	-260	Hydrogen	5000	2.25	3	1,850	0.44 - 0.72

\* Range includes strain hardening - softening effects.

Table IV-4. Elevated Temperature Low Cycle Fatigue Properties of Materials in High Pressure Gaseous Environment

Material	Test Conditions			Test Results			
	Test Temperature, °F	Environment	Pressure, psig	Total Strain Range, %	Cyclic Rate, Cycles/Minute	Cycles to Failure	Plastic Strain Range, % *
AMS 5662 (INCO 718) 1750 °F	1250	Helium	5000	2.0	3	145	0.59 - 0.72
	1250	Helium	5000	1.45	4	570	0.15 - 0.28
	1250	Helium	5000	1.25	4	940	0.04 - 0.16
	1250	Helium	5000	1.0	4	1,820	0.026-0.10
	1250	Hydrogen	5000	1.75	3	175	0.45 - 0.59
	1250	Hydrogen	5000	1.50	3	330	0.21 - 0.39
	1250	Hydrogen	5000	1.25	4	815	0.05 - 0.18
	1250	Hydrogen	5000	1.0	4	1,810	0.05
AMS 5662 (INCO 718) 1900 °F Sol.	1250	Helium	5000	2.0	3	260	0.64 - 0.85
	1250	Helium	5000	1.6	3	510	0.43 - 0.52
	1250	Helium	5000	1.35	4	950	0.15 - 0.28
	1250	Helium	5000	1.0	4	1,730	0.11 - 0.22
	1250	Hydrogen	5000	1.75	3	320	0.50 - 0.67
	1250	Hydrogen	5000	1.6	3	285	0.33 - 0.48
	1250	Hydrogen	5000	1.3	4	685	0.22 - 0.39
	1250	Hydrogen	5000	1.0	4	1,350	0.10 - 0.17
AMS 5735 (A-286)	1250	Helium	5000	2.0	3	405	0.82 - 0.89
	1250	Helium	5000	1.5	3	1,000	0.31 - 0.42
	1250	Helium	5000	1.25	4	1,600	0.08 - 0.14
	1250	Helium	5000	1.0	4	2,290	0.05 - 0.15
	1250	Hydrogen	5000	2.0	3	410	0.70 - 0.89
	1250	Hydrogen	5000	1.6	3	650	0.39 - 0.57
	1250	Hydrogen	5000	1.25	4	1,260	0.057-0.063
	1250	Hydrogen	5000	1.0	4	2,050	0.03 - 0.14

IV-24

Table IV-4. Elevated Temperature Low Cycle Fatigue Properties of Materials in High Pressure Gaseous Environment (Continued)

Material	Test Conditions			Test Results			
	Test Temperature, °F	Environment	Pressure, psig	Total Strain Range, %	Cyclic Rate, Cycles/Minute	Cycles to Failure	Plastic Strain Range, % *
AMS 4928 (Ti 6-4)	200	Helium	5000	1.25	4	11,270	0.033 - 0.047
	200	Helium	5000	1.6	3	2,130	0.03 - 0.08
	200	Helium	5000	1.8	3	1,650	0.14 - 0.19
	200	Helium	5000	2.15	3	1,050	0.45 - 0.56
	200	Hydrogen	5000	1.25	4	5,880	0.02 - 0.04
	200	Hydrogen	5000	1.5	3	3,020	0.043
	200	Hydrogen	5000	1.9	3	1,050	0.17 - 0.25
	200	Hydrogen	5000	2.1	3	970	0.24 - 0.32
AMS 4926 (A-110)	200	Helium	5000	1.25	4	5,300	0.04 - 0.07
	200	Helium	5000	1.6	3	2,900	0.23 - 0.26
	200	Helium	5000	1.9	3	1,620	0.26 - 0.42
	200	Helium	5000	2.05	3	1,400	0.32 - 0.46
	200	Hydrogen	5000	1.0	4	14,200	0.03 - 0.036
	200	Hydrogen	5000	1.3	4	4,100	0.035 - 0.09
	200	Hydrogen	5000	1.6	3	215	0.14 - 0.24
	200	Hydrogen	5000	2.0	3	130	0.32 - 0.45

\* Range includes strain hardening - softening effects.

IV-25/IV-26

## SECTION V HIGH CYCLE FATIGUE

### A. INTRODUCTION

Tests were accomplished on nickel, iron, and titanium base alloys (INCO 718, AISI 347, and A-110, respectively) to evaluate the high cycle fatigue (HCF) behavior of these materials when subjected to high pressure gaseous helium and hydrogen atmospheres at ambient and elevated temperatures, and to establish the susceptibility of these alloys to hydrogen degradation.

High Cycle Fatigue (HCF) tests were conducted in 5000-psig gaseous helium and hydrogen at 80°F for all materials investigated and at 1250°F for the nickel base alloy, INCO 718. Results of the tests in helium provided a baseline for comparison with the hydrogen tests.

### B. CONCLUSIONS AND DISCUSSION

Tests of the AMS 5662 (INCO 718) alloy with 1750°F and 1900°F solution plus age heat treatments at both 80°F and 1250°F in 5000-psig hydrogen indicated appreciable HCF life degradation for both heat treatments. Conclusions as to the degree of HCF degradation of this alloy by gaseous hydrogen are restricted due to data scatter inherent in this type of test, and because of the limited number of tests. Additional testing of a sufficient number of samples for a statistical analysis is required before definite conclusions as to the degree of hydrogen degradation can be made. The HCF life of the iron base alloy, AMS 5646 (AISI 347), and the titanium base alloy, AMS 4926 (A-110), which were tested at 80°F only, was not appreciably affected by 5000-psig hydrogen.

High cycle fatigue test results are presented graphically in figures V-1 through V-6.

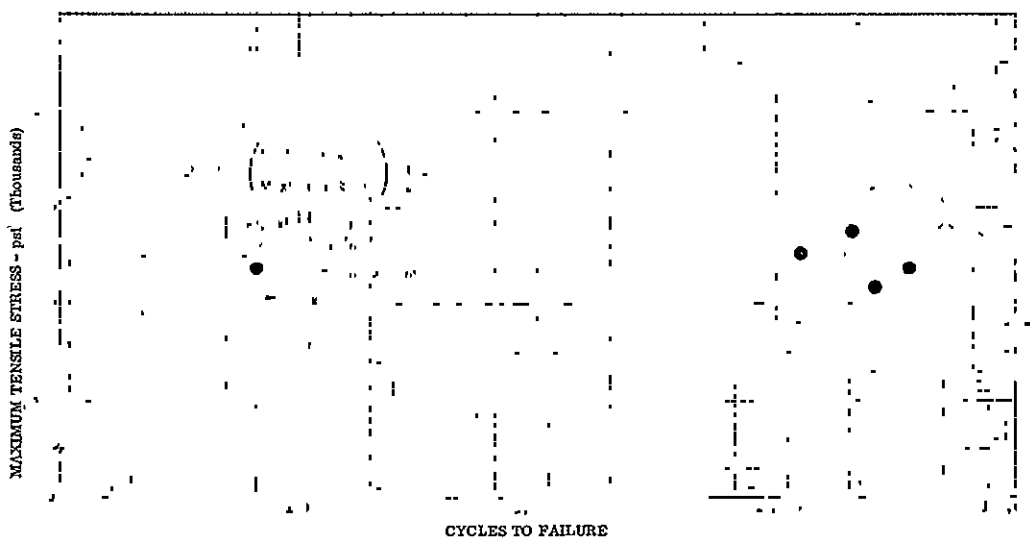


Figure V-1. Life of AMS 5662 at 80°F (INCO 718,  
1750°F Solution Plus Age)

DF 86852

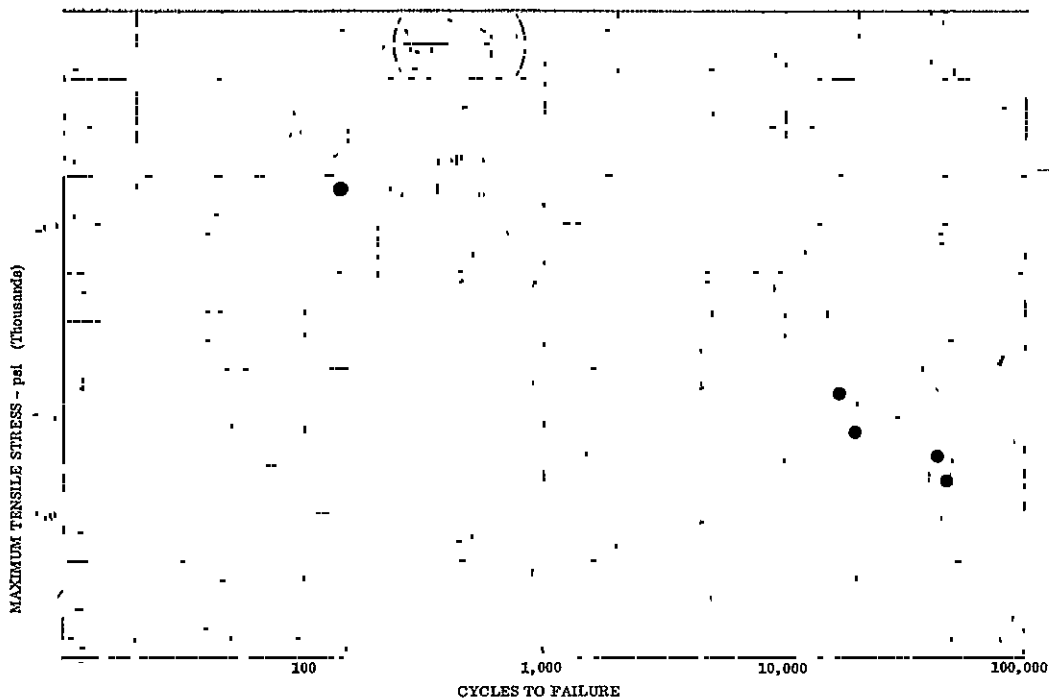


Figure V-2. High Cycle Fatigue Life of AMS 5662      DF 86853  
at 80 °F (INCO 718, 1900 °F Solution  
Plus Age)

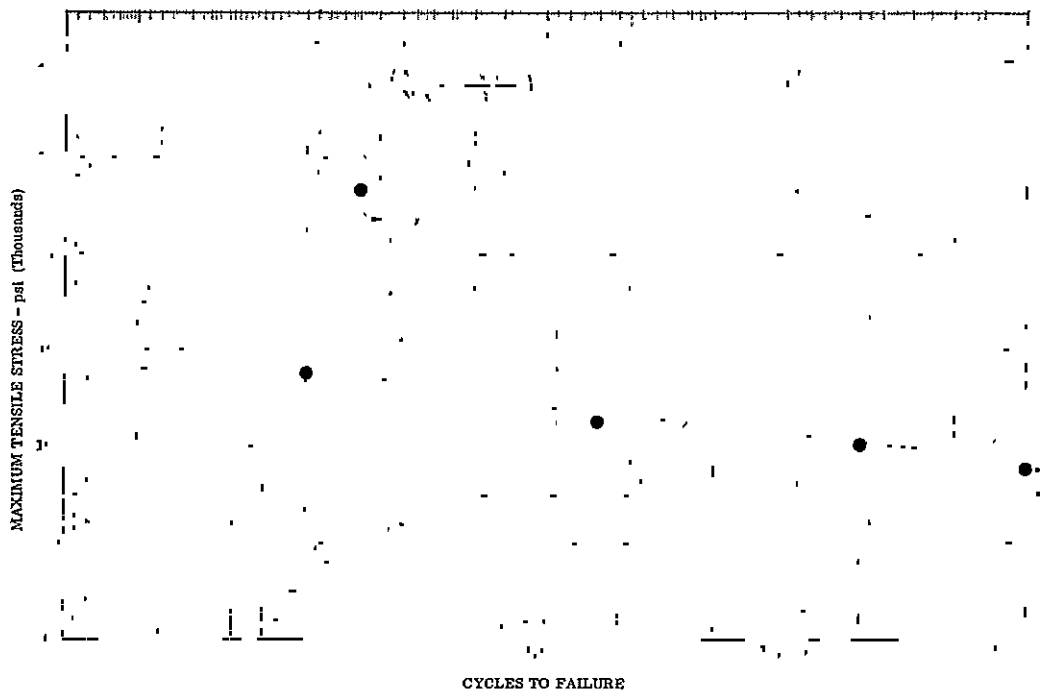


Figure V-3. High Cycle Fatigue Life of AMS 5646      DF 86854  
(AISI 347) at 80 °F

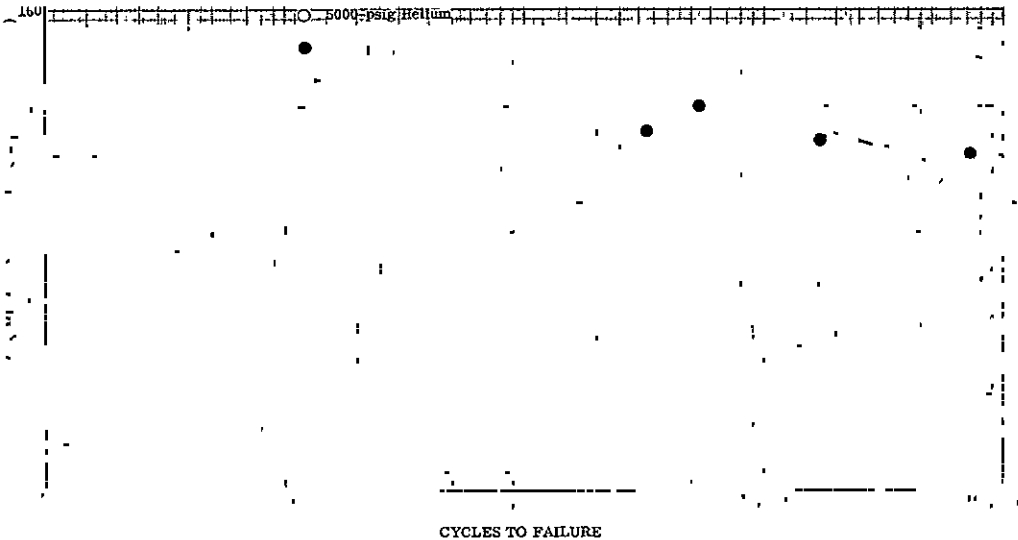


Figure V-4. High Cycle Fatigue Life of AMS 4926 (A-110) at 80 °F DF 86855

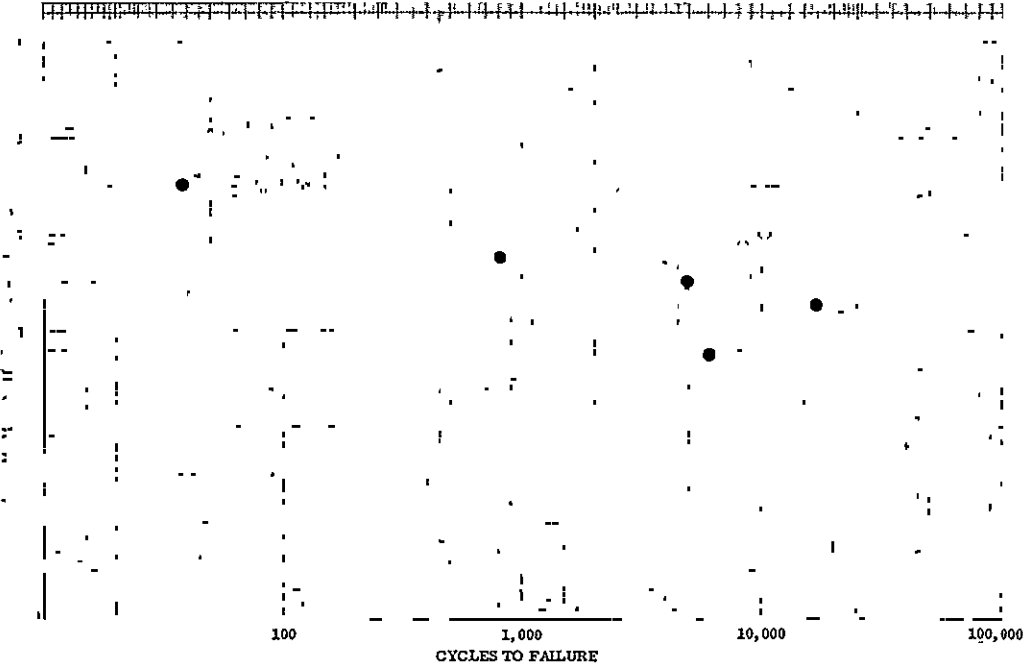


Figure V-5. High Cycle Fatigue Life of AMS 5662 (INCO 718) 1750 °F Solution at 1250 °F DF 86856

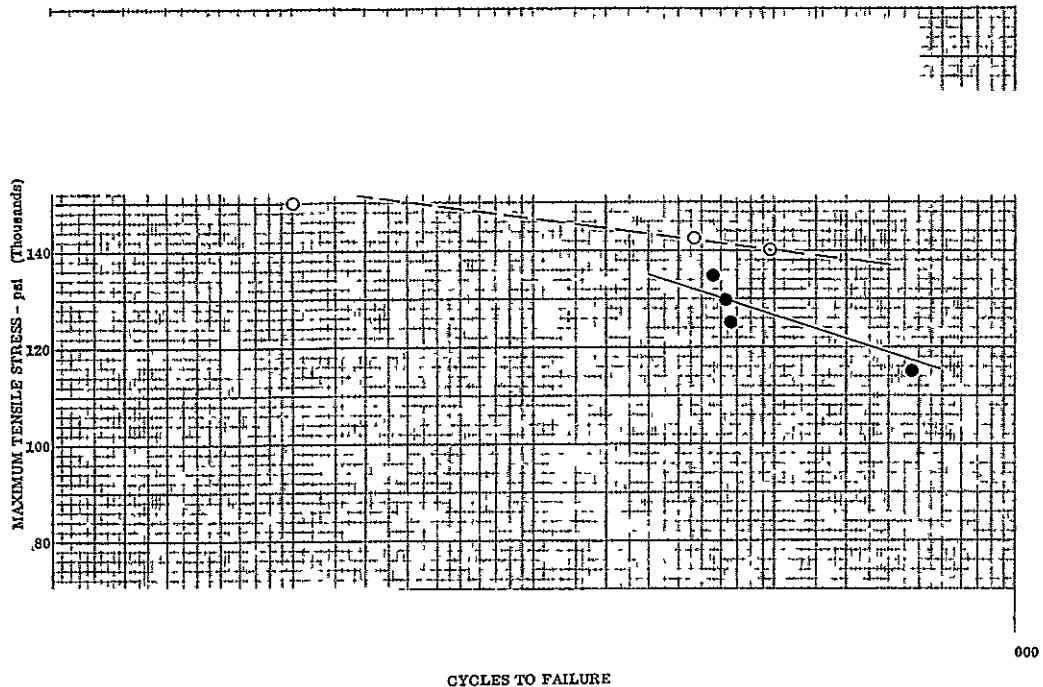


Figure V-6. High Cycle Fatigue Life of AMS 5662  
(INCO 718) 1900 °F Solution at 1250 °F

DF 86857

### C. TEST PROCEDURE

Smooth, round specimens were used for the high cycle fatigue tests discussed in this report. The test specimen used is illustrated in Section III and detailed by print FML 95212B, also included in that section.

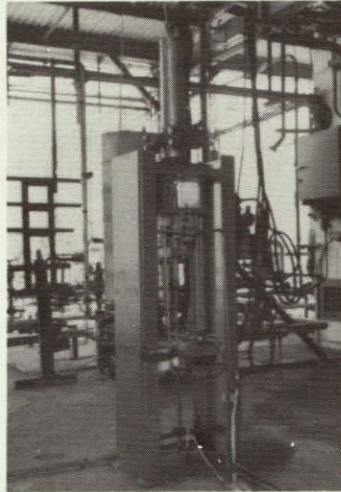
After machining, specimen material was verified, each specimen was inspected visually for any machining discrepancies, the minimum cross section was measured with a micrometer, and the specimen cleaned with acetone.

The HCF life data were established by a load (stress) controlled tension-tension test. A typical test cycle is a tensile load that varies sinusoidally about a constant tensile preload at a cyclic rate of 20 Hz. All specimens were tested at an R ratio (minimum stress/maximum stress) of 0.1.

Tests were conducted using a Pratt & Whitney Aircraft designed and fabricated closed-loop, servo-controlled, hydraulically actuated test machine located in an isolated test cell, figure V-7 (top). A heavy walled pressure vessel made of AISI 321 stainless steel was mounted on the upper platen of the test machine. The pressure vessel, shown in figure V-7 (bottom) is similar to those used for other testing under this contract.

Specimen load was measured and controlled by a strain gage load cell, integral with the specimen loading rod and inside the pressure vessel. Prior to the initial test and periodically throughout the test program, the load cell was calibrated (using an instrumented and calibrated specimen) at 5000-psig pressure so that axial tensile load on the specimen due to high pressure acting over differential specimen and loading rod areas could be eliminated. As the

load cell was internal and was calibrated to give true specimen load, friction loss through the loading rod O-ring seals is of no consequence. Electrical connections to all internal strain gages, load cell, thermocouples and heating devices were made through the bottom of the pressure vessel via an instrumentation manifold and high pressure bulkhead connectors. During testing, the load cycle and number of cycles to failure were constantly monitored on a calibrated oscilloscope and electronic counter using the internal load cell output.



FC 23389

Test Machine Located in Isolated Test Cell



Test Vessel Open



Test Vessel Closed

Figure V-7. High Pressure Gaseous Environment  
High Cycle Fatigue Testing Equipment

FD 53128



Elevated temperature testing (1250°F) was accomplished using a dc power supply and a high power density, single zone furnace mounted inside the pressure vessel. Analysis of gas samples, before and after the specimen tests, indicated no oxygen contamination of the test media due to the heating device. Thermocouples attached to the specimen were used to monitor and control the specimen temperature during testing.

Test system shutdown was provided at the instant of specimen failure by a linear variable differential transformer (LVDT), which sensed load rod position, in combination with a meter relay. This proved an accurate means of determining the total number of test cycles to failure.

Test specimens were mounted in the pressure vessel load frame by threading the ends into tapped loading rods (top and bottom) and securing each end with lock-nuts. The specimen and the sealed pressure vessel were subjected to a purge cycle consisting of evacuation, nitrogen purge, two successive "pop" purges with the test media (helium or hydrogen), and final pressurization to test pressure (5000 psig).

#### D. RESULTS

Maximum stress level and cycles to failure data were obtained for each material and are listed in table V-1 for 80°F and table V-2 for 1250°F tests. These data were plotted graphically (figures V-1 through V-6) to obtain stress vs cycles to failure (S-N) curves for each material. The difference in the HCF curves for the helium and hydrogen tests represents the degradation of high cycle fatigue life caused by a high pressure hydrogen atmosphere.

Table V-1. Room Temperature High Cycle Fatigue Properties of Materials  
 In High Pressure Gaseous Environment (Continued)

Material	Test Temperature, °F	Environment	Test Conditions		Cyclic Rate, cycles/sec	Cycles to Failure
			Pressure, psig	Stress Level* Maximum, ksi Minimum, ksi		
AMS 5646 (AISI 347)	80	Helium	5000	90.0 9.0	20	100,000 + (Runout)
	80	Helium	5000	100.0 10.0	20	70,800
	80	Helium	5000	105.0 10.5	20	3,640
	80	Helium	5000	110.0 11.0	20	700
	80	Hydrogen	5000	95.0 9.5	20	100,000 + (Runout)
	80	Hydrogen	5000	100.0 10.0	20	20,600
	80	Hydrogen	5000	105.0 10.5	20	1,620
	80	Hydrogen	5000	115.0 11.5	20	100
AMS 4926 (A-110)	80	Helium	5000	120.0 12.0	20	196,600 (Runout)
	80	Helium	5000	125.0 12.5	20	51,900
	80	Helium	5000	130.0 13.0	20	46,900
	80	Helium	5000	135.0 13.5	20	17,500
	80	Hydrogen	5000	130.0 13.0	20	73,600
	80	Hydrogen	5000	132.5 13.25	20	17,200
	80	Hydrogen	5000	135.0 13.5	20	3,200
	80	Hydrogen	5000	140.0 14.0	20	5,300

\*Stress levels for R ratio  $\left( \frac{\text{Minimum Stress}}{\text{Maximum Stress}} \right) = 0.1.$

Table V-2. Elevated Temperature High Cycle Fatigue Properties of Materials in High Pressure Gaseous Environment

01-A/6-A

Material	Test Temperature, °F	Environment	Pressure, psig	Stress Level*		Cyclic Rate, cycles/sec	Cycles to Failure
				Maximum, ksi	Minimum, ksi		
AMS 5662 (INCO 718) 1750°F Solution	1250	Helium	5000	140.0	14.0	20	10,200
	1250	Helium	5000	145.0	14.5	20	13,400
	1250	Helium	5000	150.0	15.0	20	2,400
	1250	Helium	5000	137.5	13.75	20	8,400
	1250	Hydrogen	5000	115.0	11.5	20	6,100
	1250	Hydrogen	5000	125.0	12.5	20	16,800
	1250	Hydrogen	5000	130.0	13.0	20	4,900
	1250	Hydrogen	5000	135.0	13.5	20	800
AMS 5662 (INCO 718) 1900°F Solution	1250	Helium	5000	140.0	14.0	20	9,600
	1250	Helium	5000	142.5	14.25	20	4,530
	1250	Helium	5000	150.0	15.0	20	100
	1250	Helium	5000	160.0	16.0	20	20
	1250	Hydrogen	5000	115.0	11.5	20	37,200
	1250	Hydrogen	5000	125.0	12.5	20	6,500
	1250	Hydrogen	5000	135.0	13.5	20	5,560
	1250	Hydrogen	5000	130.0	13.0	20	6,200

\*Stress levels for R ratio  $\left( \frac{\text{Minimum Stress}}{\text{Maximum Stress}} \right) = 0.1.$

## SECTION VI FRACTURE TOUGHNESS

### A. INTRODUCTION

Fracture toughness tests were conducted in 5000 psig gaseous hydrogen at a temperature of approximately 80°F. For comparison, and to determine the degree of susceptibility to hydrogen degradation and/or embrittlement, similar tests were also conducted in 5000-psig helium. The materials tested (Section III) were AMS 5662 (INCO 718), AMS 5666 (INCO 625), AMS 5735 (A-286), AMS 5646 (AISI 347), AMS 4928 (Ti 6-4), and AMS 4926 (Ti A-110).

### B. CONCLUSIONS AND DISCUSSION

The following conclusions were made from the results of this fracture toughness testing program and the metallographic investigations:

1. There was no severe hydrogen degradation in any of the materials tested. Only a slight sensitivity was evident in AMS 5662 (INCO 718), as indicated by slightly lower fracture toughness values and by the somewhat smoother fracture face when compared to results in helium.
2. Although there was no evidence of hydrogen degradation in fracture toughness values in AMS 4928 (Ti 6-4), the metallographic examination revealed a slight sensitivity to hydrogen in this material.
3. From the metallographic examinations, it was concluded that the most severely hydrogen embrittled alloy was AMS 5666 (INCO 625). This was not consistent with the obtained fracture toughness values, as if anything, they showed a slight increase in hydrogen.
4. A comparison of welded to parent material revealed a general decrease in magnitude of the fracture toughness values, but no susceptibility to hydrogen degradation. GTA-welded AMS 5662 (INCO 718) 1900°F solution was less ductile than the parent material, as was evidenced by the appearance of the fracture face and the attained valid  $K_{IC}$  value. This was not the case with AMS 5666 (INCO 625) in that it remained very ductile and a valid  $K_{IC}$  was not attainable.
5. When comparing longitudinal to transverse fracture toughness values there was generally no difference, although there was a slight increase in magnitude in the transverse direction in both titanium materials tested.

Although the primary aim of this investigation was to determine the degree of susceptibility to high pressure hydrogen degradation, additional interpretation of the fracture toughness data is required for characterization of these alloys in terms of critical flaw size and stress level required for failure. Pelling, W. S.<sup>1</sup>, and R. W. Judy, Jr., R. J. Goode, and C. N. Freed<sup>2</sup> have used Ratio Analysis Diagrams (RAD) to reduce the complex problem of interpretation of fracture toughness data. These diagrams have compared  $K_{IC}$  with Dynamic Test (DT) and Charpy V-notch ( $C_V$ ) tests.

Correlation of engineering fracture toughness tests with  $K_{IC}$  provides the necessary information to express the fracture toughness, regardless of type of test, of materials in terms of critical flaw size and nominal stress level required for fracture. The equation:

$$\frac{K_{IC}}{\sigma} = \frac{1.1 \sqrt{\pi a}}{\sqrt{Q}}$$

where:

$K_{IC}$	=	Plane Strain Fracture Toughness, ksi $\sqrt{\text{in.}}$
$\sigma$	=	Nominal Stress (ksi)
$1.1/\sqrt{Q}$	=	Flaw Geometry Factor
$a$	=	Critical Crack Depth (in.)

defines the critical flaw-stress conditions for plane strain conditions.

The ratio  $K_{IC}/\sigma$  ys, termed "engineering ratio," is the basic parameter in the equations used for calculating flaw size. Generalizing various  $K_{IC}/\sigma$  ys ratios as follows:

Ratios between 1 and 1.5 - Nominal stresses in excess of yield are required for fracture propagation.

Ratios between 0.5 and 1.0 - High elastic nominal stresses and detectable flaws required for fracture propagation.

Ratios below 0.5 - Low elastic nominal stresses and flaws that may be too small for reliable detectability are required for fracture propagation.

---

<sup>1</sup>Pellini, W. S., "Advances in Fracture Toughness Characterization Procedures and in Quantitative Interpretations to Fracture-Safe Design for Structural Steels," Naval Research Laboratory, Washington, D. C., April 3, 1968.

<sup>2</sup>Judy, R. W., Jr. R. W. Goode, and C. N. Freed, "Fracture Toughness Characterization Procedures and Interpretations to Fracture-Safe Design for Structural Aluminum Alloys," Naval Research Laboratory, Washington, D. C., March 31, 1969.



These guidelines serve as a simple index for engineering assessment and/or comparing materials.

In figure VI-1, INCO 718 (1900 °F solution) GTA-welded, Ti 6-4 and Ti A-110 tested in both 5000-psig gaseous helium and hydrogen are generally below the 0.5 ratio. INCO 718 (1900 °F solution) has a higher ratio than INCO 718 with 1750 °F solution with the hydrogen data lower than helium in both cases. INCO 625 and A-286 fall between ratios of 0.5 and 1.0. AISI 347 and GTA-welded INCO 625 have ratios of 1.0 or better.

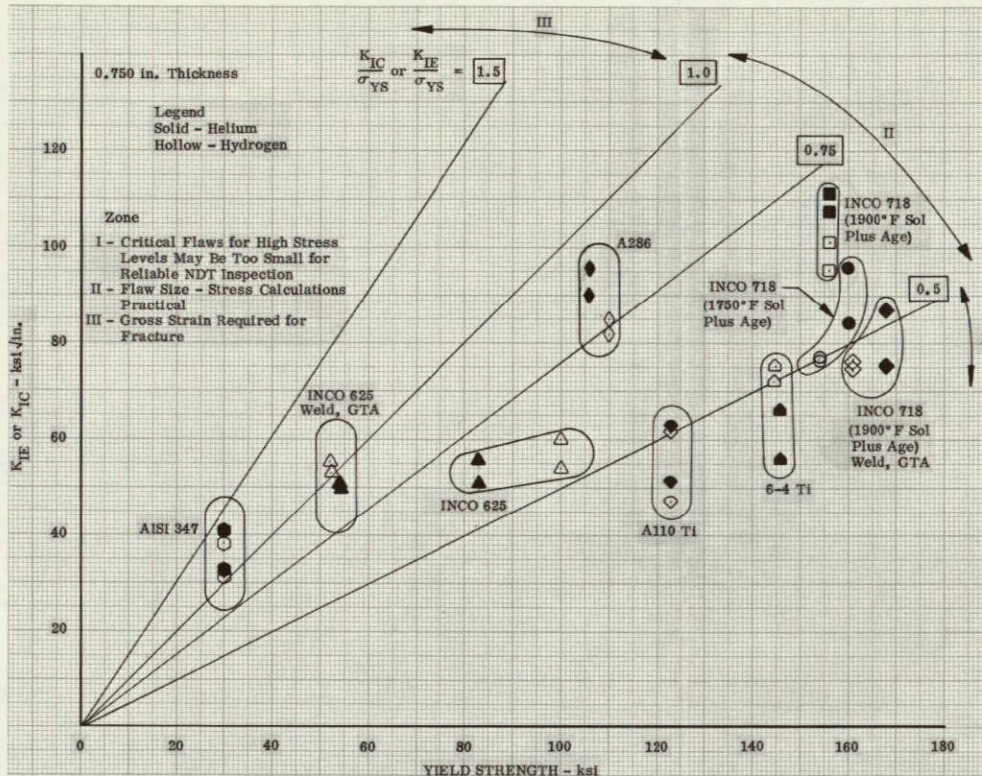


Figure VI-1. Engineering Ratio,  $K_{IC}/\sigma_{YS}$  or  $K_{IIE}/\sigma_{YS}$ , for Alloys Tested in High Pressure Gaseous Environments

DF 86788

### C. TEST PROCEDURE

Longitudinal and transverse specimen blanks were cut from bar stock, heat treated if required, and machined per ASTM specifications for compact tension specimens. (See Print FML 95559C.) The specimens were all 0.750-in. thick. This thickness was chosen to stay within the load limits of the existing high pressure tensile testing rig. All specimens were precracked in tension - tension using a Sonntag fatigue machine, which operates at 1800 cpm. All precracking was conducted in air at approximately 80 °F at load levels ( $K_f$ ), which later were verified not to exceed 60% of  $K_Q$ .



1. Equipment

Fracture toughness testing was conducted on a 30,000-lb Tinius Olsen testing machine, equipped with a Pratt & Whitney designed pressure vessel. This equipment is shown in figures VI-2 and VI-3. The pressure vessel is shown open in figure VI-4 with a standard compact tension specimen and clip gage in place. The vessel is made of AISI 347 stainless steel and incorporates a high pressure Gray-Loc connector. An internal load cell is used, thus the effects of friction on the load rod are not recorded on the readout equipment. To make the necessary gas analyses, a gas sampling system is incorporated in the test cell.

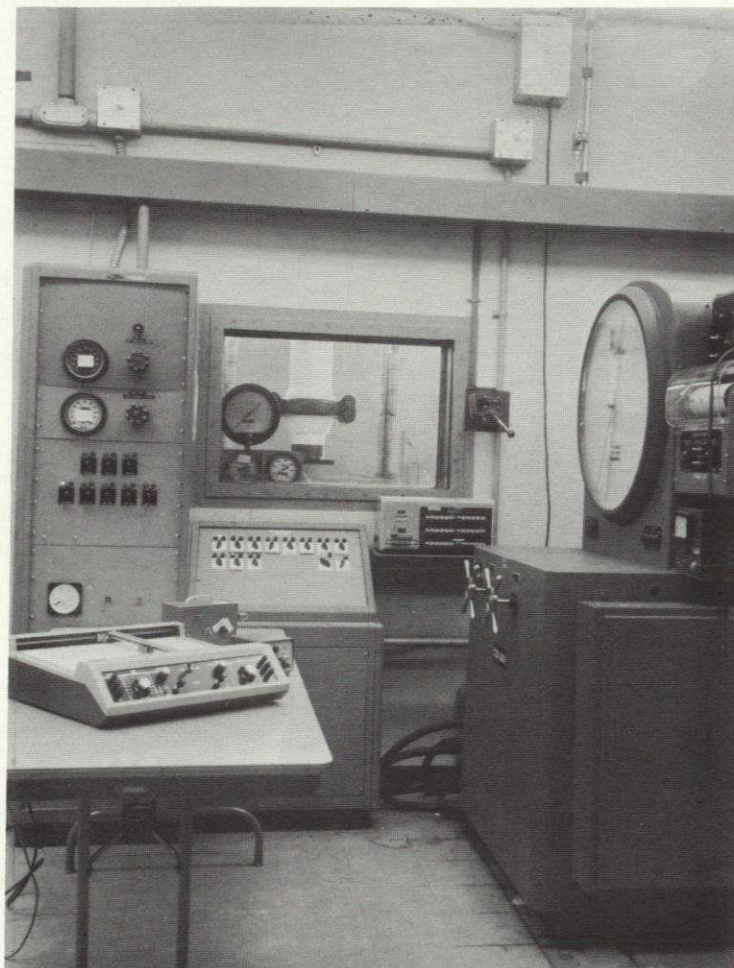


Figure VI-2. Tensile Machine, Test Environment  
Controls, and Data Acquisition Equipment  
Located in the Blockhouse

FC 21272



VI-5

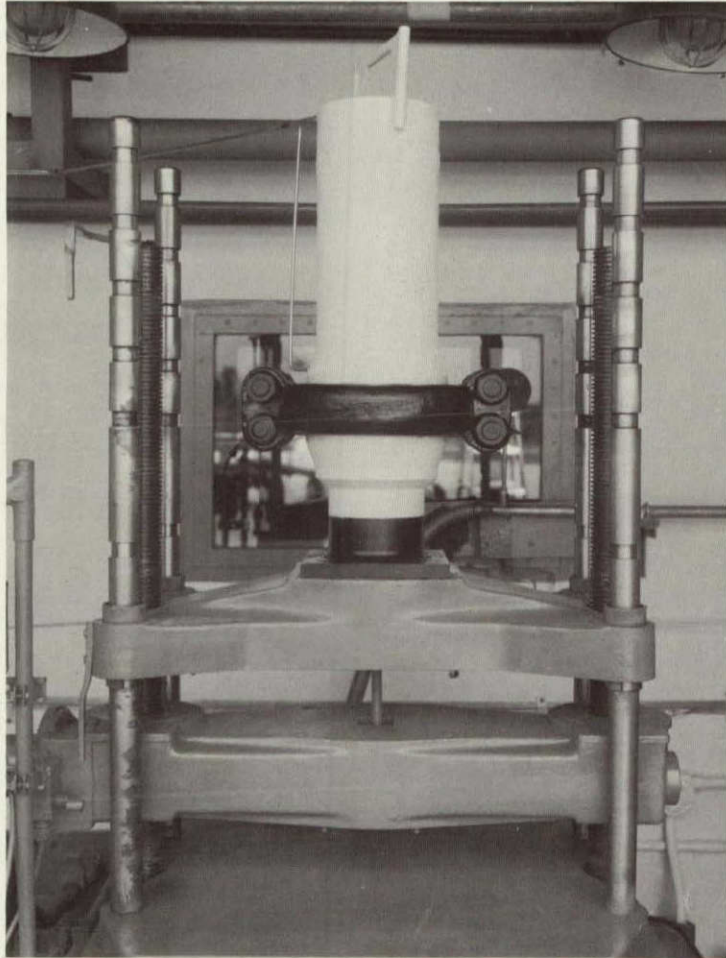


Figure VI-3. High Pressure Gaseous Environment Fracture Toughness Test Vessel Installed on Tensile Machine in the Test Cell

FC 21268

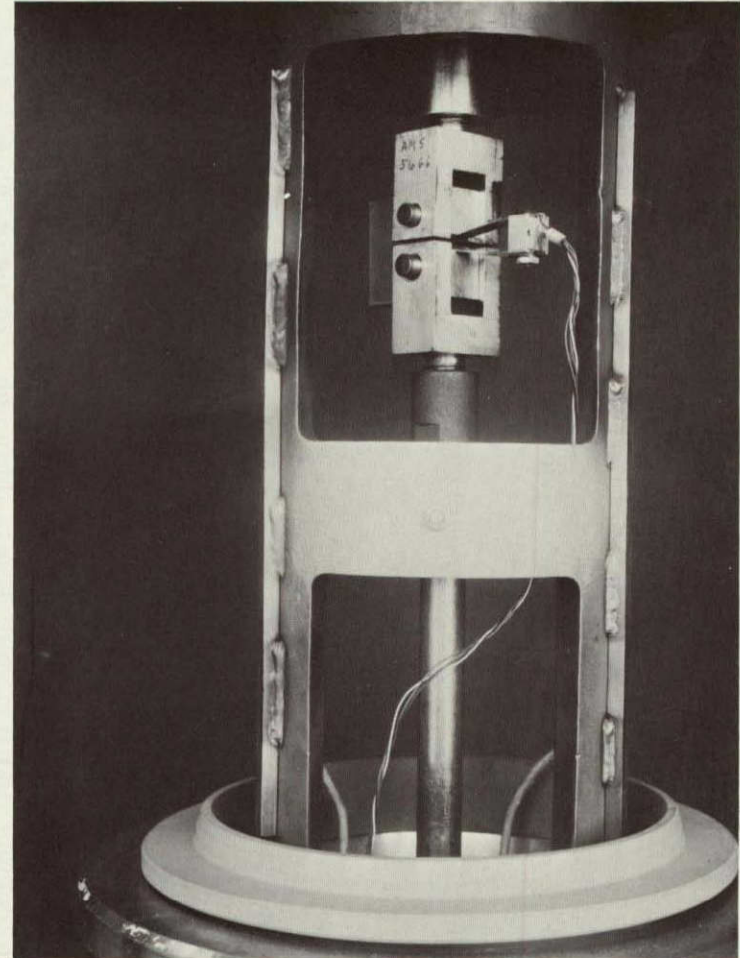


Figure VI-4. High Pressure Gaseous Environment Fracture Toughness Test Vessel With Outer Chamber Removed and Fracture Toughness Specimen With COD Gage Attached

FE 107942



## 2. Test Method

The following procedure is used during testing:

1. Specimen is precracked per tentative ASTM Designation E 399-70T for precracking compact tension specimens.
2. Chamber is opened, the prepared specimen installed, and the COD gage attached, as shown in figure VI-4.
3. Instrumentation continuity checks are conducted.
4. Chamber is closed, sealed, and evacuated.
5. Chamber is backfilled with nitrogen and purged.
6. Chamber is backfilled and "pop" purged twice in succession with the test gas.
7. Chamber is pressurized with test gas to 5000 psig.
8. Test is conducted. During the test, a load-displacement curve is plotted by an X-Y recorder from the output of a strain-gage-type internal load cell, and a crack opening displacement (COD) gage placed in the notch opening of the specimen.
9. After specimen failure, the chamber is vented and opened, and the failed specimen is removed.
10. Fracture toughness values are calculated from the load-displacement curve per tentative ASTM Designation E 399-70T for compact tension fracture toughness specimens.

## D. TEST RESULTS

The fracture toughness value is calculated from the load ( $P_Q$ ) established by a 5% deviation from the linear portion of the recorded load-displacement curve, the specimen thickness (B), width (W), and crack length (a) after fracture by the equation:

$$K_Q = \frac{P_Q}{BW^{1/2}} \left[ \begin{array}{l} 29.6 (a/W)^{1/2} - 185.5 (a/W)^{3/2} + 655.7 (a/W)^{5/2} \\ -1017.0 (a/W)^{7/2} + 638.9 (a/W)^{9/2} \end{array} \right]$$

$K_Q$  is a valid  $K_{IC}$  (plain strain fracture toughness) value if both the specimen thickness (B) and the crack length (a) exceed  $2.5 (K_{IC}/\sigma_{ys})^2$ , where  $\sigma_{ys}$  is the 0.2% offset yield strength of the material for the temperature of the test. In addition, there are requirements upon the precracking conditions and the shape of the fatigue precrack.

Table VI-1. Fracture Toughness of Materials in High Pressure Gaseous Environment

VI-8

Material	Test Conditions			Specimen Parameters			Test Results					
	Notch Orientation	Gaseous Environment	Load Rate $K_I/\text{min}$ (ksi $\sqrt{\text{in.}}/\text{min}$ )	Thickness "B" (in.)	Depth "W" (in.)	Crack Length (in.)	Fracture Appearance (% Oblique)	$2.5 \left( \frac{K_Q}{\sigma_{ys}} \right)^2$	Fracture Toughness (ksi $\sqrt{\text{in.}}$ )		Yield Strength (ksi)	$\frac{K_I}{\sigma_{ys}}$
									$K_{Ic}$	$K_{Ic}$		
AMS 5662 (INCO 718) 1750° F Sol	Long	Helium	80.0	0.750	1.501	0.852	3	0.686	--	84.0	160.4	0.52
	Trans	Helium	80.0	0.745	1.502	0.785	3	0.881	95.5 <sup>B</sup>	--	160.4	0.59
	Long	Hydrogen	80.0	0.751	1.500	0.855	3	0.613	--	76.2	154.1	0.49
	Trans	Hydrogen	80.0	0.740	1.496	0.848	3	0.620	--	76.7	154.1	0.50
AMS 5662 (INCO 718) 1900° F Sol	Long	Helium	80.0	0.747	1.501	0.865	4	1.270	111.5 <sup>B</sup>	--	156.4	0.71
	Trans	Helium	80.0	0.751	1.500	0.868	6	1.181	107.6 <sup>B</sup>	--	156.4	0.69
	Long	Hydrogen	80.0	0.750	1.500	0.852	5	1.029	101.0 <sup>AB</sup>	--	157.4	0.64
	Trans	Hydrogen	80.0	0.748	1.500	0.872	5	0.916	95.2 <sup>B</sup>	--	157.4	0.61
AMS 5662 (INCO 718) 1900° F Sol Welded	Long	Helium	80.0	0.752	1.503	0.852	3	0.660	--	86.8	168.9	0.51
	Trans	Helium	80.0	0.753	1.499	0.915	2	0.503	--	75.7	168.9	0.45
	Long	Hydrogen	80.0	0.748	1.498	0.868	2	0.550	--	76.0	161.7	0.47
	Trans	Hydrogen	80.0	0.751	1.503	0.885	3	0.531	--	74.6	161.7	0.46
AMS 5666 (INCO 625)	Long	Helium	80.0	0.751	1.509	0.855	15	0.954	51.8 <sup>B</sup>	--	83.9	0.61
	Trans	Helium	80.0	0.749	1.504	0.975	14	1.142	56.6 <sup>AB</sup>	--	83.9	0.68
	Long	Hydrogen	80.0	0.748	1.500	0.885	10	0.888	59.7 <sup>B</sup>	--	100.7	0.59
	Trans	Hydrogen	80.0	0.747	1.500	0.862	8	0.731	54.2 <sup>A</sup>	--	100.7	0.54
AMS 5666 (INCO 625) Welded	Long	Helium	80.0	0.750	1.502	0.912	16	2.260	51.0 <sup>B</sup>	--	53.6	0.95
	Trans	Helium	80.0	0.752	1.503	0.892	15	2.180	49.8 <sup>AB</sup>	--	53.6	0.92
	Long	Hydrogen	80.0	0.749	1.504	0.912	13	2.730	55.0 <sup>AB</sup>	--	52.7	1.04
	Trans	Hydrogen	80.0	0.751	1.504	0.958	12	2.560	53.4 <sup>AB</sup>	--	52.7	1.0
AMS 5735 (A-286)	Long	Helium	80.0	0.752	1.505	0.865	6	1.740	89.4 <sup>B</sup>	--	106.9	0.86
	Trans	Helium	80.0	0.749	1.498	0.888	5	2.000	95.6 <sup>B</sup>	--	106.9	0.90
	Long	Hydrogen	80.0	0.749	1.500	0.848	4	1.485	85.3 <sup>B</sup>	--	110.7	0.76
	Trans	Hydrogen	80.0	0.749	1.488	0.878	4	1.403	82.9 <sup>B</sup>	--	110.7	0.75
AMS 5646 (AISI 347)	Long	Helium	80.0	0.749	1.499	0.872	12	0.925	40.7 <sup>B</sup>	--	30.0	1.36
	Trans	Helium	80.0	0.750	1.500	0.925	13	0.582	--	32.2	30.0	1.07
	Long	Hydrogen	80.0	0.750	1.497	0.902	9	0.559	--	31.2	30.0	1.04
	Trans	Hydrogen	80.0	0.747	1.498	0.686	10	0.815	37.7 <sup>AB</sup>	--	30.0	1.27
AMS 4928 (Ti 6-4)	Long	Helium	80.0	0.742	1.501	0.802	16	0.368	--	56.0	146.1	0.38
	Trans	Helium	80.0	0.724	1.498	0.792	13	0.515	--	66.4	146.1	0.45
	Long	Hydrogen	80.0	0.748	1.499	0.898	17	0.681	--	75.7	144.9	0.52
	Trans	Hydrogen	80.0	0.740	1.499	0.748	16	0.522	72.4 <sup>A</sup>	--	144.9	0.50
AMS 4926 (A-110)	Long	Helium	80.0	0.747	1.495	0.825	8	0.433	--	51.2	122.9	0.42
	Trans	Helium	80.0	0.751	1.499	0.868	4	0.665	--	63.5	122.9	0.52
	Long	Hydrogen	80.0	0.745	1.497	0.842	2	0.343	--	47.0	127.3	0.37
	Trans	Hydrogen	80.0	0.742	1.494	0.844	3	0.605	--	62.6	127.3	0.49

A - Does not meet tentative ASTM designation E399-70T, paragraphs 7.2.3 and 7.2.4.

B - Does not meet tentative ASTM designation E399-70T, paragraph 8.1.5.

All fatigue precracking done per tentative ASTM designation E399-70T, paragraphs 6.5.1 through 6.5.4.

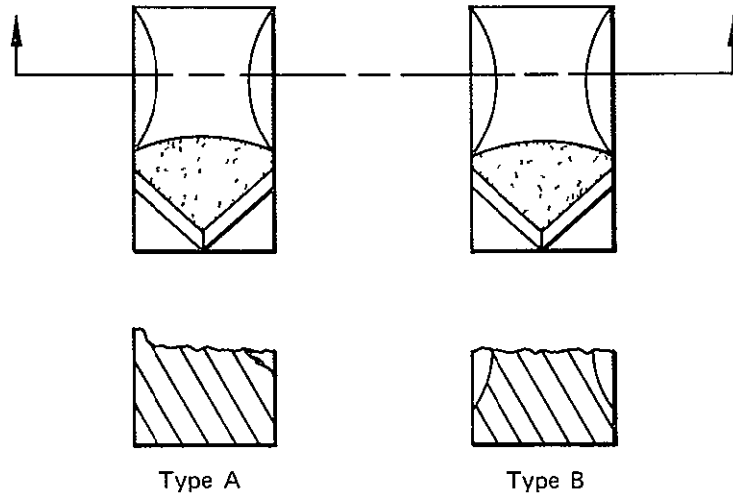


Figure VI-6. Fracture Appearances

FD 51883

## SECTION VII CREEP RUPTURE

### A. INTRODUCTION

Creep rupture properties were evaluated under 5000-psig hydrogen and 5000-psig helium gaseous environments at either 200 °F or 1250 °F. Creep rate, rupture life, percent elongation and percent reduction of area were determined for two nickel, two iron, and two titanium base alloys.

### B. CONCLUSIONS

Creep and rupture properties were degraded in 5000-psig hydrogen for all nickel, iron, and titanium base alloys tested except AISI 347 stainless steel. Degradation in rupture life is expressed as percent reduction of stress in hydrogen compared to helium to obtain identical rupture life (hr).

Degradation (%) for Life (hr) of:

$$\left[ \frac{H_e \text{ Stress} - H_2 \text{ Stress}}{H_e \text{ Stress}} \right] \times 100$$

Nickel Base	<u>10 hr</u>	<u>100 hr</u>
AMS 5662 (INCO 718) 1750 °F Solution + Age	30%	32%
AMS 5662 (INCO 718) 1900 °F Solution + Age	26%	28%
AMS 5666 (INCO 625)	17%	28%
 Iron Base		
AMS 5735 (A-286)	16%	21%
AMS 5646 (AISI 347)	0	0
 Titanium		
AMS 4928 (Ti 6-4)	*	*
AMS 5926 (A-110)	*	*

Stress rupture curves are shown in figures VII-1 through VII-7 for all alloys.

---

\*Results inconclusive for limited tests conducted.

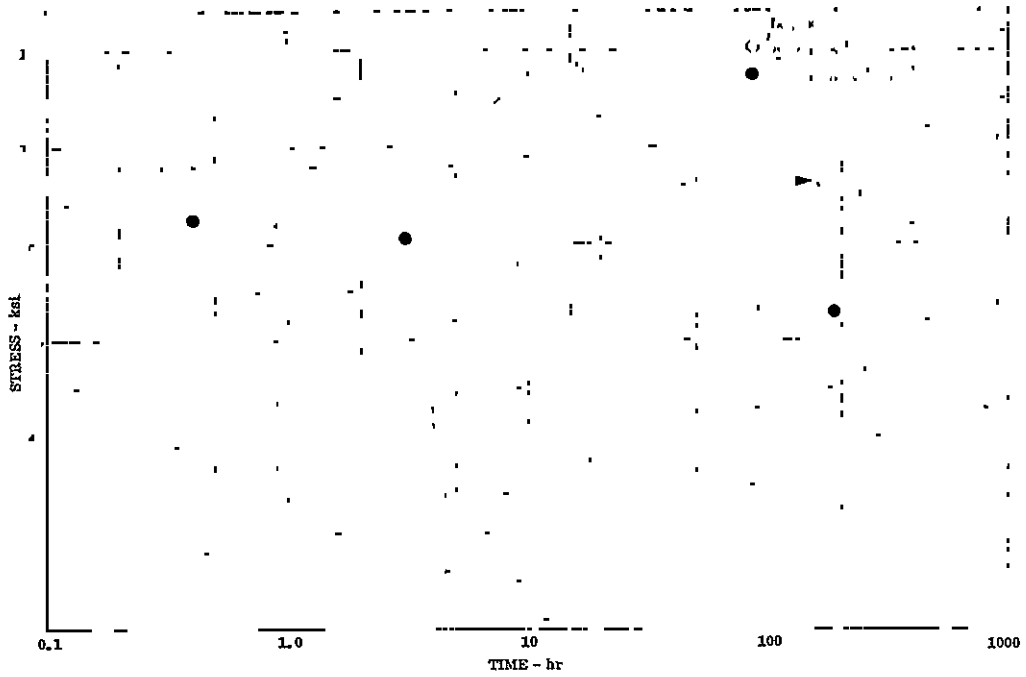


Figure VII-1. Stress Rupture of AMS 5662 at 1250 °F (INCO 718, 1750 °F Solution Plus Age) DF 86815

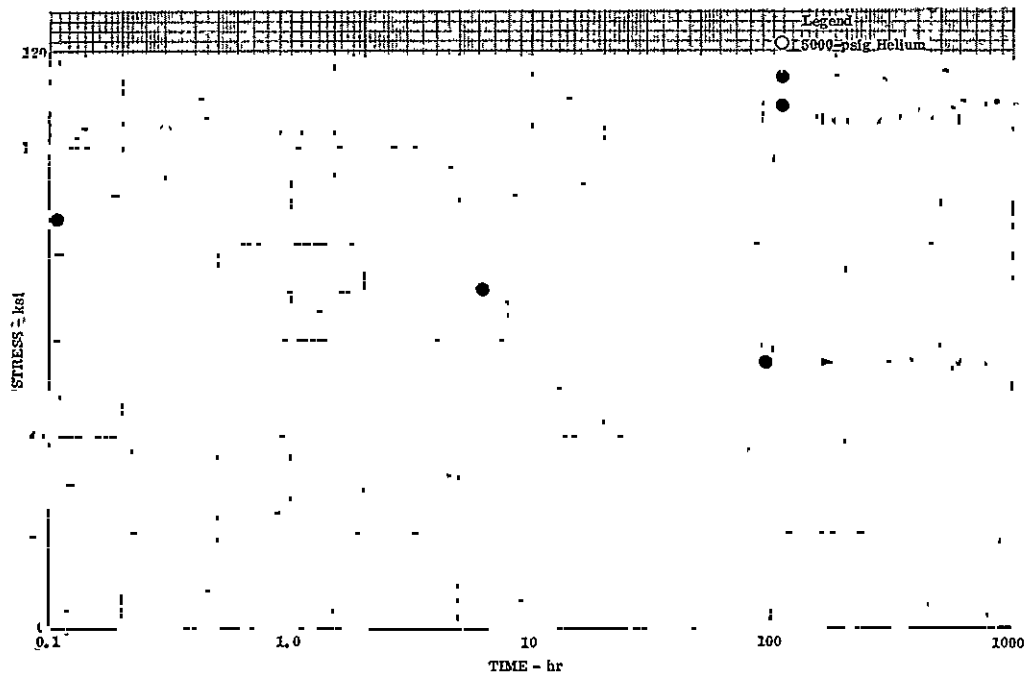


Figure VII-2. Stress Rupture of AMS 5662 at 1250 °F (INCO 718, 1900 °F Solution Plus Age) DF 86816

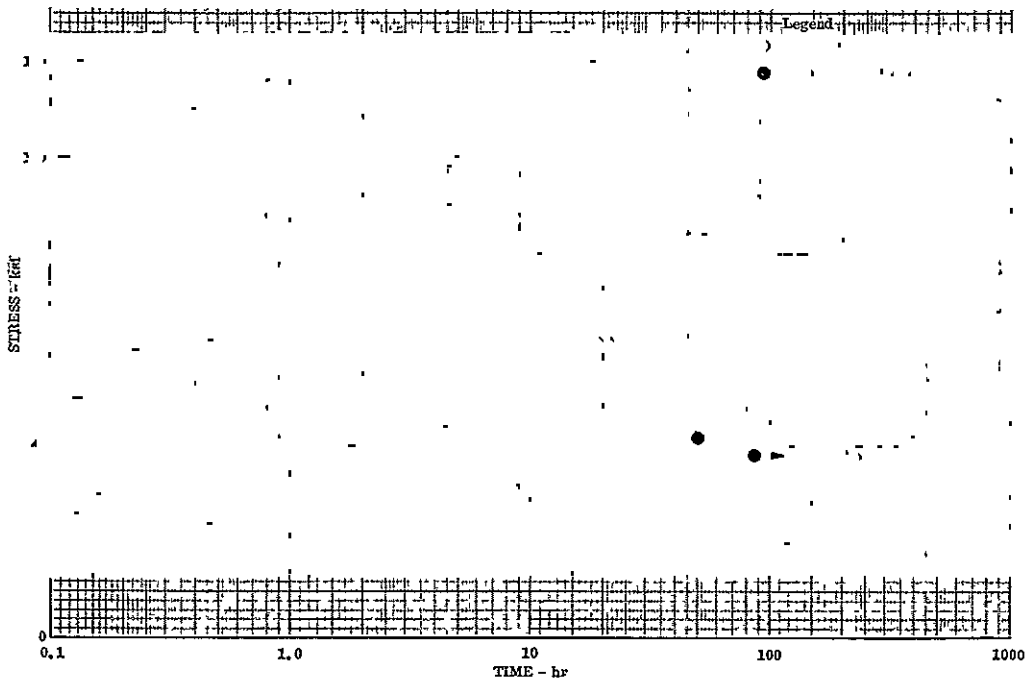


Figure VII-3. Stress Rupture of AMS 5662 (INCO 625) at 1250°F

DF 86817

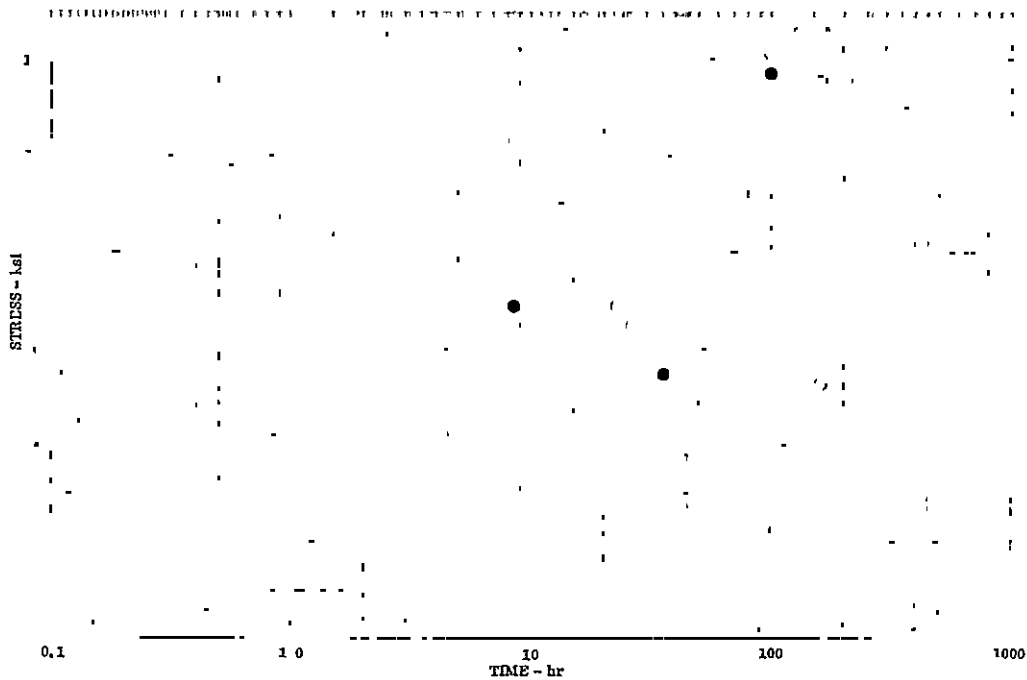


Figure VII-4. Stress Rupture of AMS 5735 (A-286) at 1250°F

DF 86818



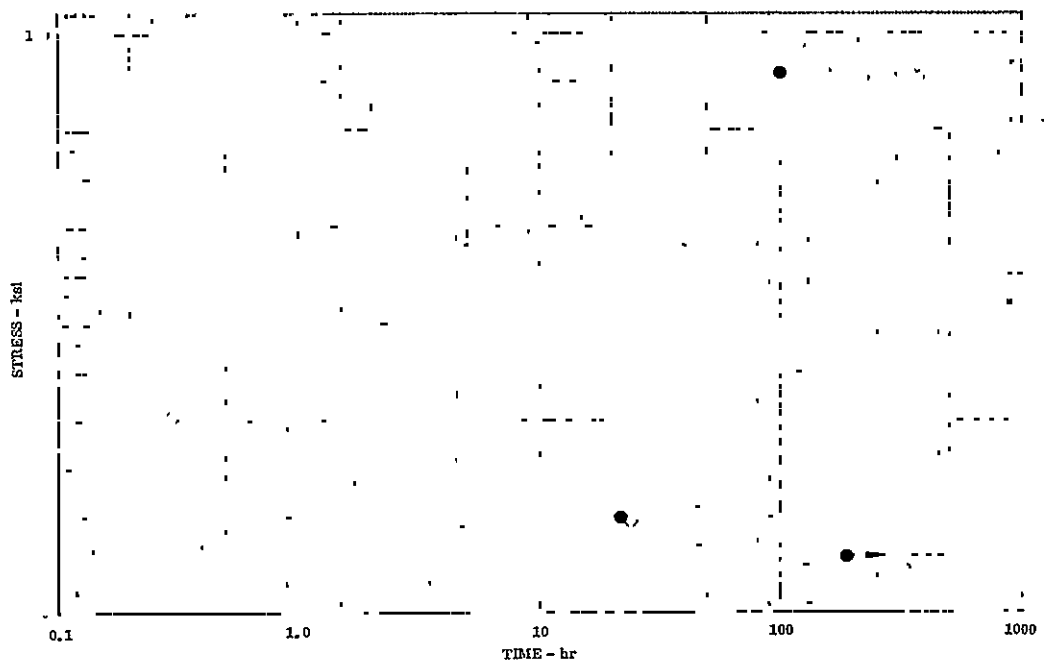


Figure VII-5. Stress Rupture of AMS 5646  
(AISI 347) at 1250°F

DF 86819

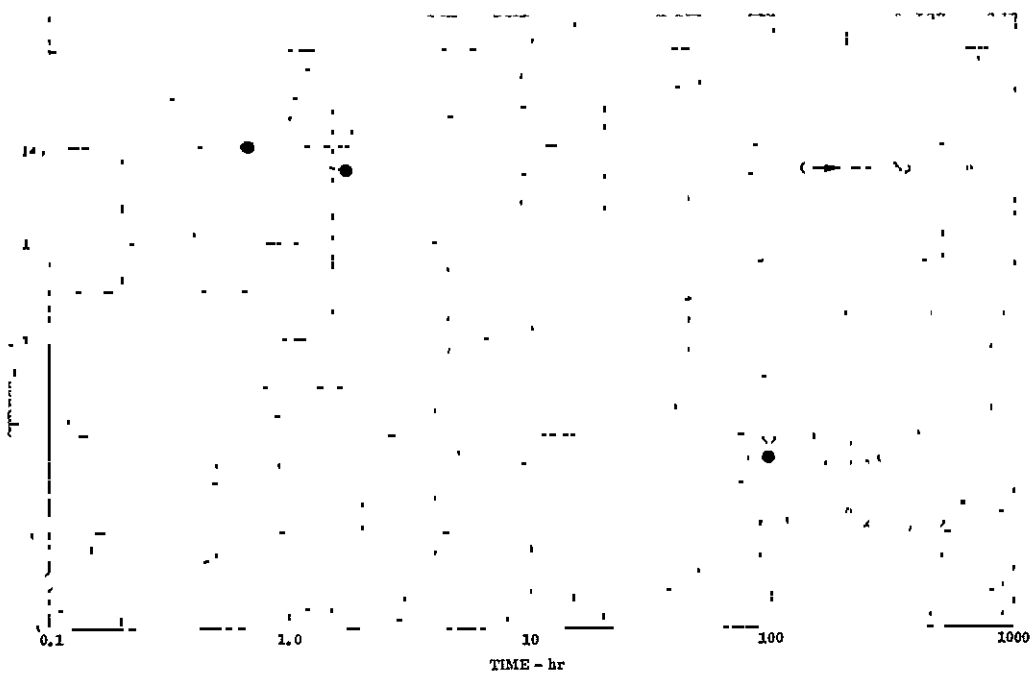


Figure VII-6. Stress Rupture of AMS 4928  
(Ti 6-4) at 200°F

DF 86820

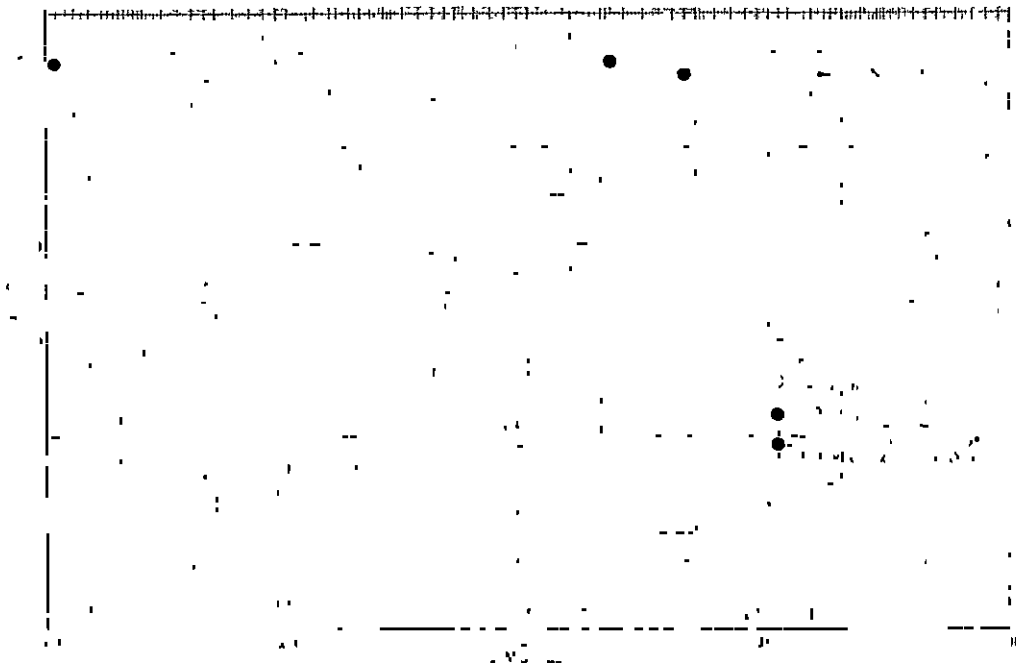


Figure VII-7. Stress Rupture of AMS 4926  
(A-110) at 200°F

DF 86821

Degradation was also quite evident in time required to obtain a given percent of creep. Limited available data (figures VII-8 and VII-9) for a constant stress level are given below.

Stress (ksi)	Time (hr) to Creep (%) of:						
	0.5%		1.0%		2.0%		
	<u>H<sub>e</sub></u>	<u>H<sub>2</sub></u>	<u>H<sub>e</sub></u>	<u>H<sub>2</sub></u>	<u>H<sub>e</sub></u>	<u>H<sub>2</sub></u>	
AMS 5662 (INCO 718) 1750°F Solution + Age	81	>100	1	>100	1.6	>100	2
AMS 5735 (A-286)	52	66	9	90	15	120	22

Generally, creep rates were greater in hydrogen for all alloys with the possible exception of AISI 347 stainless steel. This is evident in cases where it was possible to test in hydrogen and helium at same stress levels. Creep-rate curves are shown in figures VII-10 through VII-15.

The titanium base alloys were loaded to stress levels beyond the initial yield to obtain a desired stress rupture life between 10 and 100 hours. This did not allow a substantial margin between operating stress and ultimate stress. Hydrogen influence was visibly evident as a flaking off of surface material (figure VII-16). Metallographic analysis identified this as hydriding. All these factors combined to make results inconclusive for the limited tests conducted. Data are listed in table VII-1.

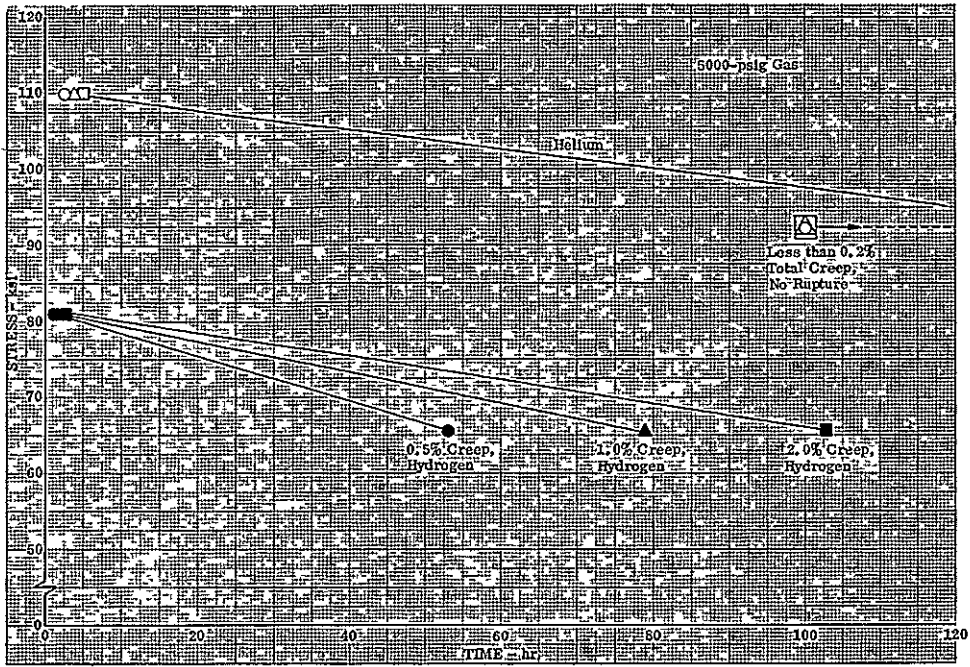


Figure VII-8. Creep-Stress-Time of AMS 5662  
at 1250°F (INCO 718, 1750°F  
Solution Plus Age)

DF 86822

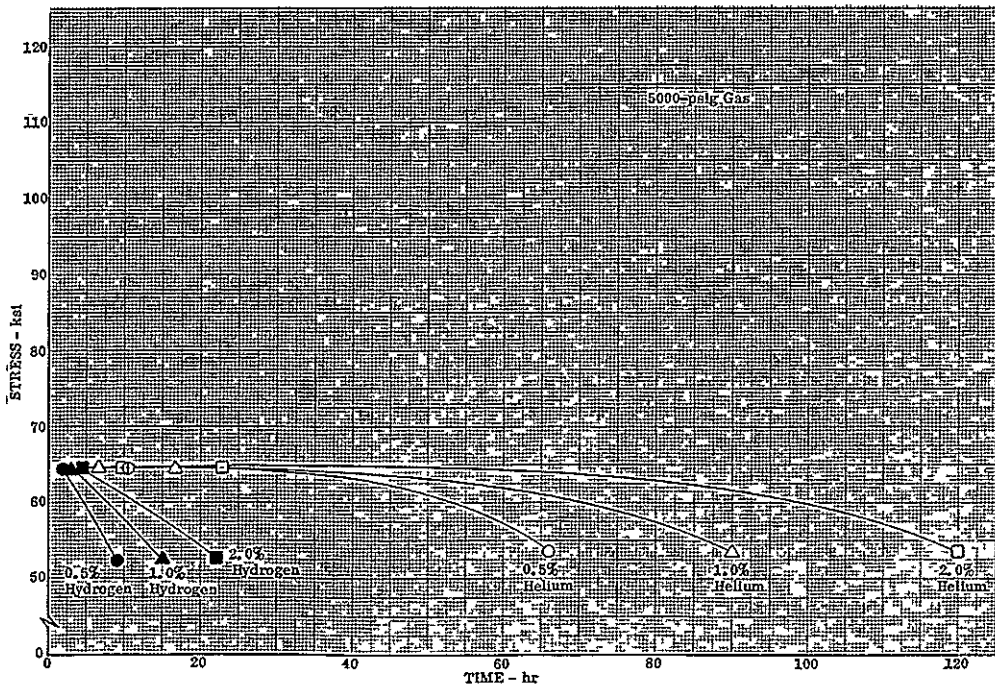


Figure VII-9. Creep-Stress-Time AMS 5735  
(A-286) at 1250°F

DF 86823

Figure VII-10. Creep-Stress Rupture of AMS 5662 at 1250 °F (INCO 718, 1750 °F Solution Plus Age)

DF 86824

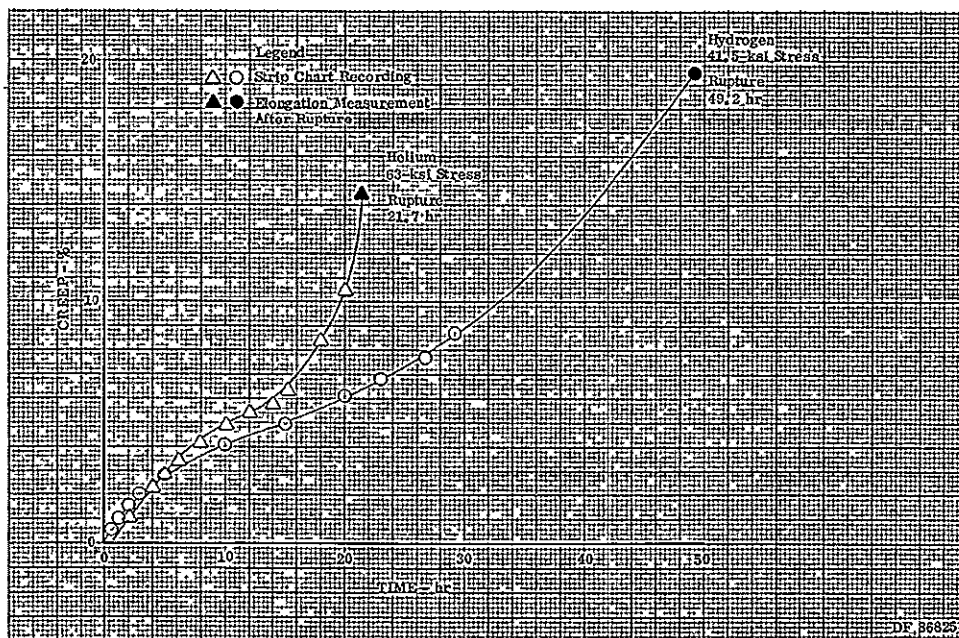


Figure VII-11. Creep-Stress Rupture of AMS 5666 (INCO 625) at 1250 °F

DF 86825

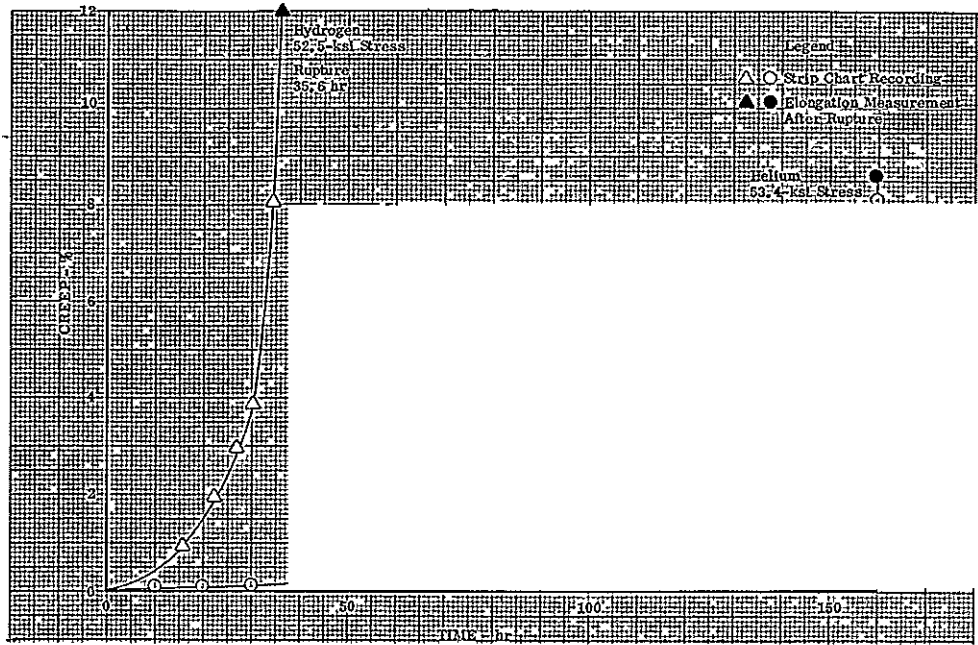


Figure VII-12. Creep-Stress Rupture of AMS 5735 (A-286) at 1250°F

DF 86826

Figure VII-13. Creep-Stress Rupture of AMS 5646 (AISI 347) at 1250°F

DF 86827



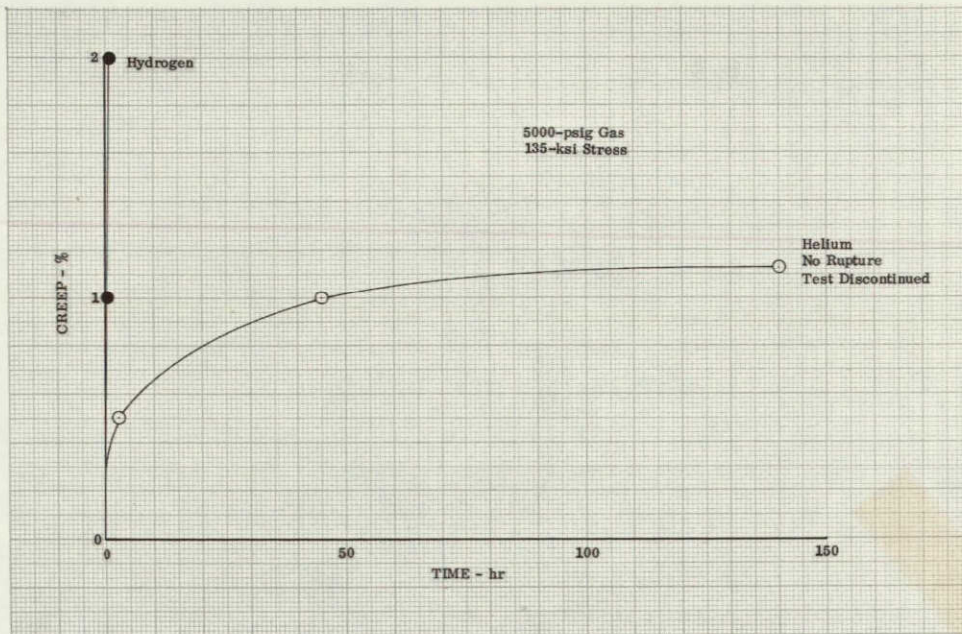


Figure VII-14. Creep-Stress Rupture of AMS 4928 (Ti 6-4) at 200°F DF 86828

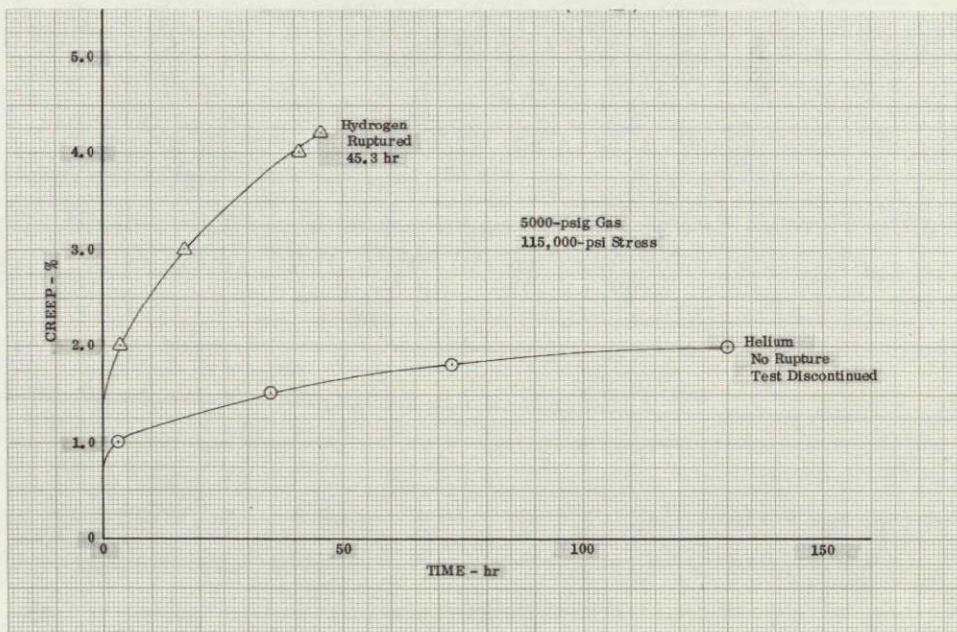


Figure VII-15. Creep-Stress Rupture of AMS 4926 (Ti A-110) at 200°F DF 86829



NOT REPRODUCIBLE

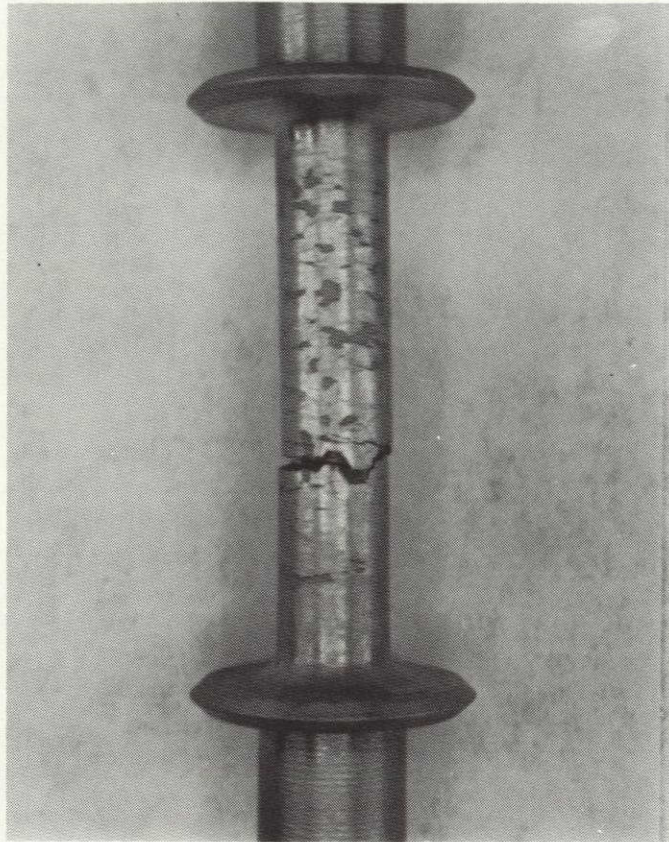


Figure VII-16. Creep-Rupture Specimen of AMS 4926 FAC 21700  
(A-110) Showing Hydriding After  
Exposure to 5000-psig Hydrogen,  
115,000-psi Stress and 200°F for  
45 hr Until Rupture



Table VII-1. Creep-Rupture Properties of Materials in High Pressure Gaseous Environment

Material	Test Temperature (°F)	Environment	Test Conditions		Time to Creep (hr)			Time to Rupture (hr)	EL (%)	RA (%)
			Pressure (psig)	Stress Level (ksi)	0.5%	1.0%	2.0%			
AMS 5662 (INCO 718) 1750 °F Solution	1250	Helium	5000	92.3	< 0.2% Total Creep			100.0 (1)		
	1250	Helium	5000	110.0	2.5	4.0	5.3	7.2	9.5	38.2
	1250	Hydrogen	5000	65.4	53.0	79.0	103.0	118.6	5.3	36.4
	1250	Hydrogen	5000	85.2	0.1	0.15	0.25	0.4	7.8	48.8
	1250	Hydrogen	5000	81.0	1.0	1.6	2.2	3.1	10.2	52.3
AMS 5662 (INCO 718) 1900 °F Solution	1250	Helium	5000	90.5	10.5	17.5	24.5	32.2	6.4	38.8
	1250	Helium	5000	113.5	< 0.3% Total Creep			0.3		(2)
	1250	Hydrogen	5000	55.4	< 0.1% Total Creep			100.0 (1)		
	1250	Hydrogen	5000	70.4	< 0.5% Total Creep			6.2	1.2	4.7
	1250	Hydrogen	5000	85.5	Failed on Loading					(2)
AMS 5666 (INCO 625)	1250	Helium	5000	53.5	0.6	1.0	1.6	4.0 (3)	7.0	51.5
	1250	Helium	5000	63.0	1.2	2.0	3.5	21.2	14.7	52.5
	1250	Helium	5000	63.0	0.45	0.7	1.2	25.7	39.2	52.4
	1250	Hydrogen	5000	45.4	Failed on Loading				18.9	76.7
	1250	Hydrogen	5000	45.6	Failed on Loading				17.6	78.4
	1250	Hydrogen	5000	38.0	< 0.25% Total Creep			86.5 (1)		
	1250	Hydrogen	5000	41.5 (5)	0.6	1.3	3	49.2	19.5	47.5
	1250	Hydrogen	5000	41.5 (5)	0.6	1.3	3	49.2	19.5	47.5
AMS 5735 (A-286)	1250	Helium	5000	53.4	66.0	90.0	120.0	159.8	8.6	36.6
	1250	Helium	5000	64.4	10.4	16.6	22.8	31.7	9.3	44.2
	1250	Helium	5000	64.4	3.5	6.5	9.8	22.8	27.5	27.8
	1250	Hydrogen	5000	57.5	<0.1	0.1	0.13	0.25	10.8	55.5
	1250	Hydrogen	5000	52.5	9	15	22	35.6	7.4	26
	1250	Hydrogen	5000	64.4	1.75	2.8	4.2	8.6	12.1	40
	1250	Hydrogen	5000	64.4	1.75	2.8	4.2	8.6	12.1	40
AMS 5646 (AISI 347)	1250	Helium	5000	40.4	<0.1	0.15	0.2	0.3	8.7	48.3
	1250	Helium	5000	19.4	3.0	9.0	16.5	24.5	8.5	43.7
	1250	Hydrogen	5000	11.8	60.0	115.0	187.0	187.0 (1)		
	1250	Hydrogen	5000	38.9	Failed on Loading				8.5	42.4
	1250	Hydrogen	5000	19.8	8.0	14.0	21.0	23.9	2.6	14.3
AMS 4928 (Ti 6-4)	200	Helium	5000	140.0	Failed on Loading					
	200	Helium	5000	135.0	2.75	45.0	1.13% Total	140.3 (1)		
	200	Hydrogen	5000	140.0	<0.1	0.3	0.67	0.67	4.2 (4)	17.9
	200	Hydrogen	5000	135.0	<0.1	0.6	1.7	1.7	3.16 (4)	11.8
AMS 4926 (A-110)	200	Helium	5000	118.0	Failed on Loading					
	200	Helium	5000	115.0	0.18	3.0	130.0	130.0 (1)		
	200	Hydrogen	5000	115.0	<0.1	0.35	3.6	45.3	5.1 (4)	10.0
	200	Hydrogen	5000	118.0	<0.1	0.25	2.75	21.7	6.5 (4)	20.9

- NOTES: 1. Test discontinued, no rupture.  
 2. Failure mode precludes accurate measurement.  
 3. Rig shutdown due to temperature loss, immediately prior to failure.  
 4. Includes initial yield.  
 5. Estimated from strip chart instantaneous elongation.

VII-11

## C. TEST PROCEDURE

Creep-rupture tests were conducted on a 12,000 lb capacity Arcweld (Satec) Model JE creep-rupture machine modified and installed in a remote test cell. The loading frame and test vessel are explosion proofed and located in an enclosure exposed to atmospheric conditions. Controls and instrumentation readout are located in an adjacent block-house. The pressure vessel (figure VII-17) is made of AISI 321 stainless steel and incorporates a high pressure Gray-Loc connector. This vessel is suspended in the creep-rupture machine which is counterbalanced to maintain the load lever arm at a level position. The interior of the vessel is shown in figure VII-18 with specimen and extensometer in place and figure VII-19 with half of the furnace in place. The creep-rupture specimen was designed with integral collars for positive location and gripping of creep measuring extensometer heads. Ends of specimen were flat pin joints rather than the conventional threaded joints and acted as part of a two pin universal joint.

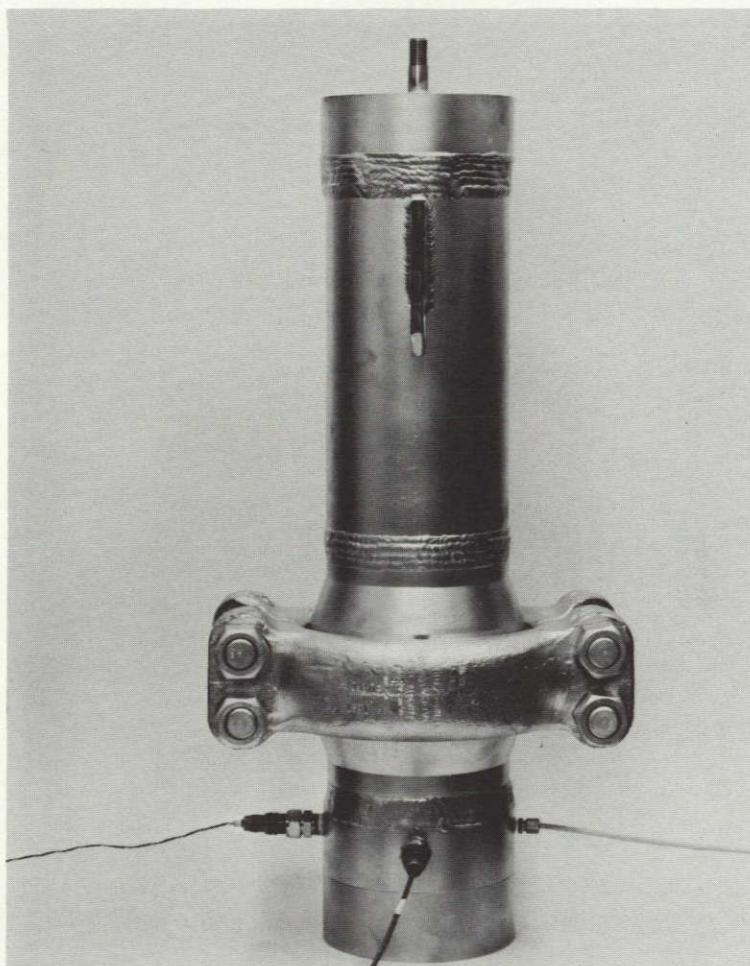


Figure VII-17. Creep-Rupture Pressure Vessel  
Complete Assembly

FC 21867



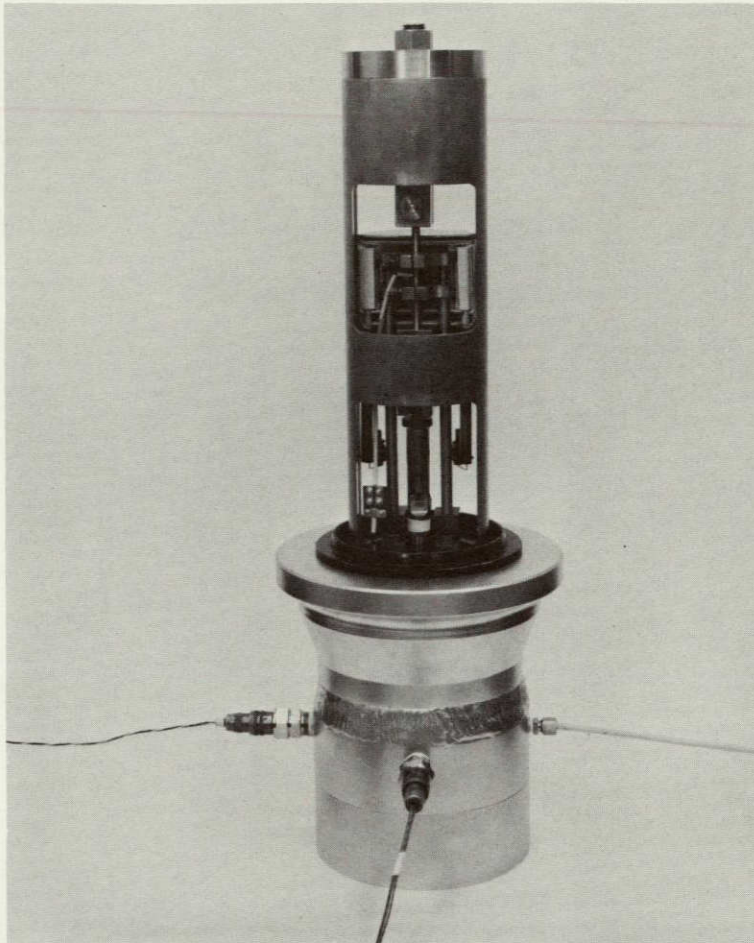
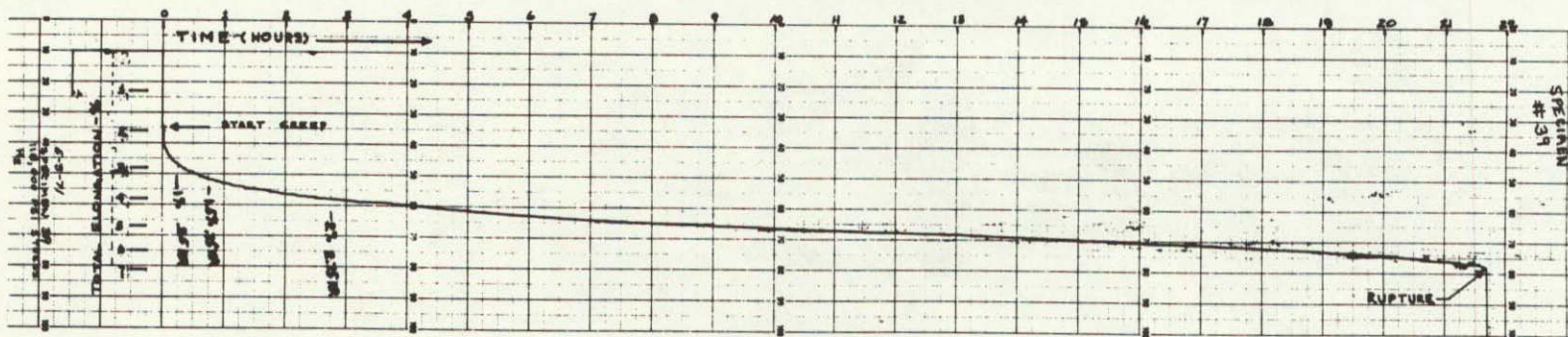


Figure VII-18. Creep-Rupture Pressure Vessel With Chamber Wall Removed. Specimen, Extensometer, Universal Pin Joints and Half of Oven in Place FC 21869





VII-14

Figure VII-19. Typical Creep-Time Strip Chart Record for Creep-Rupture Test Conducted in High Pressure Gaseous Environment

FD 53127

Load rods and adapters also incorporate pin joints. This in effect puts a universal joint at the immediate ends of the specimen and eliminates alignment errors and resulting bending stresses upon the specimen.

As the specimen ends are exposed to the high pressure gas, a compensating technique is used to eliminate any effective load on the specimen due to pressure. The extensometer is inside the vessel and is of the averaging type. The output of the extensometer is recorded as elongation vs time (figure VII-19). Time run meter was used to validate rupture life indicated on strip chart.

Specimen heater was a resistance wire, split, clam shell configuration. Two zones were provided with independent control to minimize temperature gradient along gage length. Three chromel-alumel thermocouples were looped tight around gage section with ceramic beads. Split heater was positioned around specimen and extensometer heads. Pressure vessel was closed with Gray Loc clamps and connected to load rod adapters in creep-rupture machine.

Gas pressure lines, water cooling lines and electric power leads were connected. Low pressure leak check was performed with gaseous nitrogen. Pressure vessel was evaluated to 10-microns of mercury and pop-purged 10 times with test gas.

Vessel was pressurized to 4000-psig test gas and stabilized to check for high pressure leaks. Temperature was applied to specimen and allowed to stabilize by adjusting primary temperature controller. Temperature increased gas pressure which was vented as necessary to stabilize at 5000-psig. Stable temperature and pressure were obtained in 1-1/2 to 2 hr. Test load was applied by activating automatic lever arm leveling unit. Dead weights were lifted off rest pan to a position where lever arm was maintained level. Load was corrected for frictional losses by using the internal load cell to verify the stress on the specimen gage section. Test system was secured for automatic control and monitor. When specimen failed all control equipment was automatically deactivated. Specimen was removed and final gage length and diameter were measured and recorded to determine percent elongation and percent reduction of area.



## SECTION VIII TENSILE PROPERTIES

### A. INTRODUCTION

Tensile properties were investigated in 5000-psig hydrogen and helium gaseous environments at temperatures of -260°F, 80°F and 200°F or 1250°F. Both smooth and notched ( $K_t = 8.0$ ) tests were conducted on nickel, iron, and titanium base alloys.

### B. CONCLUSIONS

Both solution heat treatments of AMS 5662 (INCO 718) tested were degraded in hydrogen at room temperature, as evidenced by a severe decrease in ductility. The 1750°F solution had a 75% decrease in ductility as compared to helium, while the 1900°F solution had a 20% decrease. However, at 1250°F there was no hydrogen degradation in either solution heat treatment, with the smaller grained 1750°F solution material having the better tensile properties.

Of the nickel-base alloys tested in this study (INCO 718, INCO 625, and Hastelloy X) only AMS 5754 (Hastelloy X) experienced no hydrogen degradation at ambient (80°F) or elevated temperature (1250°F). AMS 5666 (INCO 625) was degraded, as evidenced by the 50% decrease in ductility as compared to helium at room temperature (80°F). However, at elevated temperatures (1250°F) there was only a 12% decrease in ductility as compared to helium.

Although AMS 5662 (INCO 718) is degraded in hydrogen at ambient temperatures, at elevated temperatures the 1750°F solution heat treatment demonstrated the best tensile properties of the nickel-base alloys.

Comparing welded AMS 5662 (INCO 718 1900°F solution) to welded AMS 5666 (INCO 625) reveals INCO 718 to be superior in strength, but not in ductility, to INCO 625. GTA-welded INCO 718 was degraded by hydrogen, as evidenced by a decrease in ductility, while welded INCO 625 was not degraded. Comparing welded to parent material, INCO 718 maintained strength but lost ductility, while INCO 625 lost strength but experienced only a small loss in ductility.

The iron-base alloys AMS 5735 (A-286) and AMS 5646 (AISI 347) experienced no degradation in tensile properties in high pressure hydrogen. AISI 347 demonstrated superior tensile properties at cryogenic temperatures, but decreased significantly in strength with increasing temperature.

Both titanium-base alloys AMS 4928 (Ti 6-4) and AMS 4926 (A-110) experienced hydrogen degradation, as was evidenced by a 20% decrease in ductility as compared to helium. At temperatures of 200°F both alloys experienced severe hydrogen degradation, as evidenced by the 45% decrease in percent reduction of area as compared to helium.



C. TEST PROCEDURE

Specimen blanks were cut from 0.750-inch diameter bar stock, heat-treated if required, and machined as per ASTM Designations E8-69 for smooth and notched tensile specimens. (See Section III Prints FML 95224B and FML 95620B.) All smooth round tensile specimens have a 0.252-inch gage diameter and a gage length of 1.00 inch. Notched specimens ( $K_t$  of 8.0) have a large diameter of 0.500 inch and a notch diameter of 0.315 inch machined in the center of the specimen gage at a 60-degree angle with a 0.002-inch radius at the apex of the notch.

Tensile testing was done with a Tinius Olsen 30,000-lb capacity tensile machine equipped with a P&WA-designed pressure vessel. All controls and instrumentation readout equipment are located inside the adjacent block house. This equipment is shown in figures VIII-1 and VIII-2a. The pressure vessel is shown open in figure VIII-2b with a notched specimen in place and in figure VIII-2c with a smooth specimen and room temperature extensometer in place. The vessel is made of AISI 347 stainless steel and incorporates a high pressure Gray-Loc connector. A special compensating device built into the base of the vessel compensates for any blowoff load resulting from specimen failure. Both internal and external load cells are used, thus the effect of friction on the load rods passing through the seals is known and accounted for.

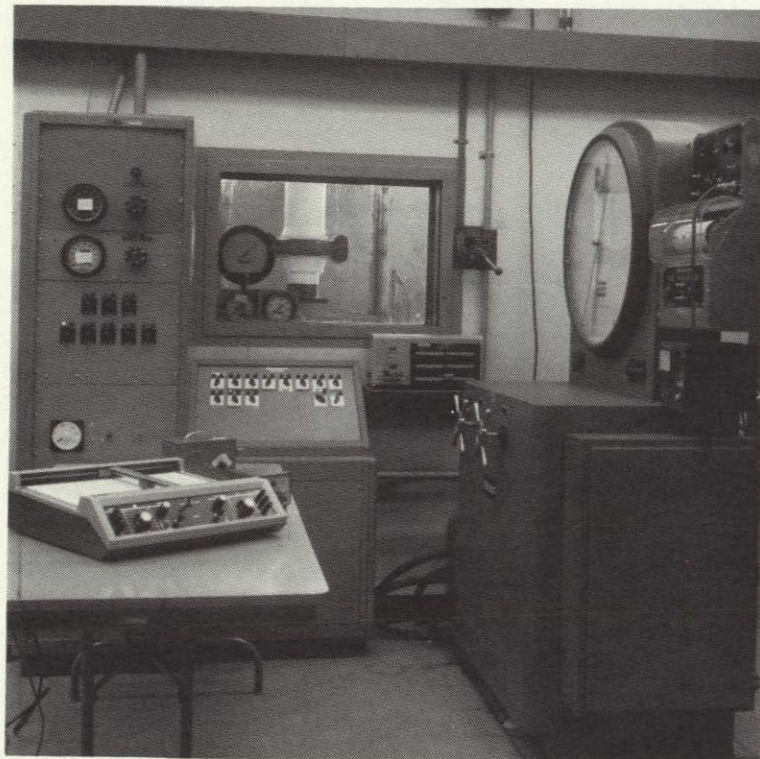
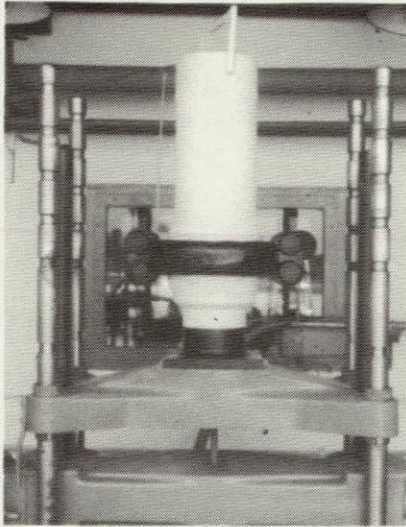


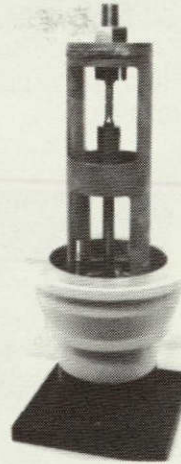
Figure VIII-1. Tensile Machine and Test Environment  
Controls and Data Acquisition Equipment

FC 21272

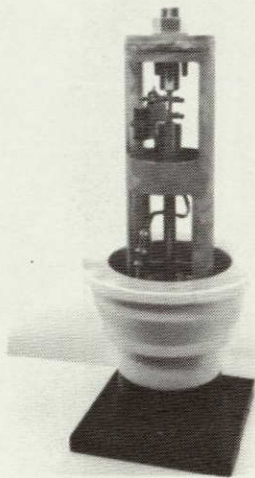




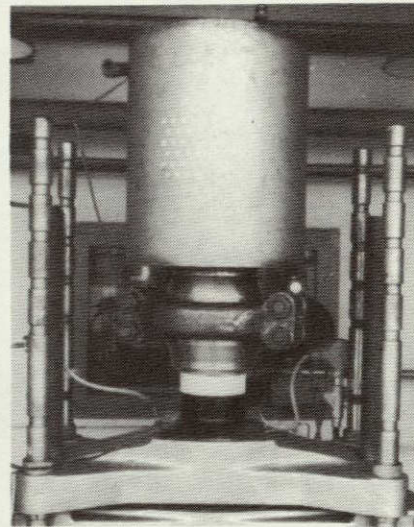
FC 21268  
a) Test Vessel Installed on Tensile Machine in Remote Test Cell



FC 21572  
b) Test Vessel Open With Notch Tensile Specimen in Place



FC 21573  
c) Test Vessel Open With Smooth Specimen in Place and Room Temperature Extensometer Attached



FE 107940  
d) Test Vessel With Cryogenic Jacket Installed

Figure VIII-2. Various Views of Test Vessel

FD 53125

To conduct cryogenic tests, the pressure vessel was modified by the addition of an insulated jacket placed over the upper portion. (See figure VIII-2d.) This jacket has provisions for flowing LN<sub>2</sub>, thus providing cryogenic temperature inside the pressure vessel. To enhance cooling, the hydrogen gas passes through a heat exchanger coil located inside the LN<sub>2</sub> jacket before passing into the pressure vessel.

To conduct elevated temperature tests, a two-zone furnace and separate control systems for each zone were prepared to minimize any heat gradient due



to the high conductivity of the gases. The upper zone uses a Research Incorporated Model 625 temperature-power controller, while the lower zone uses a Barber Colman Model 477P proportional controller. The high temperature extensometer system, developed by P&WA, is shown attached in place with thermocouples on a smooth tensile specimen in figure VIII-3. This extensometer system uses conventional linear differential transformers to measure specimen strain at elevated temperatures.

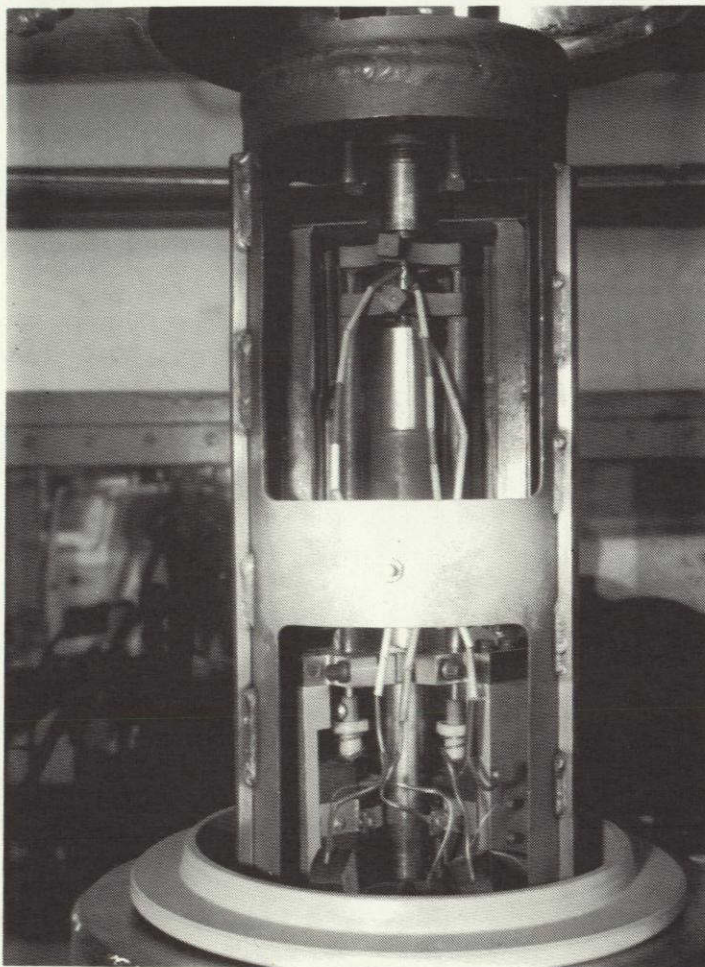


Figure VIII-3. Test Vessel With Outer Chamber  
Removed Showing Specimen,  
Extensometer, and Half of Furnace  
in Place

FE 107943

To make the necessary gas analyses, a gas sampling system is incorporated in the test cell. All the controls for the gas sampling system are operated by remote control inside the block house.



Table VIII-1. Room Temperature Tensile Properties of Materials in High Pressure Gaseous Environment (Continued)

Material	Test Conditions					Test Results				
	Test Temp, °F	Stress Concentration Factor	Environment	Pressure, psig	Load Rate in/min		Strength		Ductility	
					0 Load to Yield	Yield to Ultimate	Yield, ksi	Ultimate, ksi	EL, (1) %	RA, (2) %
AMS 5735 (A-286) (Cont'd)	80	Smooth	Hydrogen	5000	0.050	0.100	110.2	155.8	28.5	46.4
	80	Smooth	Hydrogen	5000	0.050	0.100	111.2	155.6	27.0	45.8
	80	8.0	Hydrogen	5000		0.100		225.4		8.1
	80	8.0	Hydrogen	5000		0.100		224.3		8.6
	80	8.0	Hydrogen	5000		0.100		225.4		7.2
AMS 5646 (AISI 347)	80	Smooth	Helium	5000	0.050	0.100	69.7	102.0	38.0	70.1
	80	Smooth	Helium	5000	0.050	0.100	63.9	99.4	36.5	70.5
	80	8.0	Helium	5000		0.100		170.0		20.7
	80	8.0	Helium	5000		0.100		173.3		20.1
	80	Smooth	Hydrogen	5000	0.050	0.100	64.6	109.7	41.5	71.1
	80	Smooth	Hydrogen	5000	0.050	0.100	67.4	108.3	39.0	70.4
	80	8.0	Hydrogen	5000		0.100		166.8		18.3
	80	8.0	Hydrogen	5000		0.100		172.1		18.0
	80	8.0	Hydrogen	5000		0.100		127.8		19.5
AMS 5754 (Hastelloy X)	80	Smooth	Helium	5000	0.050	0.100	48.6	106.7	54.0	63.0
	80	Smooth	Helium	5000	0.050	0.100	44.6	103.0	53.5	62.8
	80	8.0	Helium	5000		0.100		127.7		17.2
	80	8.0	Helium	5000		0.100		163.8		18.3
	80	Smooth	Hydrogen	5000	0.050	0.100	48.6	105.5	51.5	60.5
	80	Smooth	Hydrogen	5000	0.050	0.100	50.1	105.3	54.5	66.4
	80	8.0	Hydrogen	5000		0.100		124.0		13.5
	80	8.0	Hydrogen	5000		0.100		125.5		9.2
	80	8.0	Hydrogen	5000		0.100		130.8		19.4

Table VIII-1. Room Temperature Tensile Properties of Materials in High Pressure Gaseous Environment (Continued)

Material	Test Conditions					Test Results				
	Test Temp, °F	Stress Concentration Factor	Environment	Pressure, psig	Load Rate in/min		Strength		Ductility	
					0 Load to Yield	Yield to Ultimate	Yield, ksi	Ultimate, ksi	EL, (1) %	RA, (2) %
AMS 4928 (T1 6Al-4V)	80	Smooth	Helium	5000	0.050	0.100	145.4	151.1	15.0	45.4
	80	Smooth	Helium	5000	0.050	0.100	146.7	151.0	15.0	44.0
	80	8.0	Helium	5000		0.100		205.3		4.3
	80	8.0	Helium	5000		0.100		209.5		3.0
	80	Smooth	Hydrogen	5000	0.050	0.100	144.1	147.8	13.5	34.0
	80	Smooth	Hydrogen	5000	0.050	0.100	145.7	152.7	13.5	37.8
	80	8.0	Hydrogen	5000		0.100		189.7		2.1
	80	8.0	Hydrogen	5000		0.100		183.5		1.2
	80	8.0	Hydrogen	5000		0.100		178.8		1.0
AMS 4926 (A-110)	80	Smooth	Helium	5000	0.050	0.100	115.6	132.5	20.0	44.6
	80	Smooth	Helium	5000	0.050	0.100	130.3	133.1	18.5	43.9
	80	8.0	Helium	5000		0.100		204.9		2.0
	80	8.0	Helium	5000		0.100		197.2		3.1
	80	Smooth	Hydrogen	5000	0.050	0.100	121.0	134.8	14.5	35.4
	80	Smooth	Hydrogen	5000	0.050	0.100	133.6	138.9	16.5	31.4
	80	8.0	Hydrogen	5000		0.100		158.2		1.4
	80	8.0	Hydrogen	5000		0.100		173.3		2.3
	80	8.0	Hydrogen	5000		0.100		167.1		2.3

(1) Elongation in 1 inch.

(2) Reduction of Area.

6-VIII-9

Table VIII-2. Cryogenic Temperature Properties of Materials in High Pressure Gaseous Environment

Material	Test Conditions				Test Results					
	Test Temp, °F	Stress Concentration Factor	Environment	Pressure, psig	Load Rate, in/min		Strength		Ductility	
					0 Load to Yield	Yield to Ultimate	Yield, ksi	Ultimate, ksi	EL, (1) %	RA, (2) %
AMS 5646 (AISI 347)	-260	Smooth	Helium	5000	0.050	0.100	99.8	196.9	43.5	64.0
	-260	Smooth	Helium	5000	0.050	0.100	109.0	202.4	42.5	64.6
	-260	Smooth	Hydrogen	5000	0.050	0.100	96.5	190.0	42.5	64.6
	-260	Smooth	Hydrogen	5000	0.050	0.100	96.0	177.2	43.5	62.8
	-260	8.0	Helium	5000		0.100		230.4		11.6
	-260	8.0	Helium	5000		0.100		227.4		12.1
	-260	8.0	Hydrogen	5000		0.100		221.3		11.9
	-260	8.0	Hydrogen	5000		0.100		225.9		13.1
	-260	8.0	Hydrogen	5000		0.100		222.6		11.9

(1) Elongation in 1 inch.

(2) Reduction of area.

Table VIII-3. Elevated Temperature Tensile Properties of Materials in High Pressure Gaseous Environment

Material	Test Conditions					Test Results				
	Test Temp, °F	Stress Concentration Factor	Environment	Pressure, psig	Load Rate in/min		Strength		Ductility	
					0 Load to Yield	Yield to Ultimate	Yield, ksi	Ultimate ksi	EL, (1) %	RA, (2) %
AMS 5662 (INCO 718) 1750°F Sol	1250	Smooth	Helium	5000	0.050	0.100	136.7	155.9	20.0	19.7
	1250	Smooth	Helium	5000	0.050	0.100	131.3	154.3	25.0	47.5
	1250	8.0	Helium	5000		0.100		202.5		3.3
	1250	8.0	Helium	5000		0.100		210.5		4.6
	1250	Smooth	Hydrogen	5000	0.050	0.100	137.5	150.3	22.0	46.8
	1250	Smooth	Hydrogen	5000	0.050	0.100	136.0	155.5	21.5	34.9
	1250	8.0	Hydrogen	5000		0.100		187.5		4.6
	1250	8.0	Hydrogen	5000		0.100		196.5		3.3
	1250	8.0	Hydrogen	5000		0.100		199.1		5.3
AMS 5662 (INCO 718) 1900°F Sol	1250	Smooth	Helium	5000	0.050	0.100	134.9	150.3	17.5	31.8
	1250	Smooth	Helium	5000	0.050	0.100	141.3	150.4	11.5	18.0
	1250	8.0	Helium	5000		0.100		190.0		5.4
	1250	8.0	Helium	5000		0.100		196.6		4.0
	1250	Smooth	Hydrogen	5000	0.050	0.100	133.3	150.3	17.0	27.0
	1250	Smooth	Hydrogen	5000	0.050	0.100	134.5	151.8	15.5	19.6
	1250	8.0	Hydrogen	5000		0.100		176.2		3.9
	1250	8.0	Hydrogen	5000		0.100		174.7		6.5
	1250	8.0	Hydrogen	5000		0.100		180.8		4.7
AMS 5666 (INCO 625)	1250	Smooth	Helium	5000	0.050	0.100	75.3	116.9	62.5	70.4
	1250	Smooth	Helium	5000	0.050	0.100	71.7	120.8	59.0	66.2
	1250	8.0	Helium	5000		0.100		150.0		15.3
	1250	8.0	Helium	5000		0.100		135.8		17.0
	1250	Smooth	Hydrogen	5000	0.050	0.100	72.7	119.1	57.5	64.2
	1250	Smooth	Hydrogen	5000	0.050	0.100	77.4	127.4	52.5	55.9
	1250	8.0	Hydrogen	5000		0.100		146.0		19.5
	1250	8.0	Hydrogen	5000		0.100		147.4		13.2
	1250	8.0	Hydrogen	5000		0.100		148.0		14.9

VI-III  
II-11

Table VIII-3. Elevated Temperature Tensile Properties of Materials in High Pressure Gaseous Environment (Continued)

Material	Test Conditions				Test Results					
	Test Temp, °F	Stress Concentration Factor	Environment	Pressure, psig	Load Rate in/min		Strength		Ductility	
					0 Load to Yield	Yield to Ultimate	Yield, ksi	Ultimate, ksi	EL, (1) %	RA, (2) %
AMS 5735 (A-286)	1250	Smooth	Helium	5000	0.050	0.100	104.6	119.0	25.5	52.1
	1250	Smooth	Helium	5000	0.050	0.100	104.0	122.4	29.0	54.5
	1250	8.0	Helium	5000		0.100		166.5		9.6
	1250	8.0	Helium	5000		0.100		182.0		12.5
	1250	Smooth	Hydrogen	5000	0.050	0.100	106.7	118.9	22.0	44.6
	1250	Smooth	Hydrogen	5000	0.050	0.100	122.3	109.3	25.0	46.6
	1250	8.0	Hydrogen	5000		0.100		173.5		6.7
	1250	8.0	Hydrogen	5000		0.100		184.5		9.6
	1250	8.0	Hydrogen	5000		0.100		186.2		7.2
AMS 5646 (AISI 347)	1250	Smooth	Helium	5000	0.050	0.100	57.8	60.4	24.5	66.3
	1250	Smooth	Helium	5000	0.050	0.100	57.4	59.6	25.0	68.1
	1250	8.0	Helium	5000		0.100		104.0		19.7
	1250	8.0	Helium	5000		0.100		102.7		18.1
	1250	Smooth	Hydrogen	5000	0.050	0.100	54.7	58.8	25.5	68.3
	1250	Smooth	Hydrogen	5000	0.050	0.100	60.3	64.2	25.0	66.7
	1250	8.0	Hydrogen	5000		0.100		101.4		15.0
	1250	8.0	Hydrogen	5000		0.100		100.0		16.5
	1250	8.0	Hydrogen	5000		0.100		99.8		15.3
AMS 5754 (Hastelloy X)	1250	Smooth	Helium	5000	0.050	0.100	35.2	82.1	53.0	57.5
	1250	Smooth	Helium	5000	0.050	0.100	33.1	77.5	53.0	57.6
	1250	8.0	Helium	5000		0.100		90.2		18.1
	1250	8.0	Helium	5000		0.100		91.2		18.3
	1250	Smooth	Hydrogen	5000	0.050	0.100	33.9	80.8	51.5	58.2
	1250	Smooth	Hydrogen	5000	0.050	0.100	34.1	80.3	51.0	48.9
	1250	8.0	Hydrogen	5000		0.100		88.6		20.2
	1250	8.0	Hydrogen	5000		0.100		90.8		17.6
	1250	8.0	Hydrogen	5000		0.100		91.0		18.8

VIII-12

Table VIII-3. Elevated Temperature Tensile Properties of Materials in High Pressure Gaseous Environment (Continued)

Material	Test Conditions					Test Results				
	Test Temp, °F	Stress Concentration Factor	Environment	Pressure, psig	Load Rate in/min		Strength		Ductility	
					0 Load to Yield	Yield to Ultimate	Yield, ksi	Ultimate, ksi	EL, (1) %	RA, (2) %
AMS 4928 (Ti 6-4)	200	Smooth	Helium	5000	0.050	0.100	138.3	152.5	15.0	46.6
	200	Smooth	Helium	5000	0.050	0.100	139.2	147.6	16.0	47.0
	200	8.0	Helium	5000		0.100		207.5		3.6
	200	8.0	Helium	5000		0.100		207.5		5.0
	200	8.0	Helium	5000		0.100		206.5		4.7
	200	Smooth	Hydrogen	5000	0.050	0.100	141.0	146.3	10.5	22.6
	200	Smooth	Hydrogen	5000	0.050	0.100	138.5	144.7	12.0	31.4
	200	8.0	Hydrogen	5000		0.100		209.0		3.7
	200	8.0	Hydrogen	5000		0.100		184.4		4.2
	200	8.0	Hydrogen	5000		0.100		183.3		4.2
AMS 4926 (A-110)	200	Smooth	Helium	5000	0.050	0.100	111.8	127.6	20.5	45.4
	200	Smooth	Helium	5000	0.050	0.100	113.6	132.7	17.5	46.6
	200	8.0	Helium	5000		0.100		190.5		3.5
	200	8.0	Helium	5000		0.100		185.3		5.0
	200	8.0	Helium	5000		0.100		187.0		3.5
	200	Smooth	Hydrogen	5000	0.050	0.100	114.4	126.0	14.0	20.8
	200	Smooth	Hydrogen	5000	0.050	0.100	112.5	130.0	17.0	31.9
	200	8.0	Hydrogen	5000		0.100		160.2		3.0
	200	8.0	Hydrogen	5000		0.100		168.0		2.7
	200	8.0	Hydrogen	5000		0.100		175.5		2.3

(1) Elongation in 1 inch.

(2) Reduction of Area.

VIII-13



VIII-14

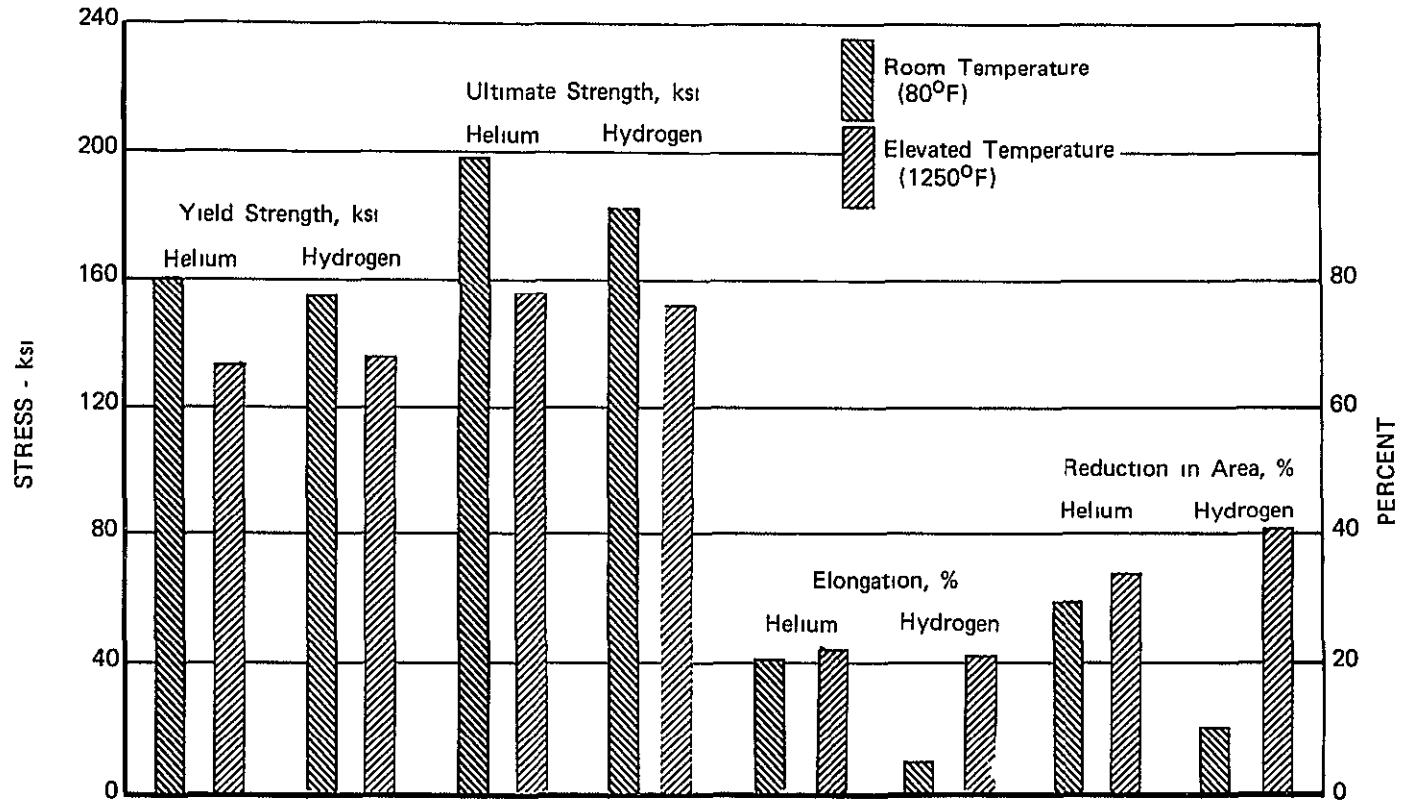


Figure VIII-4. Tensile Properties of AMS 5662 (INCO 718), 1750°F Solution in High Pressure Gaseous Environments

FD 53124

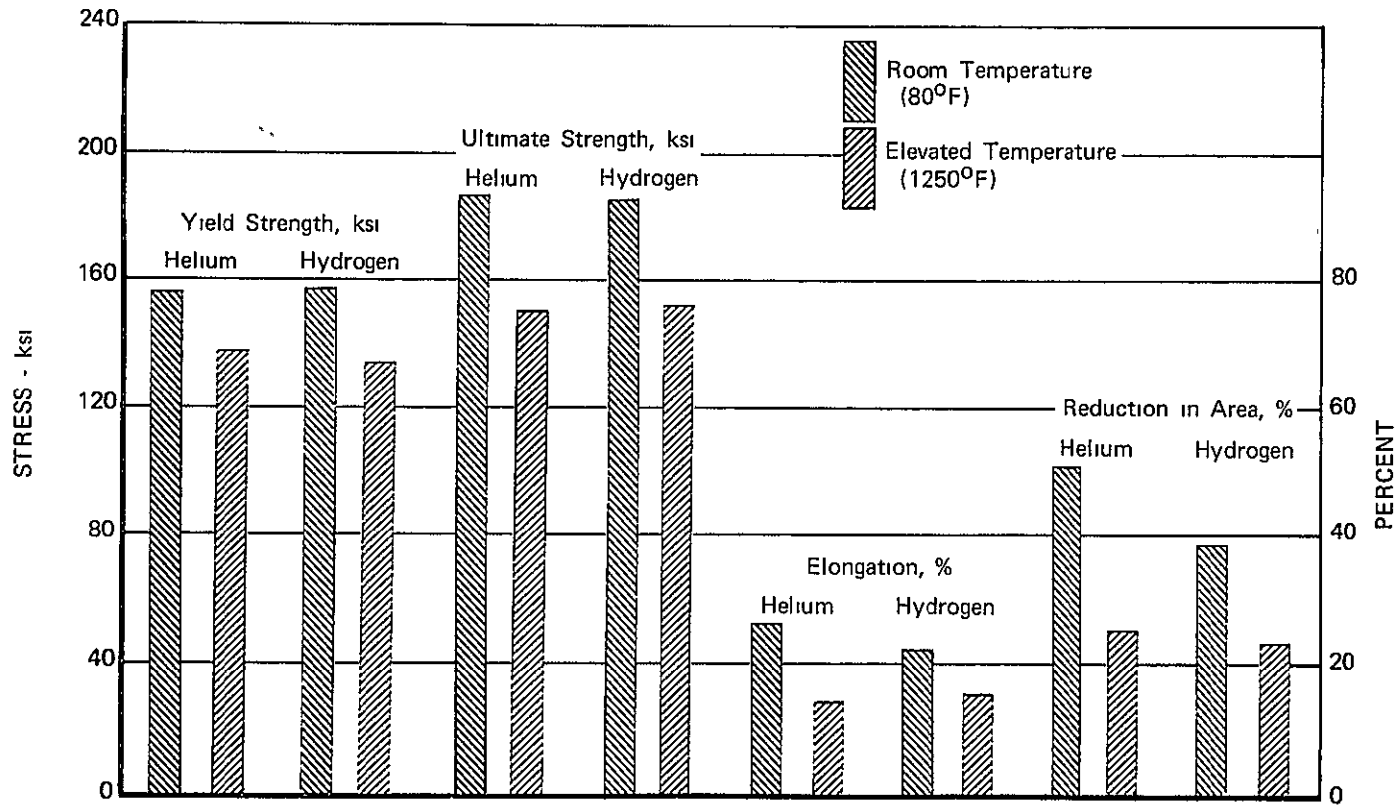


Figure VIII-5. Tensile Properties of AMS 5662 (INCO 718), 1900°F Solution in High Pressure Gaseous Environments

FD 53123

VIII-16

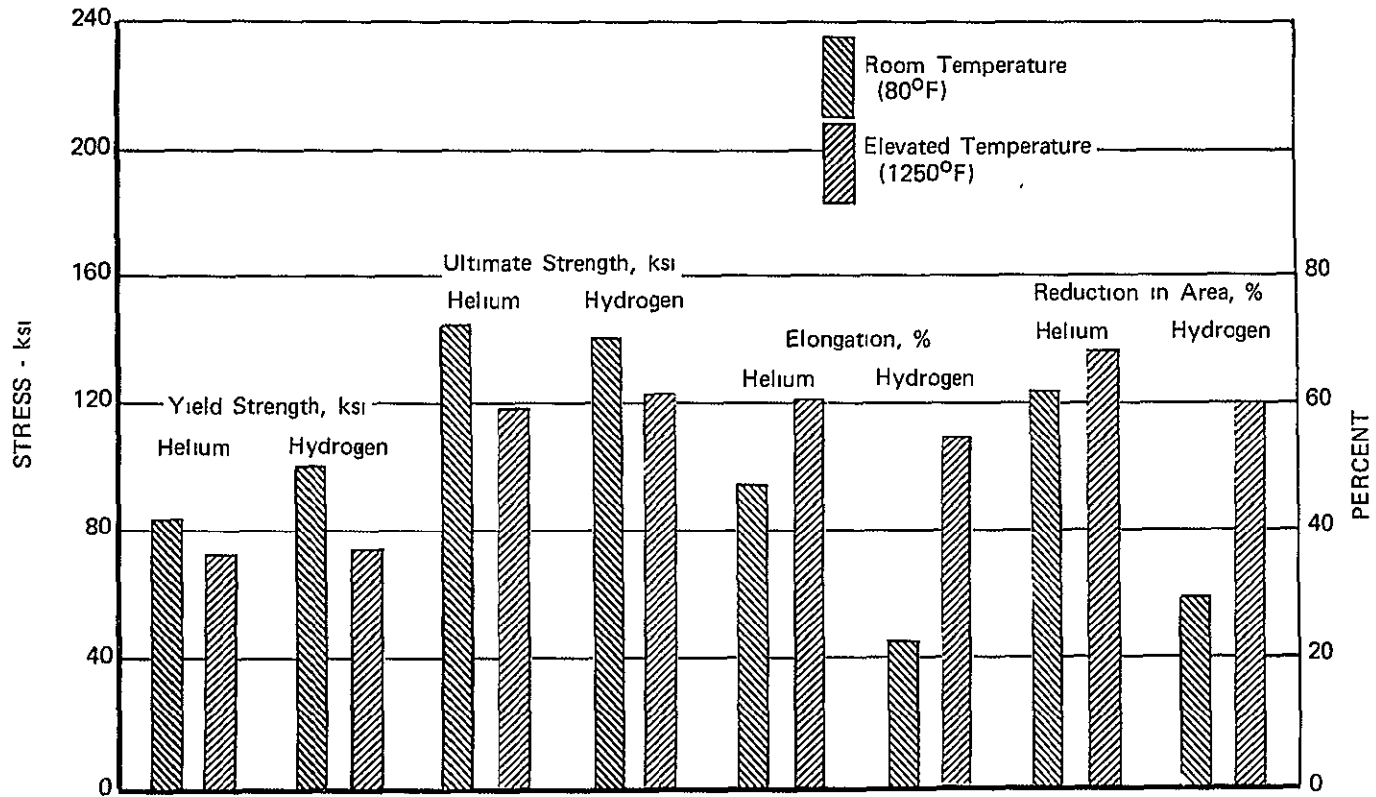


Figure VIII-6. Tensile Properties of AMS 5666 (INCO 625) in High Pressure Gaseous Environments

FD 53122

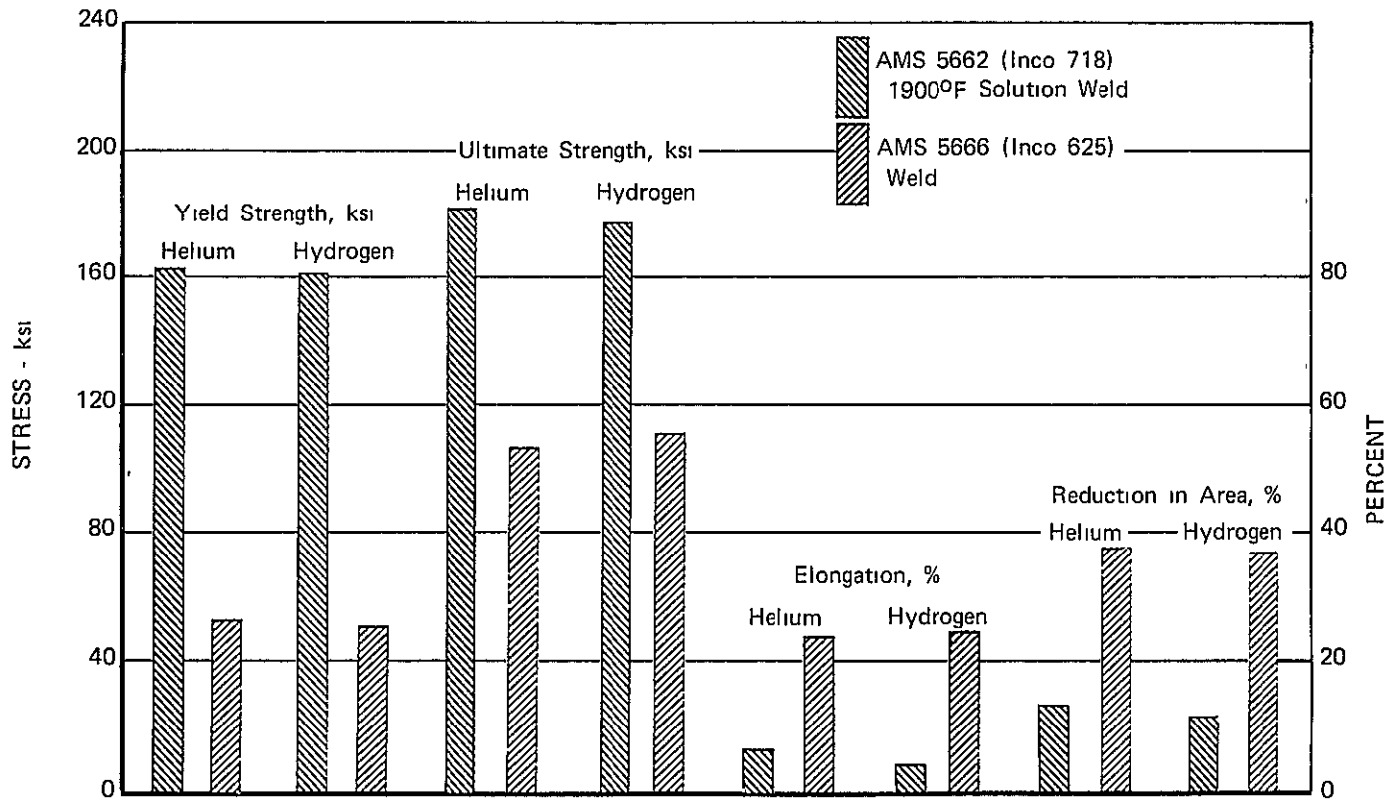


Figure VIII-7. Tensile Properties of AMS 5662 (INCO 718), 1900°F Solution Welds, and AMS 5666 (INCO 625) welds, in High Pressure Gaseous Environments at Room Temperature (80°F)

FD 53121

VIII-18

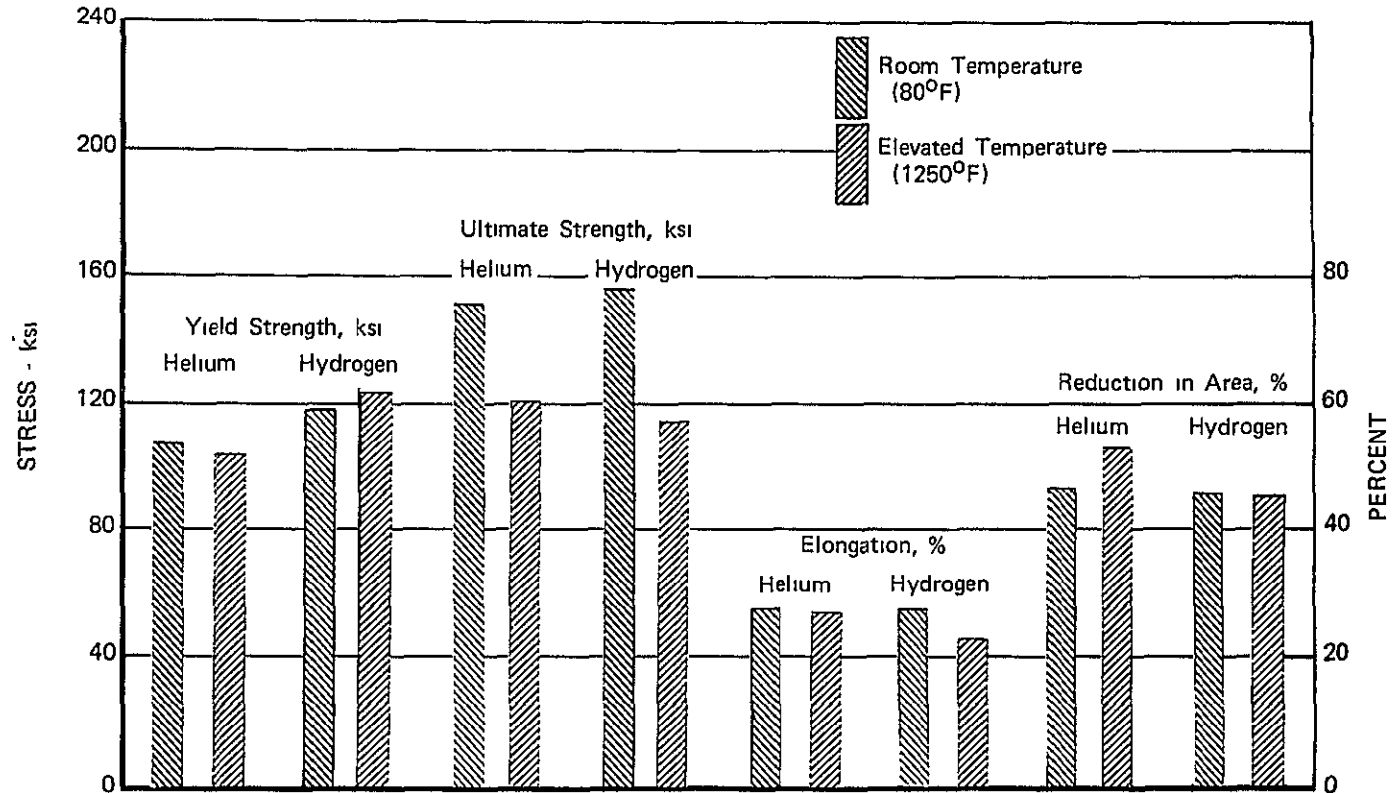


Figure VIII-8. Tensile Properties of AMS 5735 (A-286) in High Pressure Gaseous Environments

FD 53120



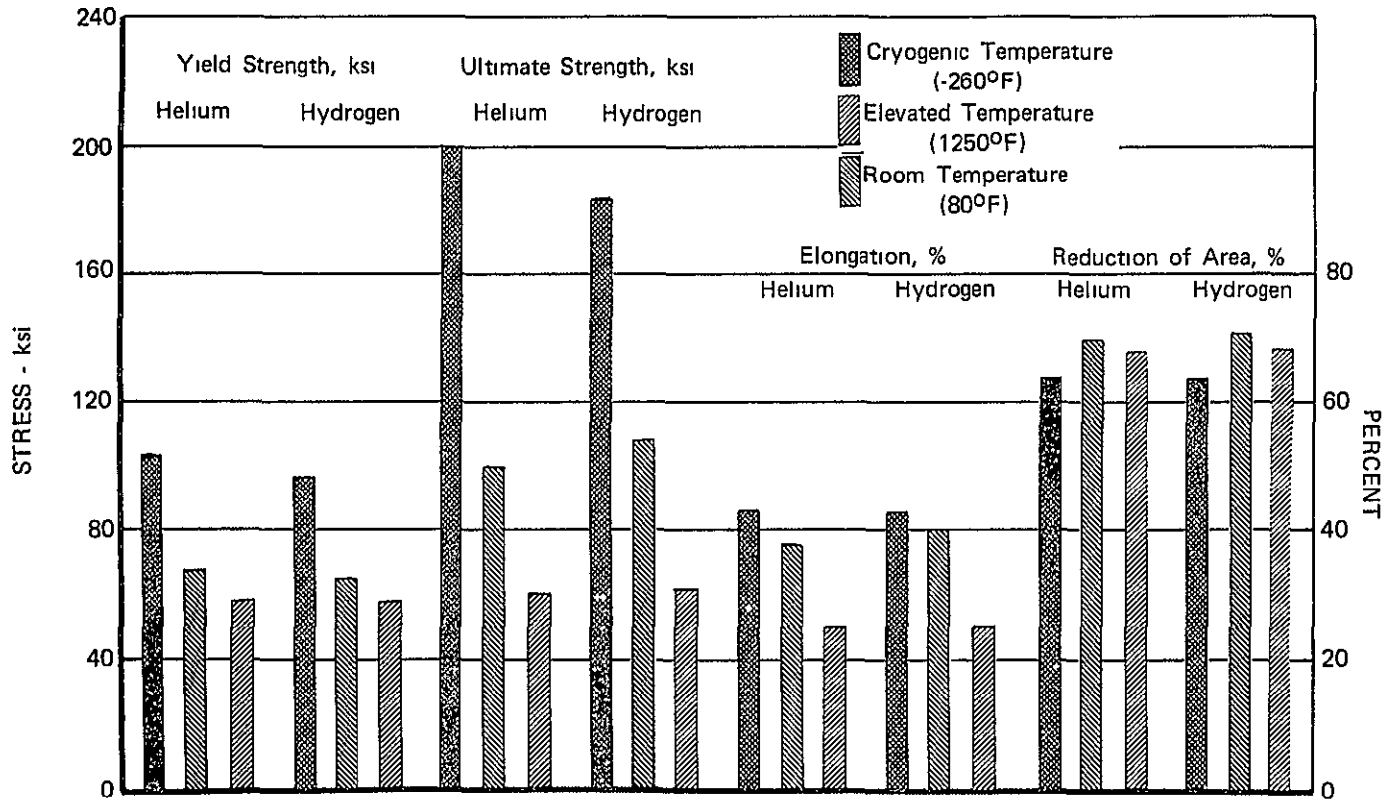


Figure VIII-9. Tensile Properties of AMS 5646 (AISI 347) in High Pressure Gaseous Environments

FD 53119

VIII-20

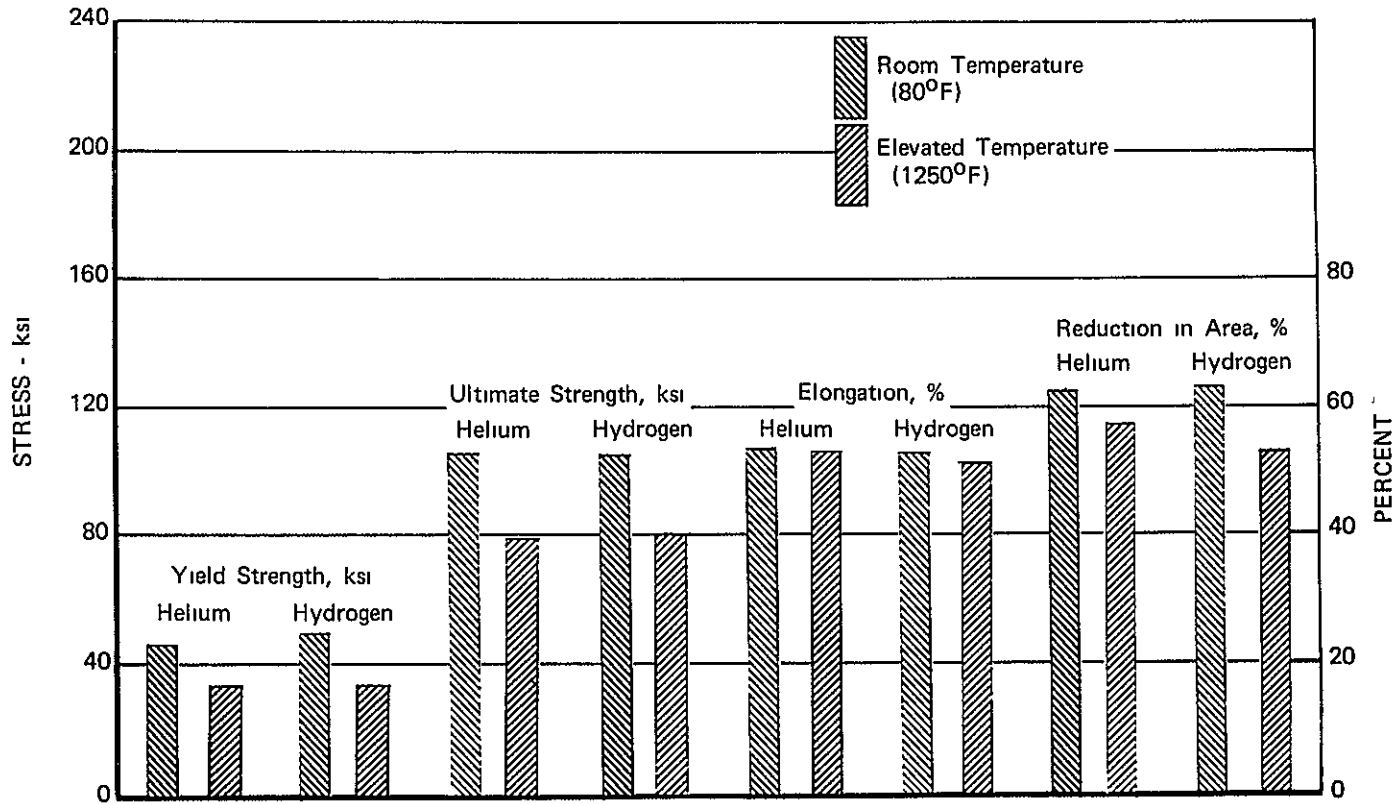


Figure VIII-10. Tensile Properties of AMS 5754 (Hastelloy X) in High Pressure Gaseous Environments

FD 53118

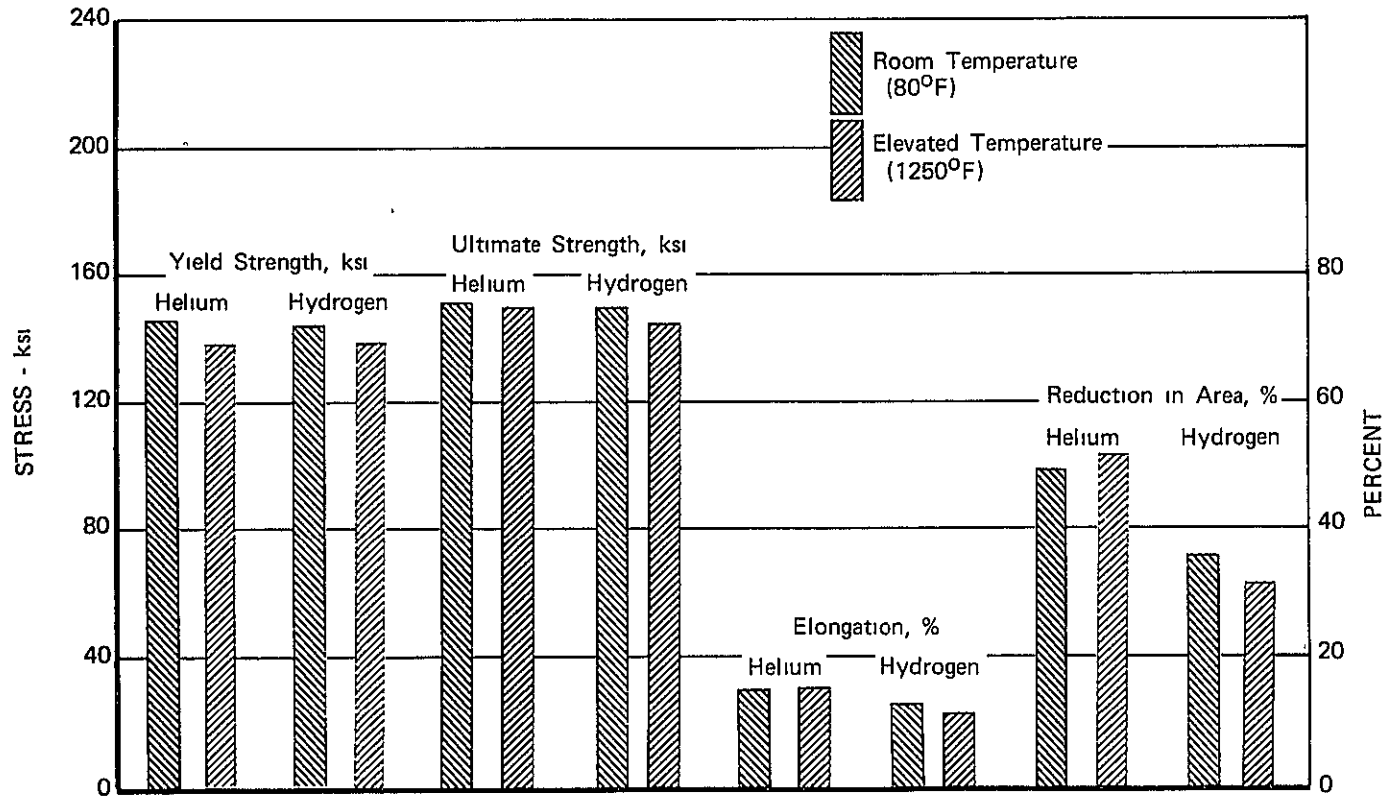


Figure VIII-11. Tensile Properties of AMS 4928 (Ti 4-6) in High Pressure Gaseous Environments

FD 53117

VIII-22

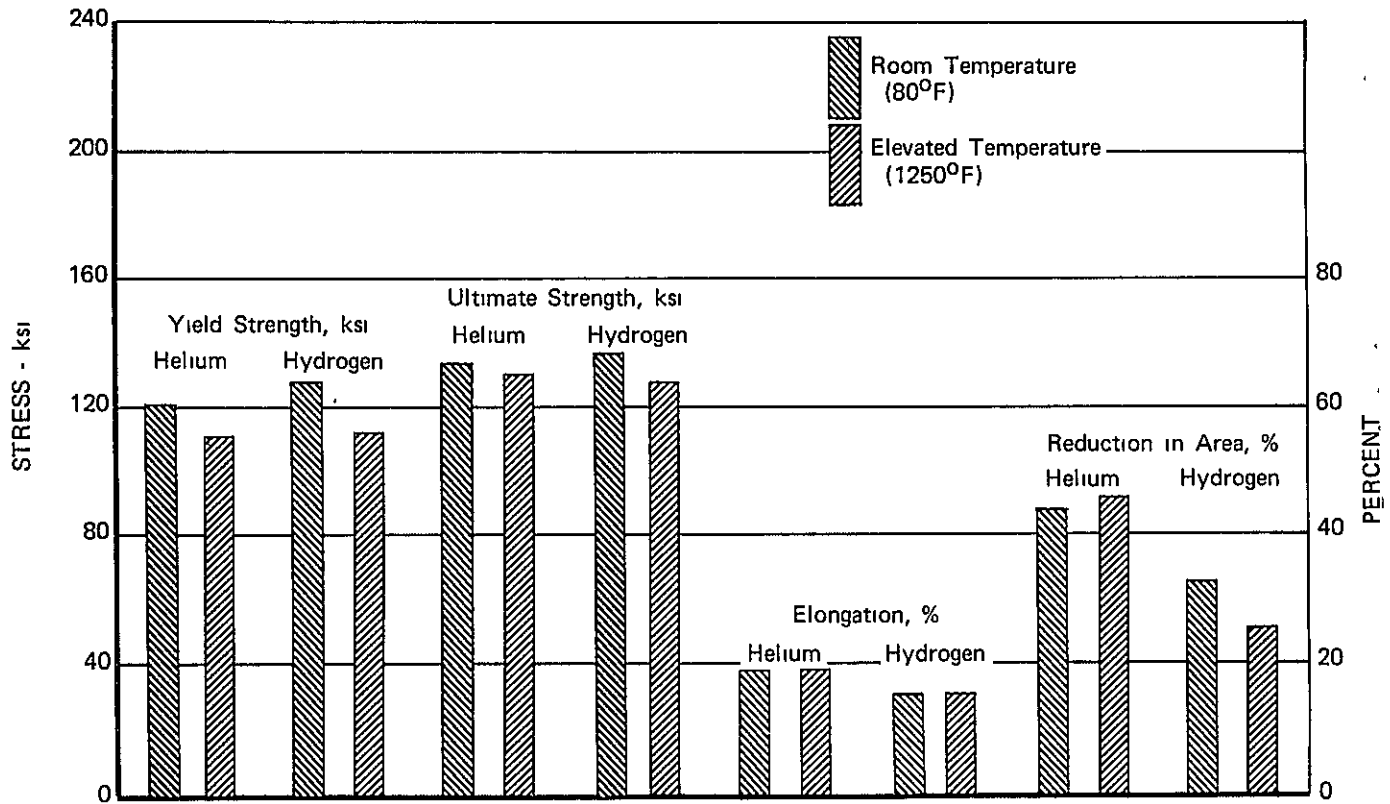


Figure VIII-12. Tensile Properties of AMS 4926 (A-110) in High Pressure Gaseous Environments

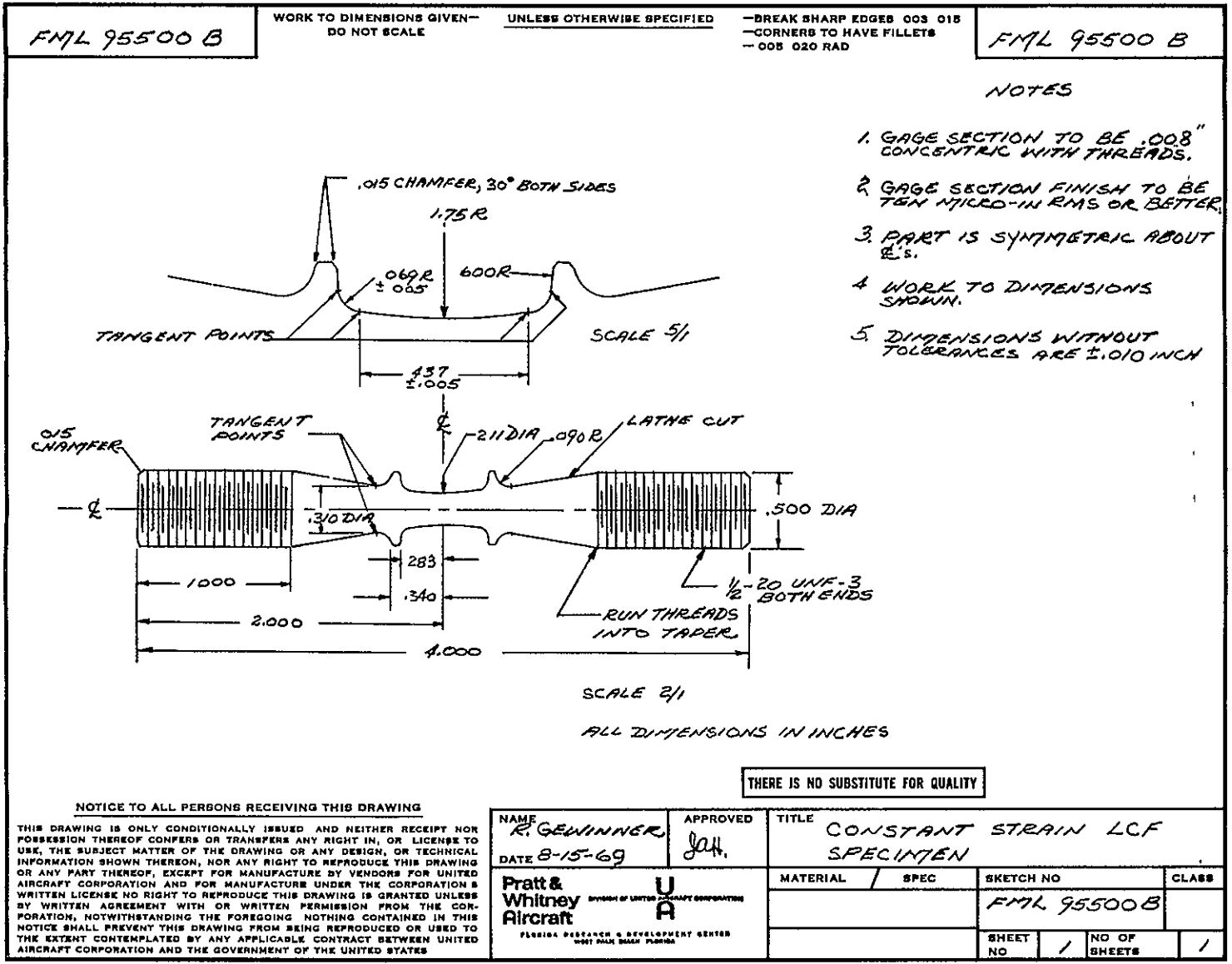
FD 53116

Welded specimens were machined from blanks prepared as previously discussed; manual GTA welding was done on oversized blanks to ensure specimen finished dimensions. Both the root pass and the finished weld were X-ray inspected and judged radiographically sound. Prior to finish machining, specimens were given a light etch to define weld location. After finish machining, all specimens were polished to produce desired surface finish.

Table III-2. Specimens Used to Determine Influence of Elevated Temperature on Metals in Gaseous Hydrogen

Name	Print Number	Figure
Constant Strain Low Cycle Fatigue Specimen	FML 95500B	III-3
Smooth Axial Fatigue Specimen (High Cycle Fatigue)	FML 95212B	III-4
Fracture Toughness Specimen	FML 95559 C	III-5
Flat End Creep Rupture Specimen	FML 95623B	III-6
Ambient-Cryogenic Tensile Specimen (notch)	FML 95620B	III-7
Ambient-Elevated Temperature Tensile Specimen (Smooth)	FML 95224B	III-8

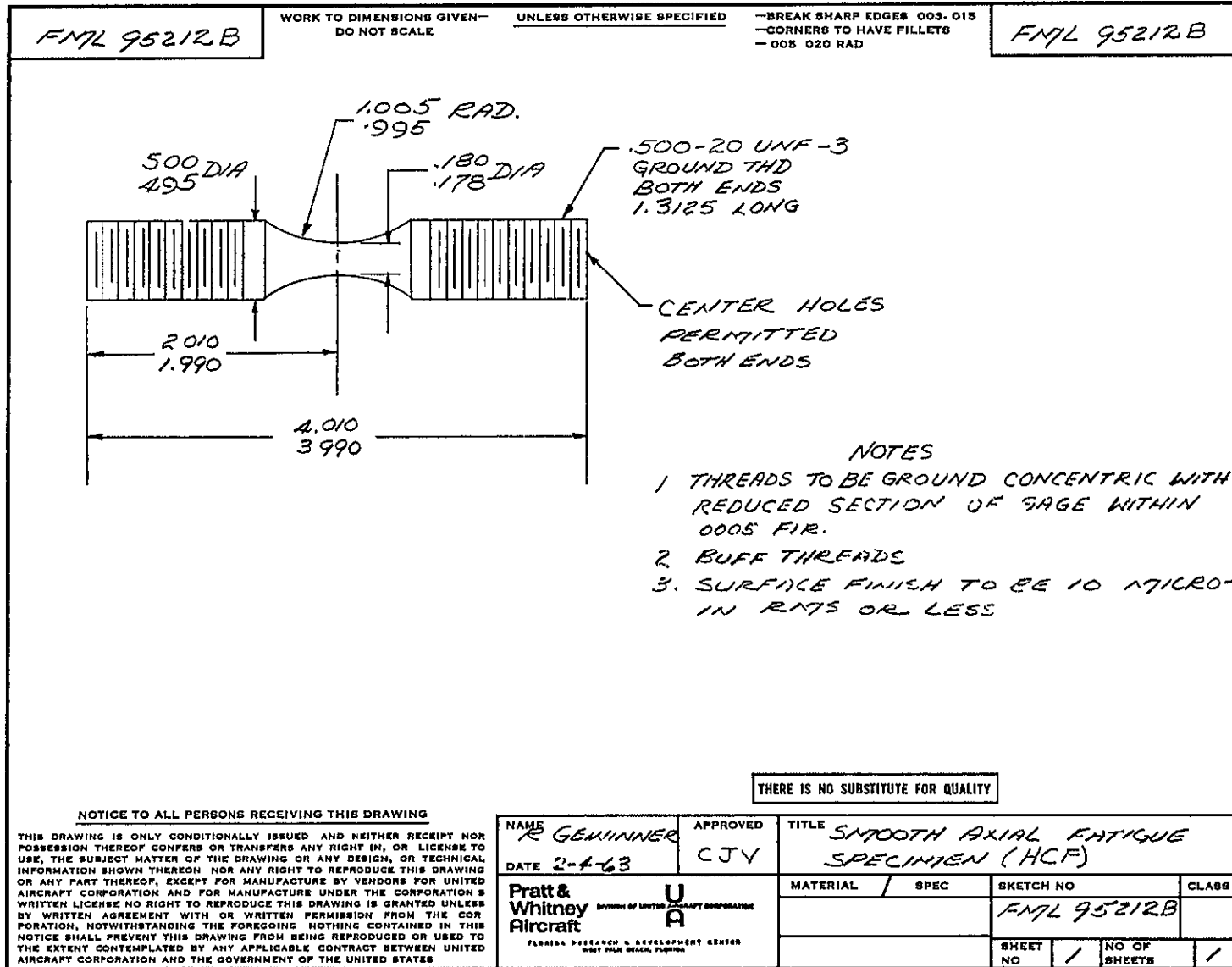




III-9

Figure III-3. Constant Strain Low Cycle Fatigue Specimen

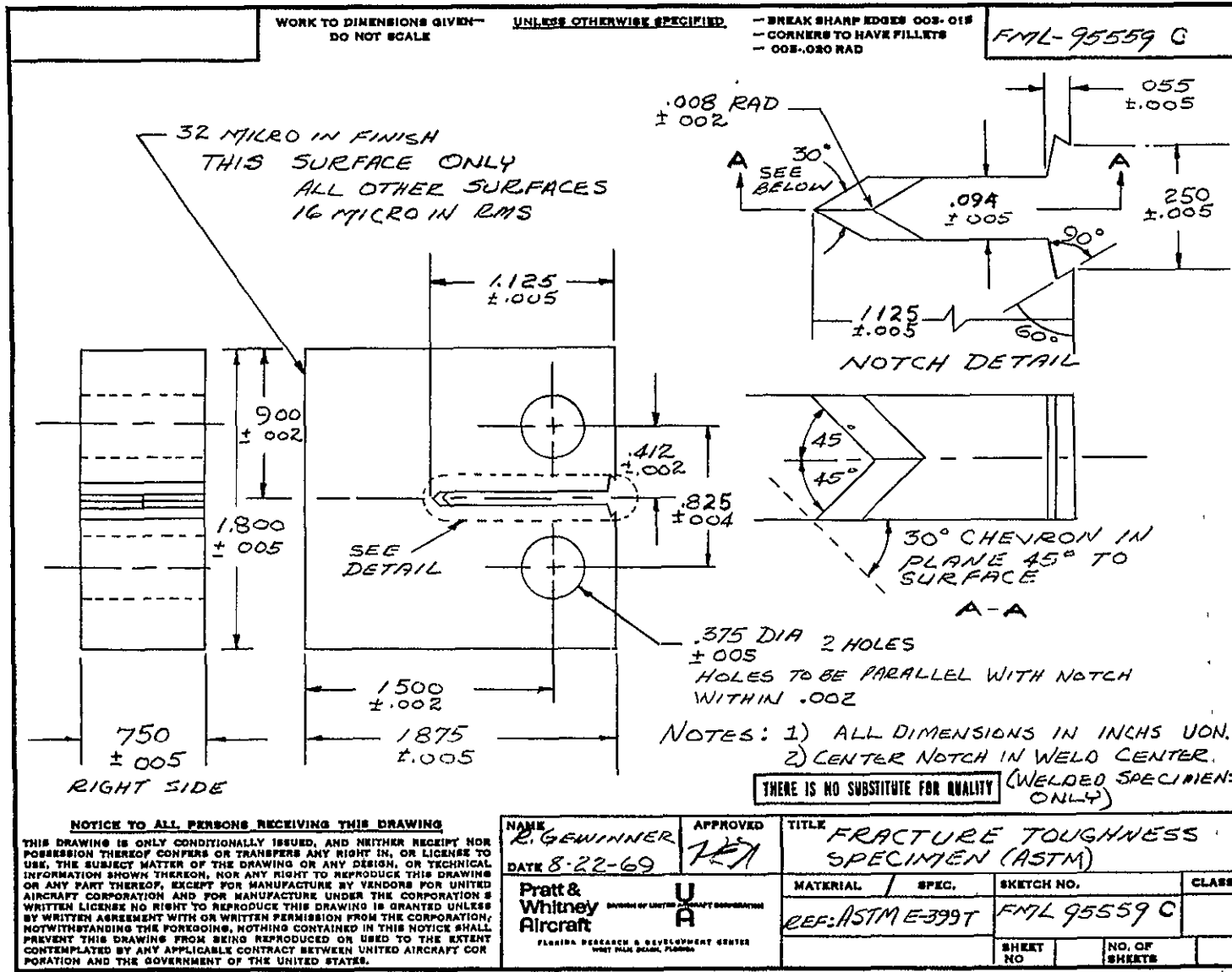
FML 95500B



III-7

Figure III-4. Smooth Axial High Cycle Fatigue Specimen

FNL 95212B



III-8

Figure III-5. Fracture Toughness Specimen (ASTM)

FML 95559C

FML 95623 B

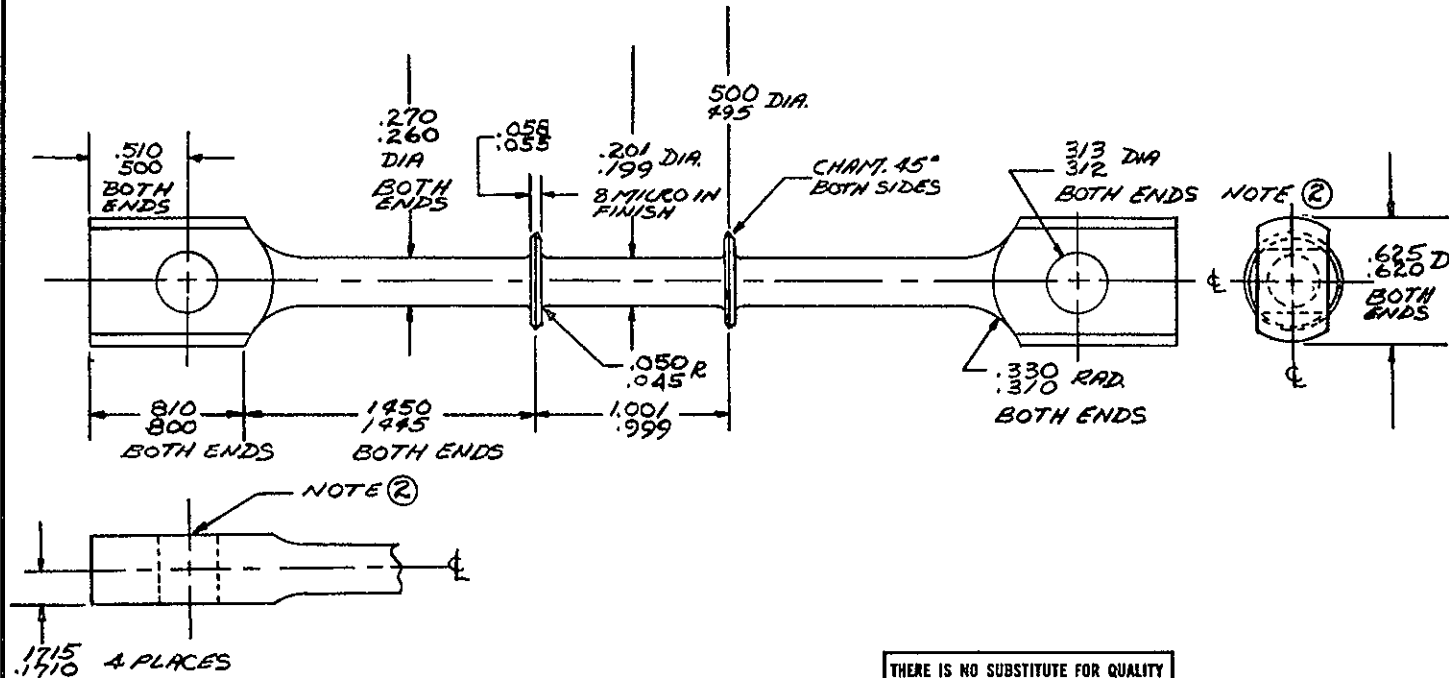
WORK TO DIMENSIONS GIVEN—  
DO NOT SCALE

UNLESS OTHERWISE SPECIFIED

—BREAK SHARP EDGES .003 .015  
—CORNERS TO HAVE FILLETS  
—.005 .020 RAD

FML 95623 B

- ①-ALL DIAMETERS TO BE CONCENTRIC WITHIN  $\pm .002$
- ②-HOLES TO BE PERPENDICULAR TO  $\phi$  WITHIN  $\pm .002$



THERE IS NO SUBSTITUTE FOR QUALITY

NOTICE TO ALL PERSONS RECEIVING THIS DRAWING

THIS DRAWING IS ONLY CONDITIONALLY ISSUED, AND NEITHER RECEIPT NOR POSSESSION THEREOF CONFERS OR TRANSFERS ANY RIGHT IN, OR LICENSE TO USE, THE SUBJECT MATTER OF THE DRAWING OR ANY DESIGN, OR TECHNICAL INFORMATION SHOWN THEREON, NOR ANY RIGHT TO REPRODUCE THIS DRAWING OR ANY PART THEREOF, EXCEPT FOR MANUFACTURE BY VENDORS FOR UNITED AIRCRAFT CORPORATION AND FOR MANUFACTURE UNDER THE CORPORATION'S WRITTEN LICENSE NO RIGHT TO REPRODUCE THIS DRAWING IS GRANTED UNLESS BY WRITTEN AGREEMENT WITH OR WRITTEN PERMISSION FROM THE CORPORATION, NOTWITHSTANDING THE FOREGOING, NOTHING CONTAINED IN THIS NOTICE SHALL PREVENT THIS DRAWING FROM BEING REPRODUCED OR USED TO THE EXTENT CONTEMPLATED BY ANY APPLICABLE CONTRACT BETWEEN UNITED AIRCRAFT CORPORATION AND THE GOVERNMENT OF THE UNITED STATES

NAME R. GENWINNER		APPROVED J.S		TITLE FLAT END CREEP RUPTURE SPECIMEN			
DATE Jan '70				MATERIAL / SPEC		SKETCH NO	
Pratt & Whitney Aircraft		DIVISION OF UNITED AIRCRAFT CORPORATION				FML 95623 B	
FLORIDA RESEARCH & DEVELOPMENT CENTER WEST PALM BEACH, FLORIDA				SHEET NO		NO OF SHEETS	

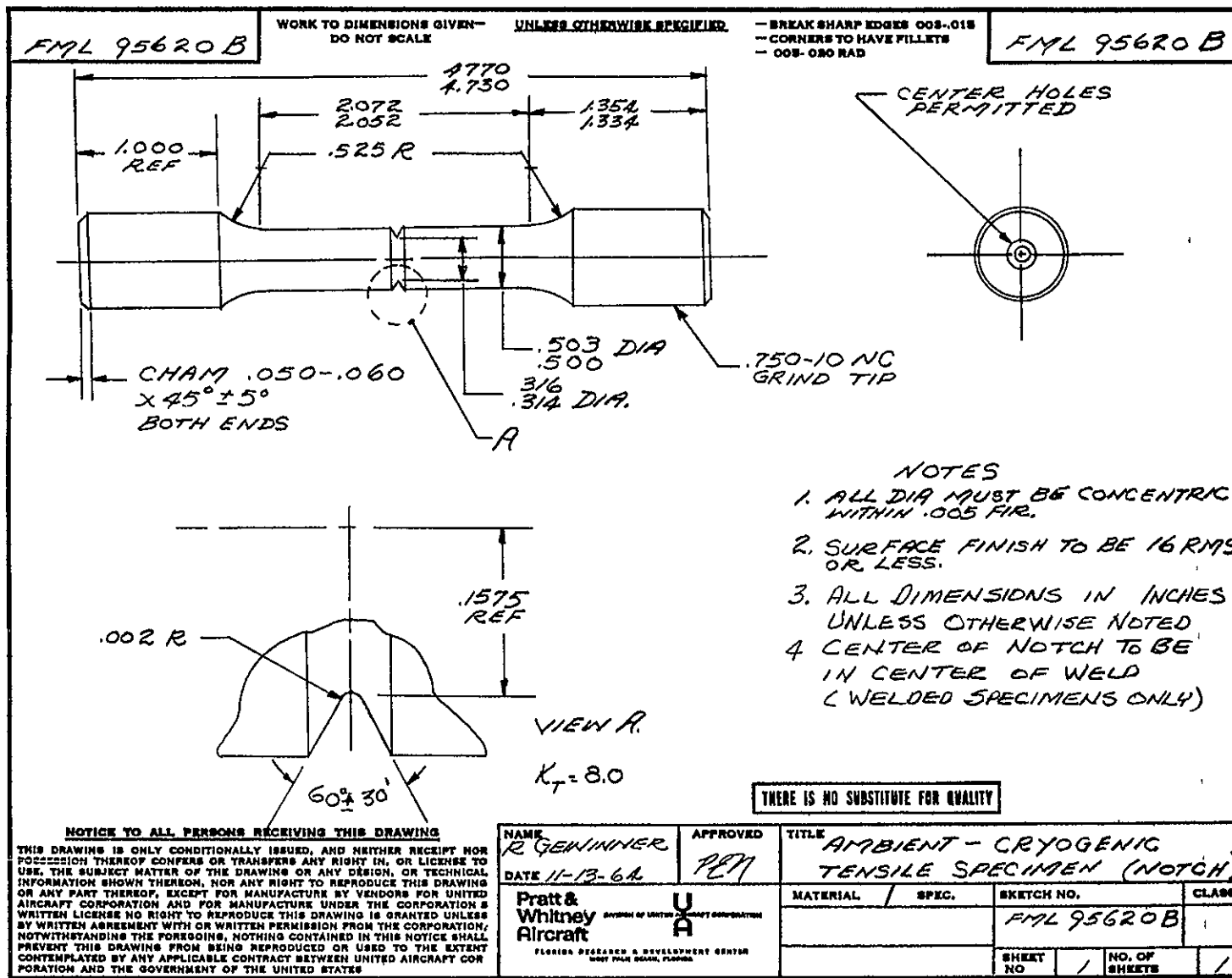
PWA 10000 REV 5 63

6-III

Figure III-6. Flat End Creep Rupture Specimen

FML 95623B

Pratt & Whitney Aircraft  
PWA FR-4566



III-10

Figure III-7. Ambient-Cryogenic Tensile Specimen (Notch)

FML 95620B



III-11/III-12

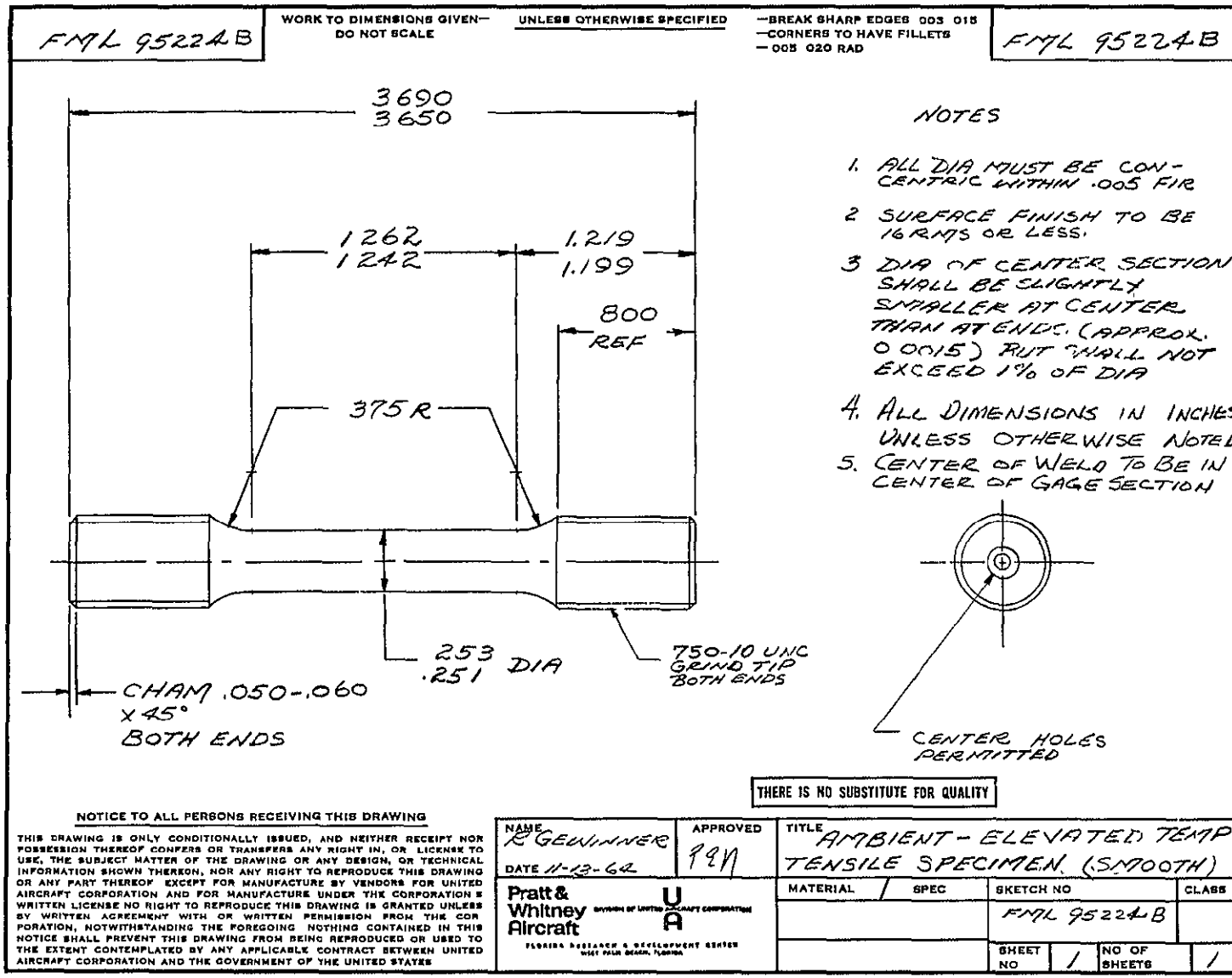


Figure III-8. Ambient-Elevated Temperature Tensile Specimen (Smooth)

FML 95224B

Pratt & Whitney Aircraft  
PWA FR-4566

## SECTION IV LOW CYCLE FATIGUE

Low cycle fatigue tests were conducted under this contract to determine the gaseous hydrogen degradation of various nickel-base, iron-base, and titanium-base alloys. Comparison of results of axial constant strain tests in a high pressure hydrogen environment to results of similar tests in a helium environment establishes the degradation due to the hydrogen environment. The low cycle fatigue tests performed under this contract have been of the strain-controlled type with the material cycling through a constant total (elastic plus plastic) strain range (figure IV-1) until complete specimen fracture.

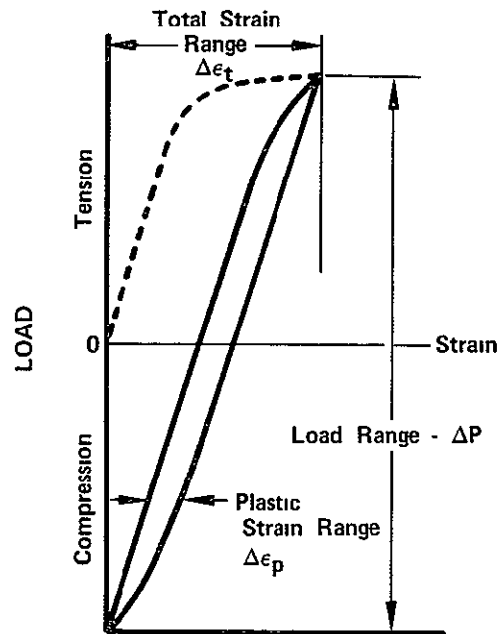


Figure IV-1. Typical Load-Strain Hysteresis Curve FD 48672  
Obtained During a Specimen Low Cycle  
Fatigue Test

### A. CONCLUSIONS AND DISCUSSION

#### 1. Summary

Except for AMS 5646 (AISI type 347, tested at 80°F only) materials tested in general exhibited degradation in LCF life due to high pressure hydrogen of at least one of the conditions tested. This degradation appears to be dependent upon both temperature and strain range. The nickel-base alloys were most susceptible to hydrogen effects, followed by the titanium-base alloys with the iron-base alloys the least susceptible. Table IV-1 summarizes the test findings; materials are listed in decreasing order of degree of hydrogen degradation based upon average degradation for tests in the range of 1.0 to 2.0% cyclic strain for the temperatures tested.

To fully characterize the LCF performance of these materials in hydrogen, testing should be conducted at additional temperatures.

Table IV-1. Degradation of Alloys Due to High Pressure Hydrogen

Material	Average Degradation			
	-260°F	80°F	200°F	1250°F
Nickel Base				
AMS 5666 (INCO 625)	NT	85%	NT	NT
AMS 5662 (INCO 718, 1900°F Sol.)	0*	82%	NT	29%
AMS 5662 (INCO 718, 1750°F Sol.)	NT	80%	NT	28%
AMS 5754 (Hastelloy X)	NT	66%	NT	NT
Titanium Base				
AMS 4926 (A-110)	NT	0	74%	NT
AMS 4928 (Ti 6-4)	NT	0	26%	NT
Iron Base				
AMS 5735 (A-286)	NT	0	NT	9%
AMS 5646 (AISI 347)	NT	0	NT	NT

NT - Not Tested  
\* - See specific conclusions.

## 2. INCO 625 (AMS 5666)

INCO 625 material was tested at 80°F only, and exhibited the most severe degradation of all alloys tested at that temperature, ranging from 80 to almost 90% over total strain levels of 1.0 to 2.0%. Some influence of strain level on degree of degradation was observed (figures IV-2 and IV-3), but even extrapolation of the LCF curves into the elastic range indicates degradation would occur at very low strain levels.